CDSD IN THE TYPE III SECRETION APPARATUS OF *CHLAMYDIA PNEUMONIAE*

CHARACTERIZATION OF *CHLAMYDIA PNEUMONIAE* CDSD AND ITS ROLE IN THE BASAL BODY OF THE TYPE III SECRETION APPARATUS

By

ROBERT CURTIS CLAYDEN, B.SC.

A Thesis Submitted to the School of Graduate Studies in Partial Fulfilment

of the Requirements for the Degree Master of Science

DESCRIPTIVE NOTE

Master of Science (2012) McMaster University

Medical Sciences Hamilton, Ontario

TITLE: Characterization of *Chlamydia pneumoniae* CdsD and its role in the basal body of the type III secretion apparatus

AUTHOR: Robert Curtis Clayden, B.Sc. (Biochemistry – McMaster University)

SUPERVISOR: Dr. J.B. Mahony

NUMBER OF PAGES: viii, 126

ABSTRACT

Chlamydia pneumoniae is a Gram-negative, obligate intracellular bacterium which shares its unique biphasic developmental cycle, genus-specific lipopolysaccharide, and complement fixation antigen with the other *Chlamydia* species. Intracellular bacteria, like *Chlamydia*, require strategies to invade host cells, evade host detection, commandeer host processes, and absorb nutrients in order to support their developmental cycle and survive. The type III secretion (T3S) system meets these needs by transporting bacterial effector proteins across the bacterial membrane and through the host cell membrane. The T3S system in *C. pneumoniae* is composed of approximately twenty different proteins, whose encoding genes are dispersed throughout ten operons in the *Chlamydia* genome. CdsD (*Cpn0712*), a basal body protein component of the T3S apparatus, is suggested to localize to the inner membrane and anchor other T3S structural components of the inner membrane ring. However, the cytoplasmic N-terminal domain contains two putative forkhead-associated (FHA) domains which may play an additional functional role in cellular signalling. This large hypothetical inner-membrane protein is poorly characterized in *C. pneumoniae* and the role of the predicted phospho-threonine binding, N-terminal FHA domains has yet to be elucidated. Herein, we provide evidence that CdsD has a high affinity for five cytoplasmic (CdsQ, CdsL, CdsN, PknD and SycH) and one periplasmic (CdsF) T3S-associated proteins. We also provide the first evidence that the phosphorylation of CdsD may permit the phosphorylation-dependent oligomerization or interaction with other phosphorylated components of the T3S apparatus. Future

research will clarify the role of phosphate signalling in the T3S virulence mechanism. Ultimately, this may lead to a greater understanding of signalling mechanisms that regulate the secretion of bacterial effectors into host eukaryotic cells.

ACKNOWLEDGEMENTS

Over the past two years as a graduate student in the Mahony lab, I have met many extraordinary people. I would like to express my deepest appreciation to my supervisor, Dr. James Mahony, for providing a continual source of inspiration and enthusiasm for research. Dr. Mahony generously committed his time, interest, and assistance in the pursuit and preparation of this thesis. I have learned a great deal under his patient, thought-provoking tutelage and I consider myself extremely fortunate to have been able to train in his laboratory. I would also like to thank my committee members Dr. Brian Coombes and Dr. Murray Junop for their continual source of support and guidance. They consistently challenged me to explore scientific literature and expand my comfort zone in the laboratory.

I feel honoured to have studied in the Mahony laboratory alongside many intelligent, passionate, and talented people. I owe a great deal to my colleagues who have supported me both inside and outside the laboratory. Dr. Christopher Stone has been an excellent friend and invaluable mentor throughout this process in the laboratory and on the golf course. Our conversations over the past two years constantly motivated me to improve my skills as a scientist, second, and a graph plotter, first. In addition to his patient and sensitive approach to teaching, David Bulir's determination and passion for science was truly admirable. His hard work and high level of intelligence are a formidable combination that I aspire to emulate in my own studies. I would also like to thank Tiffany Leighton, Sylvia Chong, Jodi Gilchrist, Andrea Granados, Ken Mwawasi, Alex Ruyter, and Dan Waltho for their support, guidance, and friendship.

I owe my deepest, heartfelt gratitude to my family and friends who provided ample support, laughter, and joy throughout this process. I am particularly indebted to two of my best friends and editors; my brother, Wesley, and my girlfriend, Winnie. Wesley constantly offered a refreshing source of perspective and, throughout my life, has provided the best example of the correlation between hard work and achievement. My girlfriend, Winnie, has offered her selfless support, kindness and unconditional love throughout this entire process. Her spirit continually amazes me and has made even the longest hours enjoyable. Finally, I wish to take this opportunity to express my gratefulness to my parents. Their love and encouragement provided the inspiration and motivation required to complete this journey. I hope that this work makes them proud.

To Mom and Dad,

with all my love.

TABLE OF CONTENTS

LIST OF ABBREVIATIONS

ABC	ATP-binding Cassette
APS	Ammonium persulfate
ATP	Adenosine triphosphate
CDS	Contact Dependent Secretion
COPD	Chronic Obstructive Pulmonary Disease
C-ring	Cytoplasmic Ring
CSF	Cerebral Spinal Fluid
C-terminus	Carboxy terminus
DNA	Deoxyribonucleic acid
EB	Elementary Body
ECL	Electrochemiluminescence
EDTA	Ethylenediaminetetraacetic acid
FBS	Fetal Bovine Serum
FHA	Fork-head Associated
FITC	Fluorescein isothiocyanate
FPLC	Fast Protein Liquid Chromatography
GST	Glutathione-S-transferase
His	Polyhistidine (6x) tag
IB	Intermediate Body
IF	Immunofluorescent
ifu	Infection Forming Units
IM	Inner Membrane
IMR	Inner Membrane Ring
IPTG	Isopropyl-β-D-thiogalactopyranoside
kDa	kilodaltons
LB	Luria Bertani (or Lysogeny Broth)
MBP	Maltose Binding Protein
MEM	Minimal Essential Media
MOI	Multiplicity of Infection
MOMP	Major Outer Membrane Protein
Ni-NTA	Nickel-Nitrilotriacetic acid
N-terminus	Amino terminus
OM	Outer Membrane
OMR	Outer Membrane Ring
PAGE	Polyacrylamide gel electrophoresis
PBS	Phosphate-buffered Saline
RB	Reticulate Body
RNA	Ribonucleic Acid
RT-PCR	Reverse Transcriptase-Polymerase Chain Reaction
SDS	Sodium dodecyl sulfate
Sec	Secretion signal

STPK	Serine/Threonine Protein Kinase
T3S	Type III Secretion
TARP	Translocated Actin Recruitment Protein
TAT	Twin Arginine Translocation
TCA	Trichloroacetic Acid
TEMED	Tetramethylethylenediamine
TPK	Tyrosine Protein Kinase
UV	Ultra-violet
v/v	volume/volume ratio
WB	Western Blot
w/v	weight/volume ratio

LIST OF FIGURES

LIST OF BUFFERS AND SOLUTIONS

Buffer/Solution	Composition
Luria Bertani (LB) or Lysogeny Broth	1% (w/v) Tryptone, 0.5% (w/v)NaCl, and 1% (w/v) Yeast Extract
Kinase Activity Buffer	125 mM KCl, 50 mM Tris, and 5 mM $MnCl_2$
Nickel A Buffer	20 mM Tris-HCl pH 7.0, 0.03% (v/v) LDAO, 500 mM KCl, 10 mM Imidazole, and 10% (v/v) glycerol
Nickel B Buffer	20 mM Tris-HCl pH 7.0, 0.03% (v/v) LDAO, 500 mM KCl, 300 mM Imidazole, and 10% (v/v) glycerol
2X SPG Freeze/Thaw Media	220 mM Sucrose, 4 mM KH_2PO_4, 9 mM Na_2HPO_4, and 5 mM Glutamic Acid
1X Phosphate Buffered Saline (PBS)	140 mM NaCl, 6.5 mM Na_2HPO_4, 2.5 mM KCl, and 1.5 mM KH_2PO_4 (pH 7.25)
Cell Lysis Buffer	50 mM Tris-HCl (pH 7.2), 100 mM KCl, 1% (v/v) Triton X-100, 0.1% (v/v) SDS, and 1X Complete EDTA-free Protease Inhibitors (Roche)
8X Resolving Gel Buffer	3 M Tris-HCl (pH 8.8) and 0.8% (v/v) SDS
4X Stacking Gel Buffer	0.4 M Tris-HCl (pH 6.8) and 0.4% (v/v) SDS
1X SDS-PAGE Running Buffer	25 mM Tris, 192 mM Glycine, and 0.001% (v/v) SDS
5X Sample Loading Buffer	250 mM Tris-HCl (pH 6.8), 6.25% (v/v) SDS, 32.3% (v/v) glycerol,

	12.5% (v/v) 2-Mercaptoethanol, and 0.001% (v/v) Bromophenol Blue
4X Native Resolving Gel Buffer	1.5 M Tris-HCl (pH 8.8)
4X Native Stacking Gel Buffer	2.5 M Tris-HCl (pH 6.8)
Native Running Buffer	0.192 M Glycine and 0.025 M Tris-HCl (pH 8.3)
Reduced Glutathione Solution	1.5% (w/v) L-glutathione in 30 mL of 1 M Tris-HCl (pH 9.0)
High Salt Wash Buffer	20 mM Tris-HCl (pH 7.0), 500 mM NaCl and 0.5% (v/v) Triton X-100
0.1 M Potassium Phosphate Buffer (pH 7.0)	0.062 M K_2HPO_4 and 0.038 M KH_2PO_4
1X Binding Buffer	0.05 M Potassium Phosphate Buffer (pH 7.0), 1 mM $MgCl_2$, 150 mM KCl, and 0.02% (v/v) Triton X-100
0.6-2.0 % Agarose Gel Buffer	0.6-2.0% (w/v) Agarose and 0.005% (v/v) Ethidium bromide in 300 mL of 1X TAE buffer
1X TAE buffer	40 mM Tris, 20 mM Glacial Acetic Acid, and 1 mM EDTA
Tris-Buffered Saline	20 mM Tris-HCl, 100 mM NaCl (pH 7.5)
6X DNA Loading dye	30% (v/v) glycerol and 0.25% (m/v) bromophenol blue
Mounting media	50% (v/v) 1X PBS and 50% (v/v) glycerol
Membrane Stripping Buffer	67 mM Tris-HCl (pH 6.9), 0.02% (v/v) SDS, and 0.75% (v/v) 2-Mercaptoethanol

LIST OF TECHNICAL LABORATORY EQUIPMENT

Company	Equipment
Eppendorf	Microcentrifuge 5415R
Thermoscientific	FormaSeries II Water Jacketed CO_2 Incubator
VWR	Analog Heatblock
Biorad	PowerPac Basic
Invitrogen	iBlot
VWR	D2-500 Orbital Shaker
Beckman	Ultrospec 4300pro UV/Visible Spectrophotometer
Olympus	CK Light Microscope
VWR	Mini-Vortexer
Amersham	AKTA FPLC
ThermoScientific	Sorvall Legend RT+ Benchtop Centrifuge
Sorvall	RC-5B Refrigerated Superspeed Centrifuge
Beckman	LE-80 Ultracentrifuge
Thermoscientific	MaxQ 4000 orbital shaker/incubator
Fisher Scientific	Accumet Basic AB15 pH Meter
ClayAdams	Nutator
MJ Research	Peltier Thermal Cycler (PTC-200)
Fisher Scientific	Sonic Dismembrator Model 100
GeneQ	Manual Pump
Olympus	BX51 Fluorescent Microscope
Nanodrop	Spectrophotometer ND-1000
Konica Minolta	Medical X-ray Processor SRX-101A
Biorad	GelDoc
Mitsubishi	Thermal Printer P93D
JEOL	1200EX TEMSCAN Microscope

CHAPTER ONE

INTRODUCTION

1.1 The history and taxonomy of the *Chlamydiales* order

The *Chlamydiales* are clinically relevant as a result of their vast host range, prevalence in humans, and wide spectrum of disease in humans and other select vertebrates, such as birds, reptiles, and ruminants (Sudler, Hoelzle *et al.* 2004; Teankum, Pospischil *et al.* 2007). *Chlamydia* was first observed and recorded by Halberstaedter and von Prowazek, in 1905, as intracellular inclusions in the conjunctival samples of orangutans infected with a trachoma patient's ocular scrapings (Pospischil 2009). Originally, it was believed that these organisms were protozoa; however, they were relabelled as the "trachoma virus" when the organism was shown to be filtered and cultivatable in other animals (Grayston, Kuo *et al.* 1986). Tissue culture in the 1960s revealed that the trachoma virus was actually a type of bacteria (Grayston, Kuo *et al.* 1986). Before the advent of genetic testing, only *Chlamydia psittaci* and *Chlamydia trachomatis* were recognized under the order *Chlamydiales* and within the solitary *Chlamydiaceae* family (Everett 2000). Novel strains isolated in 1986 were serologically unique from *C. psittaci* and shown to be dissimilar to *C. trachomatis* due to their dense, round inclusion morphology in HeLa cells and the lack of glycogen within their inclusions (Grayston, Kuo *et al.* 1986; Kuo, Chen *et al.* 1986). These new isolates created a new taxonomic order and led to the reclassification of the *Chlamydiales* order into four distinct families; namely, *Chlamydiaceae*, *Simkaniaceae*, *Parachlamydiaceae*, and *Waddliaceae* (Everett, Bush et al. 1999; Rurangirwa, Dilbeck et al. 1999). Years later, TWAR strains of *Chlamydia*, isolated from TW-183 and AR-39 patients, were

designated as the third species of the *Chlamydiales* family and given the name *Chlamydia pneumoniae* (Grayston, Kuo *et al.* 1989).

The TWAR agent annotation originates from two isolated samples of *Chlamydia* in human patients. The first agent was obtained in 1965 as an unclassified *Chlamydia* strain, dubbed TW-183, from a Taiwanese child participating in a trachoma vaccine trial (Grayston 1968). After cell culture methodology was developed, TW-183 was found to form dense round inclusions more similar to *C. psittaci* than *C. trachomatis* (Kuo, Jackson *et al.* 1995). The first clinical respiratory isolate, AR-39 for acute respiratory pathogen, was obtained from a university student in Seattle with pharyngitis (Grayston, Kuo *et al.* 1986). Students in the original study had infections resembling *Mycoplasma pneumonia*; however, treatment with erythromycin proved to be ineffective (Grayston, Kuo *et al.* 1986). The acronym TWAR was applied to group the two new isolates which showed distinct morphology and sequence identity from the two known *Chlamydia* species. Also, these isolates were shown to transmit from human to human, without the aid of another animal host (Grayston, Kuo *et al.* 1986). Finally, in 1989, TWAR was established as the third species of *Chlamydia*, *C. pneumoniae*.

Even as recently as in 2009, the scientific community maintained a divergent stance on the taxonomic reorganization of the *Chlamydiaceae* family into two separate genera (Stephens, Myers *et al.* 2009). The propsed split between *Chlamydia spp.* and *Chlamydophila spp.*, in 1999, was initiated by the lack of sequence similarity between within the 16s ribosomal ribonucleic acid (rRNA) sequences of eight *Chlamydia* species (Everett, Bush *et al.* 1999). They were assembled using the principles of maximum

parsimony and neighbour joining methods (Everett, Bush *et al.* 1999). A proposed split was controversially adopted, dividing the *Chlamydiaceae* family into two separate genera, *Chlamydia* and *Chlamydophila* (Everett, Bush *et al.* 1999). Anti-reformist arguments centre around poor scientific reasoning on the part of the initial researchers, stating that the required sequence homology was set arbitrarily and is not sufficient criterion on its own to warrant change (see Figure 1.1) (Schachter, Stephens *et al.* 2001).

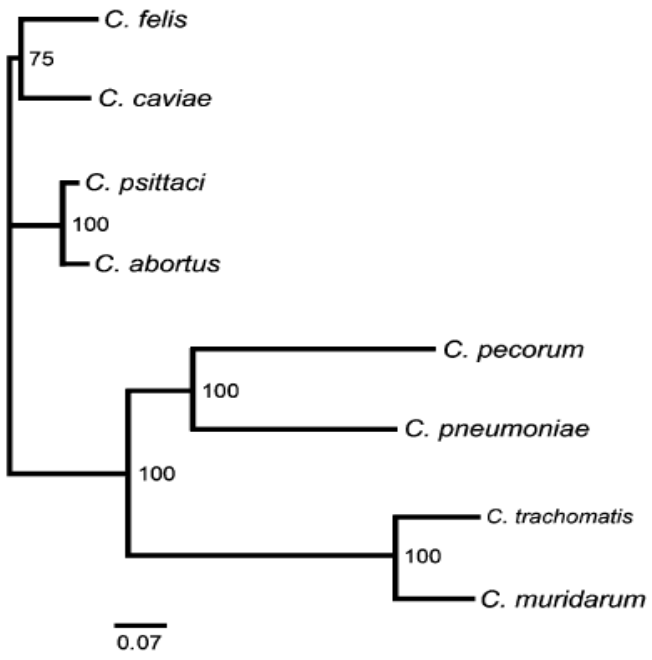

Figure 1.1 (adapted from (Stephens, Myers *et al.* 2009)) – A phylogenetic analysis of the *Chlamydiaceae* family based on the sequence of 110 concatenated genes conserved in all *Chlamydia* genomes. The sequences of *C. pneumoniae* and *C. trachomatis* may be more closely related than previously shown by Everett *et al.* (Everett, Bush *et al.* 1999). This phylogeny, developed by Stephens *et al.* argues against the separation of the two genera *Chlamydia* and *Chlamydophila*. The original proposal by Everett *et al.* set an arbitrary 16s rRNA boundary between genera at <95% and consequently grouped species based on their 16s and 23s rRNA sequence similarity. This diagram depicts the data of Stephens *et al.*, which demonstrates that a sequence comparison and realignment based on 110 concatenated genes increases the similarity between *Chlamydia* and *Chlamydophila.*

1.2 Cellular diversity and clinical epidemiology of *Chlamydia* species

There are three species of the *Chlamydiaceae* family that infect humans; however, they differ in their tissue tropism, spectrum of disease, genomic content, and morphology (Kuo, Gown *et al.* 1993). The first species, *Chlamydia trachomatis*, invades the genital and ocular mucosa of humans and is the most common reported infectious disease in the United States (Hafner, Beagley *et al.* 2008). The sequelae of disease associated with *C. trachomatis* infection consists of tubal factor infertility, ectopic pregnancy, and pelvic inflammatory disease, amongst others (Hafner, Beagley *et al.* 2008). Conversely, *C. pneumoniae* often asymptomatically infects the pharyngeal or ocular mucosal sites of humans and frequently goes undetected. One of the distinguishing features between the two species is their varying cell morphology (Wolf, Fischer *et al.* 2000). The pear-shaped structure of *C. pneumoniae* elementary bodies is a unique feature; however, it is not characteristic of all elementary bodies within the species (Popov, Shatkin *et al.* 1991; Wolf, Fischer *et al.* 2000). A loose outer membrane and large periplasmic space between the inner and outer membranes of elementary bodies has been analyzed in detail by both transmission and scanning electron microscopy (Wolf, Fischer *et al.* 2000). Regardless, the similarities between *Chlamydia* species should not be under-emphasized. The surface-exposed lipopolysaccharide is not identical within the *Chlamydia* genus, but it contains an antigenic genus-specific Kdo epitope that is often used as a marker for *Chlamydia* infection (Brade, Zych *et al.* 1997; Peterson, de la Maza *et al.* 1998). In contrast, the major outer membrane protein, one of the most abundant proteins characteristic to all *Chlamydia* membranes, is immunodominant solely in *C. trachomatis*

and is not a valid target for neutralizing antibodies in *C. pneumoniae* (Peterson, de la Maza *et al.* 1998). An interesting difference between the *Chlamydia* genus and other gram-negative bacteria is the notorious lack of peptidoglycan between the inner and outer membranes in *Chlamydia*. The "chlamydial anomaly" contends that the periplasmic space is void of this polymer, even though genes controlling the synthesis, assembly, and recycling of peptidoglycan can be found within the *Chlamydia* genome (Ghuysen and Goffin 1999). Still, *Chlamydia* remains sensitive to β-lactam antibiotics as a result of their apparent use of penicillin-binding proteins for cross-linking events to strengthen the cellular membrane (Chopra, Storey *et al.* 1998). Moulder *et al.* have hypothesized that the role of peptidoglycan may be intertwined with the division of reticulate bodies or their maturation into elementary bodies (Moulder 1993). The definitive role of peptidoglycan in *C. pneumoniae* remains to be elucidated.

With regard to its unique spectrum of disease associations, *C. pneumoniae* differs considerably from other species of *Chlamydia*. As previously mentioned, *C. trachomatis* is widely recognized as the most common sexually transmitted infection and often presents as an asymptomatic infection that progresses to pelvic inflammatory disease. Similarly, *C. pneumoniae* also presents as an asymptomatic infection. However, it is the cause of approximately 8% of all cases of "walking-pneumonia" and is associated with a wide variety of immunological-mediated pathologies such as asthma, chronic obstructive pulmonary disease (COPD), atherosclerosis, and Alzheimer's Disease (Marrie, Costain *et al.* 2012). The association between *C. pneumoniae* infection and chronic inflammatory lung diseases is well documented. In a 1999 review, nine case reports, fourteen

uncontrolled case series, and eighteen controlled studies strongly suggested that *C. pneumoniae* infection plays a role triggering wheezing and asthma exacerbations (Hahn 1999). More recently, Hahn *et al.* have shown that *C. pneumoniae*-specific IgE was correlated with asthma severity compared to controls (Hahn, Schure *et al.* 2012). A generic hypothetical model predicts that *Chlamydia* infections act as inflammation amplifiers in respiratory tract infections leading to an exacerbation of symptoms. The pathophysiological mechanism for *Chlamydia*-associated chronic airway inflammation remains unknown.

The suggested role of *C. pneumoniae* in the pathophysiology of atherosclerosis is multifaceted. The deposition of plaques in blood vessels is initiated by the formation of foam cells due to the uptake of oxidized low-density lipoprotein (LDL) by macrophages (Watson and Alp 2008). *C. pneumoniae* exposure in the lamina propria of vessels can induce the oxidation of LDL in the tunica intima leading to the uptake of LDL into foam cells (Watson and Alp 2008). Furthermore, infected endothelial cells are stimulated to secrete growth factors and cytokines that lead to the proliferation and recruitment of smooth muscle cells from the tunica media (Watson and Alp 2008). These smooth muscle cells are responsible for secreting fibrin, collagen, and proteoglycans that contribute to the formation of a fibrous cap. Lastly, the expression of matrix metalloproteinases triggered by *C. pneumoniae*-infected macrophages may precipitate plaque rupturing and thrombosis (Kol, Sukhova *et al.* 1998). Together, these mechanisms provide a possible link between the inflammatory stimulation by *C. pneumoniae* infection and the etiology of atherosclerosis.

More recently, the connection between chronic *C. pneumoniae* infection and human neuropathologies, such as Alzheimer's Disease, has become an important area of research. *C. pneumoniae* infection was initially suspected to play a role in neuroinflammatory processes as a result of its established role in the activation of inflammatory signalling. Alzheimer's Disease is commonly indicated by an increased concentration of tau protein and a decreased concentration of amyloid-β42 protein in the cerebral spinal fluid (CSF) (Paradowski, Jaremko *et al.* 2007). Paradowski *et al.* have shown that the presence of CSF *C. pneumoniae* deoxyribonucleic acid (DNA) significantly increases the occurrence of Alzheimer's Disease; however, it is not significantly related to the concentration of tau and amyloid-β42 proteins (Paradowski, Jaremko *et al.* 2007). Shima *et al.* present three separate hypotheses for the involvement of *C. pneumoniae* in the pathophysiology of Alzheimer's Disease. The infection may result in endothelial dysfunction, microglial activation, or contribute to the formation of amyloid plaques (Shima, Kuhlenbaumer *et al.* 2010). At this point, the association between *C. pneumoniae* infection and Alzheimer's Disease requires future study to support these current hypotheses.

1.3 The *Chlamydia* life cycle

There are many differences between the two most common species of *Chlamydia*, however a unique biphasic developmental cycle and greater than ninety percent 16S rRNA sequence identity are two characteristic traits to all of the species within the *Chlamydiaceae* family (Everett 2000). The intracellular life cycle of *Chlamydia* is a

complex system that involves the transition of a metabolically inactive, infectious form, known as the elementary body (EB), to a highly-replicative, metabolically active reticulate body (RB) (see Figure 1.2) (Abdelrahman and Belland 2005). The EB is the small (0.3 µm), round "spore-like" form of *Chlamydia* that is thought to maintain structural rigidity in the extracellular environment due to a high degree of cross-linking of the outer membrane complex (Wyrick 2000; Abdelrahman and Belland 2005). Histone-like proteins Hc1 and Hc2 are responsible for the highly-condensed state of nucleic acids of EBs and, consequently, an extremely compact nucleoid (Brickman, Barry *et al.* 1993). The RB is the metabolically active form of *Chlamydia* which is larger (1 µm), non-infectious, and contains a diffuse, granular-like collection of nucleic acids (Abdelrahman and Belland 2005). Electron micrographs and freeze-deep-etching have demonstrated the presence of needle-like projections organized hexagonally on the outer membrane surface of both EBs and RBs that are approximately fifty nanometres apart (Matsumoto 1982). These projections have a higher density on the surface of RBs and have been proposed to be involved in Type III Secretion (T3S), as they appear similar to T3S machinery in other gram-negative bacteria (Matsumoto 1982). An understanding of the general *Chlamydia* life cycle and T3S is essential to understanding the pathogenesis of *C. pneumoniae*.

1.3.1 The biphasic developmental cycle

The major distinguishing feature of the *Chlamydiales* order from other intracellular bacteria is their biphasic developmental cycle (see Figure 1.2). The length of the *Chlamydia* life cycle varies considerably based on the environmental conditions, host

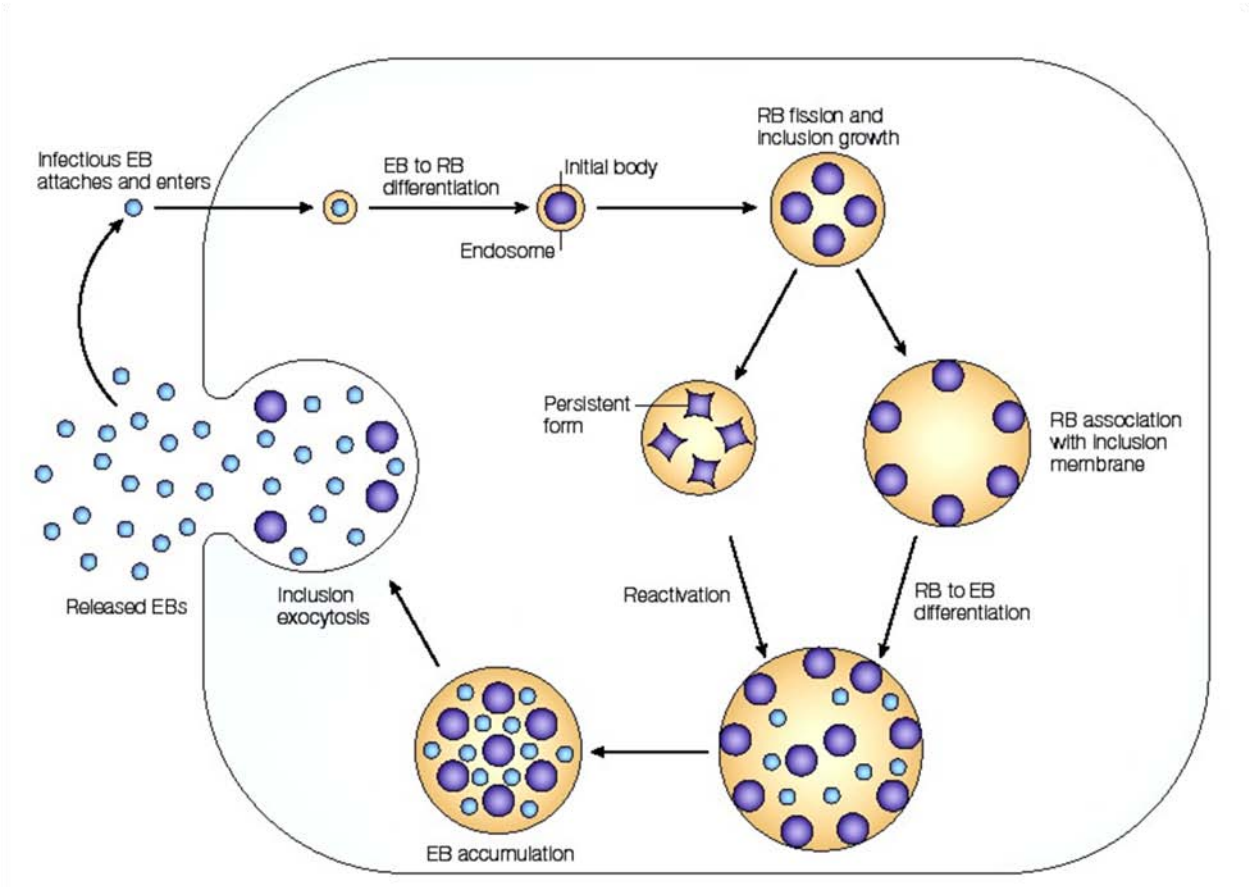

Figure 1.2 (adapted from (Simonetti, Melo *et al.* 2009) – The *Chlamydia pneumoniae* developmental cycle. The process commences with the attachment and entry of the EB (located at the top of the cycle) due to electrostatic interactions on the host cell membrane. After chromosomal decondensation in the EB, primary differentiation from the EB to an RB occurs at approximately eight hours post infection, as evident by a large, diffuse nucleoid. At about nineteen hours post infection, cell division of RBs becomes rapid. Effector proteins are secreted across the inclusion and into the host cell to prevent a host cell response and to facilitate the uptake of nutrients into the inclusion. Secondary differentiation from the RB stage to an EB takes place and at about seventy-two hours post infection, the infectious progeny are released from the host. Persistent or aberrant bodies can develop in an altered pathway through the addition of various inducers.

eukaryotic cell, and the type of strain, however it usually ranges between forty-eight and ninety-six hours (Hammerschlag 2002). The first stage of *Chlamydia* development involves the attachment of the EB to the host cell in the extracellular environment. The

exact cellular mechanism of *C. pneumoniae* attachment remains unclear, but a compilation of research using various *Chlamydia* species has been used to describe the entire developmental process. Kuo *et al.* have shown that the cleavage of N-linked oligosaccharides from the surface of *C. pneumoniae* using N-glycanase inhibited the attachment of EBs to various eukaryotic cell types (Kuo, Lee *et al.* 2004). A further investigation revealed that the mannose 6-phosphate and insulin-like growth factor 2 receptor may be the target for *C. pneumoniae* attachment (Puolakkainen, Lee *et al.* 2008). This work suggested that the initial attachment of EBs to the eukaryotic cell requires reversible electrostatic interactions between heparan sulfate-containing glycosaminoglycans on the cellular surface. Research by Su *et al.* also supports this theory, stating that a recombinant major outer membrane protein (MOMP) of *C. trachomatis* was able to competitively inhibit *Chlamydia* attachment (Su, Raymond *et al.* 1996). Furthermore, treatment with N-glycanase resulted in a lack of *Chlamydia* attachment and blocked the interaction between the eukaryotic cell and the MOMP (Su, Raymond *et al.* 1996). An irreversible binding step follows involving thiol-disulfide reactions and protein disulfide isomerase, although the exact mechanism is still poorly understood (Su, Raymond *et al.* 1996). The subsequent step in EB attachment comprises the insertion of *Chlamydia* effector proteins and internalization of the EB into the host cytoplasm. The irreversible binding of EBs to the host cell membrane is followed by the recruitment of actin to the site of attachment, the development of an actin-rich pedestal formation, and bacterial internalization (Clifton, Fields *et al.* 2004). In addition to the polymerization of the actin cytoskeleton, the activation of the MEK/ERK, PI3K, and Akt

pathways within the host cell was essential to the invasion of *C. pneumoniae* in Hep2 cells (Coombes and Mahony 2002). Clifton *et al.* have shown that the translocated actin-recruiting phosphoprotein (TARP) is delivered into the host cell immediately after the secondary attachment step and helps recruit actin to the site of attachment (Clifton, Fields *et al.* 2004). In the same study, fluorescently labelled TARP was found within the *Chlamydia* cytoplasm before cellular interactions occurred, hinting at a pre-existing functional secretion mechanism in the EB (Clifton, Fields *et al.* 2004). The authors inferred a link between TARP localization and T3S, indicating that functional T3S machinery exists prior to EB differentiation and that it may be essential for attachment and entry.

There are multiple proposed models explaining the internalization of EBs into the host. Byrne and Moulder first described a "parasite-specific" phagocytosis in 1978 to explain the host-parasite interaction and the presence of structures on the surface of both cells that aid in the internalization process (Byrne and Moulder 1978). Attenuation of *Chlamydia* phagocytosis was accomplished by protein ligand denaturation or degradation of host cell surface proteins, however none of the proteins involved were identified (Byrne and Moulder 1978). More recently, both clathrin-dependent and clathrin-independent mechanisms for *C. trachomatis* endocytosis have been proposed within caveolae-like lipid rafts in the host cell membrane (Stuart, Webley *et al.* 2003). In these cases, the addition of antibiotics which disrupt lipid function, such as Nystatin and Filipin, prevented the entry of *C. trachomatis* into eukaryotic HeLa cells (Stuart, Webley *et al.* 2003). Conversely, with the use of cholesterol-chelating agents, antibiotics, and

antibody-mediated “patching”, Gabel *et al.* have argued that lipid raft-mediated entry was not required for infection by *C. trachomatis* (Gabel, Elwell *et al.* 2004). Instead, unidentified pleiotropic effects of cholesterol depletion in the membrane were held accountable for the disruption of membrane processes and the failed bacterial entry (Gabel, Elwell *et al.* 2004). Ultimately, more research is required to reveal the true mechanism of *Chlamydia* internalization.

After endocytosis of the EB, *Chlamydia* endosomes fuse and compartmentalize within an altered membrane-bound vacuole known as an inclusion. Inclusion membrane proteins (Inc), which are not conserved between *Chlamydia* species, are known to contain a large bi-lobed hydrophobic region which commonly embeds itself in the inclusion membrane (Bannantine, Griffiths *et al.* 2000). These proteins are predicted to interact with host machinery including vesicle trafficking, inclusion development, the acquisition of nutrients, and EB reorganization (Fields and Hackstadt 2002). Modifications to the inclusion permit its deviation from the host endosomal pathway, allow entry into the host exocytic pathway, and enable its fusion with vesicles carrying lipids destined for membrane insertion (Wyrick 2000). Wolf and Hackstadt provided evidence for pathway deviation, showing that inclusion membranes lacked two ubiquitous endosomal markers, LAMP-1 and CI-M6PR (Wolf and Hackstadt 2001). In addition, the incorporation of fluorescent ceramide analogs demonstrated that sphingomyelin was rapidly incorporated into the inclusion membrane once fusion between sphingomyelin containing vesicles and the inclusion occurred (Wolf and Hackstadt 2001; Fields and Hackstadt 2002). Together, these changes encourage the survival and expansion of the inclusion body within the host

cell in order to support the differentiation and division of EBs and RBs in the intracellular milieu.

Within the internalized EB, chromosome decondensation occurs and the genome becomes highly transcriptionally active as a result of significant quantities of carryover messenger RNA (mRNA) and ribosomes (Abdelrahman and Belland 2005). The translation of immediate early genes occurs as soon as fifteen minutes post infection (Abdelrahman and Belland 2005). At approximately eight hours post infection, the EB undergoes primary differentiation into RBs, which is characterized by the appearance of a diffuse, larger nucleoid (Wolf, Fischer *et al.* 2000). This growth and developmental process is mediated by *de novo* protein synthesis which can be demonstrated with the addition of macrolide antibiotics and their subsequent inhibition of transcription and translation (Scidmore, Rockey *et al.* 1996). Multiplication and division of RBs by binary fission occurs at approximately nineteen hours post infection and between twenty-four and thirty-six hours post infection, the inclusion contains only RBs (Wolf, Fischer *et al.* 2000). At this point in the developmental cycle, RBs are extremely reliant on the host cell for sources of nutrients including iron, amino acids, and adenosine triphosphate (ATP) (Hogan, Mathews *et al.* 2004). Following cellular division, the process of secondary differentiation commences, transforming RBs into EBs. The presence of an intermediate form known as an intermediate body (IB) is detected at this point in development. The detachment of RBs from the inclusion membrane is suspected to trigger secondary differentiation. Wilson *et al.* determined by live-cell imaging that the dissociation of RBs from the inclusion membrane is related to their increased movement

within the inclusion and their secondary development (Wilson, Whittum-Hudson *et al.* 2009). Based on the contact-dependent model, separation of the T3S needle apparatus from the inclusion membrane is critical for RB to EB progression; however, this hypothesis lacks experimental evidence (Bavoil, Hsia *et al.* 2000). Finally, as shown in electron micrographs by Hybiske and Stephens, EBs are released into the extracellular space by a sequential destruction of the inclusion and cellular membranes, known as host cell lysis, or a controlled release of a portion of the inclusion called extrusion (Hybiske and Stephens 2007).

1.3.2 Nutrient acquisition and immune evasion

Chlamydiae undergo differentiation and replication within a parasitophorous, non-acidified vacuole, termed an inclusion. The inclusion milieu provides optimal conditions that are capable of supporting the growth and development of EBs and RBs within a host cell environment. For example, *Chlamydiae* avoid fusion with lysomes and endocytic vesicles as classical early endocytic markers are not present in the inclusion at five minutes post infection (Scidmore, Fischer *et al.* 2003). Hackstadt *et al.* have shown that the inclusion fuses with Golgi-derived vesicles using fluorescent ceramide analogues and thin-layer chromatography (Hackstadt, Rockey *et al.* 1996). Plasma membrane proteins are also incorporated into the inclusion membrane in the presence of cyclohexamide, signifying a lack of requirement for *de novo* eukaryotic protein synthesis (Ripa and Mardh 1977). After ten hours post infection, certain species of *Chlamydia*, excluding *C. pneumoniae*, are capable of fusing to form one large vesicle. The homotypic fusion

process is possible due to the presence of inclusion membrane protein A (IncA) and does not occur in the absence of antibody-targeted inhibition of IncA (Hackstadt, Scidmore-Carlson *et al.* 1999). The trafficking of lipids from golgi-derived vesicles into the inclusion membrane and the ability to fuse with other inclusions provides the resources to expand the parsitophorous vacuole and support *Chlamydia* survival.

Resembling most intracellular pathogens, *Chlamydia* must acquire host-derived nutrients to promote growth, survival, and proliferation inside the host cell. The inclusion membrane permits the diffusion of ions freely across the inclusion. However, molecules larger than 520 Daltons do not passively diffuse through the barrier (Heinzen and Hackstadt 1997). Adenosine triphosphate (ATP), as an example, is recruited into the inclusion and exchanged for adenosine diphosphate (ADP) by two ATP/ADP translocases that are expressed early in the *Chlamydia* life cycle (Shaw, Dooley *et al.* 2000). Beginning at approximately two hours post infection, sphingomyelin and cholesterol are sequestered by the growing inclusion through golgi-derived vesicles (Carabeo, Mead *et al.* 2003). In contrast, host-derived glycerophospholipids are delivered to the inclusion through a non-golgi, cPLA2-activated pathway where phospholipids are modified with the exchange of *Chlamydia*-derived fatty acids (Wylie, Hatch *et al.* 1997; Su, McClarty *et al.* 2004). Su *et al.* have indicated that the activation of the cPLA2 and MAPK pathway may both be involved in the recruitment of glycerophospholipids to the inclusion (Su, McClarty *et al.* 2004). Finally, iron acquisition by the *Chlamydia* inclusion may also be essential, as transferrin receptor expression is decreased in HeLa-229 cells upon *C.*

trachomatis infection (Vardhan, Bhengraj *et al.* 2009). However, mechanisms of iron delivery across the inclusion membrane have yet to be clarified.

Chlamydia must also be capable of evading host immune responses to thrive within the host cytosol. Both CD4+ and CD8+ Th1 responses are capable of detecting *Chlamydia* infections and initiating appropriate cell-mediated immune responses (Loomis and Starnbach 2002). The secreted protein Chlamydial protease-like activity factor (CPAF) is believed to cleave multiple host transcription factors, such as USF1 and RXF5, involved in the expression of major histocompatability complex (MHC) class I and II molecules (Peschel, Kernschmidt *et al.* 2010). This cleavage prevents the presentation of *Chlamydia*-specific antigens on the cell surface. Cytokine production is also affected by *Chlamydia* infection, as IL-8, IL-6, and GM-CSF expression are all increased in a pro-inflammatory response that may aid bacterial dissemination (Fields and Hackstadt 2002). This evidence supports a role for *Chlamydia* in inducing a generic pro-inflammatory response that is linked to a variety of pathologies mentioned previously.

1.3.3 Intracellular persistence

In the medical community, it has long been proposed that *Chlamydia* is capable of causing chronic asymptomatic infection within a human host. *Chlamydia* persistence has been defined by Abdelrahman and Belland as a long-term association between viable, nonculturable *Chlamydia* and its host cell (Abdelrahman and Belland 2005). *In vitro* experiments have shown that *Chlamydia* can exist in a persistent state that results from a modified or suspended developmental cycle at the RB stage (Abdelrahman and Belland

2005). For example, the application of Penicillin triggers the development of persistence by halting binary fission, creating large abnormal RBs, preventing secondary differentiation into EBs, and expelling small empty vesicles from the inclusion (Matsumoto and Manire 1970). The transcription profile changes to decrease cell division and peptide transport processes and increase general stress response and phospholipid metabolism mechanisms (Klos, Thalmann *et al.* 2009). In addition to antibiotic exposure, there are currently multiple *in vitro* conditions which result in the development of *Chlamydia* persistence including iron deficiency, amino acid deficiency, interferon gamma exposure, phage infection, monocyte infection, and heat shock (Hogan, Mathews *et al.* 2004). Specifically in *C. pneumoniae*, persistence has been observed with exposure to interferon gamma, which induces the enzyme indolemaine-2,3-dioxygenase (IDO) and depletes the intracellular supply of tryptophan (Pantoja, Miller *et al.* 2001). The creation of infectious progeny is limited by tryptophan starvation resulting from a high concentration of IFN-γ (Pantoja, Miller *et al.* 2001). Tryptophan starvation is also responsible for the creation of pleomorphic aberrant bodies and atypical inclusions which are generally smaller in diameter and contain less bacteria (Pantoja, Miller *et al.* 2001). A recovery of normal RB development and a reversal of persistence are possible when tryptophan supplementation is provided to the host cells in culture (Pantoja, Miller *et al.* 2001). It is currently unclear how accurate these *in vitro* models are of events that occur *in vivo*.

Most intracellular bacteria require an influx of iron from the host cell for use in DNA synthesis, electron transport, and, ultimately, to support their own growth. Sullivan and

Weinberg proposed that excess iron is a requirement for the establishment of *C. pneumoniae* infection in coronary arteries (Sullivan and Weinberg 1999). Iron-uptake systems exist within the genomes of most intracellular bacteria to facilitate the transport of iron from the host cell cytoplasm. Many homologous genes and proteins from other bacteria that are regulated by iron have been identified in the *Chlamydia* genome (Al-Younes, Rudel *et al.* 2001). Al-Younes *et al.* reported that a restriction in the amount of available iron to *C. pneumoniae* infected cells caused the creation of smaller inclusions and a delay in the developmental cycle (Al-Younes, Rudel *et al.* 2001). Further research by Wehrl *et al.* has shown that a large aberrant body and *Chlamydia* persistence can be induced with the addition of the iron chelator deferoxamine mesylate (DAM) (Wehrl, Meyer *et al.* 2004). Once again, the growth cycle can be reactivated with the removal of the chelator (Wehrl, Meyer *et al.* 2004). Whether any of these changes to the developmental cycle are operating *in vivo* has yet to be determined.

1.3.4 *Chlamydia* genetics

The ability to genetically manipulate prokaryotic organisms has greatly enhanced the research into novel biological processes and the invention of new therapeutic strategies to block these pathways. Until recently, the major issue when studying *Chlamydia* has been the lack of a successful technique for modifying the genomic structure of *Chlamydia* DNA (Heuer, Kneip *et al.* 2007). Multiple reasons, such as the intracellular lifestyle, metabolic inactivity of EBs, and development of persistant bodies, have been postulated to account for this genetic intractability. The intracellular habitat of

RBs implies that the transformation of exogenous DNA into the RB must travel through four membranes (namely, the cell membrane, inclusion membrane, and inner and outer membranes of the RB), which make plasmid uptake very difficult. Likewise, EBs are fairly resistant to standard methods of transformation due to their highly-crosslinked, extremely impermeable, spore-like cell wall (Heuer, Kneip *et al.* 2007). Tam *et al.* were able to successfully overcome this impediment and introduce the pPBW100 plasmid into EBs of *C. trachomatis* using electroporation and an extremely high concentration of plasmid (Tam, Davis *et al.* 1994). These authors hypothesized that in order to stably express vector transcripts, it may be necessary for the EB to undergo metabolic activation and chromosomal decondensation inside a host eukaryotic cell. Unfortunately, even though the vector was able to introduce antibiotic resistance in the initial passage, the antibiotic resistance marker was only transiently expressed and the inserted vector was unstable after four passages (Tam, Davis *et al.* 1994). Tam *et al.* propose that the exogenous plasmid may have been incompatible with the endogenous pCTE1 plasmid. In addition, the sensitivity of RBs to environmental change and their rapid transformation into persistent aberrant bodies may have also impeded the survival of transformants (Heuer, Kneip *et al.* 2007). Clearly, this combination of challenging circumstances in the developmental cycle has made studying biological pathways in *Chlamydia* difficult.

Recently, Clarke *et al.* published the first evidence of a functional transformation system for *C. trachomatis* using antibiotic resistance markers, fluorescent reporters, and iodine staining. Penicillin resistance is an excellent marker for isolating transformants due to the antibiotic's bacteriostatic effect on *Chlamydia* growth. In his method, a shuttle

plasmid carrying a β-lactamase gene, pBR325:L2, rescued transformed *C. trachomatis* from penicillin-arrested growth (Wang, Kahane *et al.* 2011). A second reporter gene, encoding green fluorescent protein (GFP), was ligated to the pL2 vector to demonstrate the general application of this technique. The resultant pGFP:SW2 vector successfully yielded penicillin-resistant strains that had green fluorescent inclusions. Furthermore, this vector was also capable of restoring glycogen synthesis in a plasmid-free strain of *C. trachomatis* as displayed by iodine staining (Wang, Kahane *et al.* 2011). The ability of the pGFP:SW2 vector to create green fluorescent stained inclusions and restore glycogen staining phenotypes confirmed the plasmid-dependent expression of recombinant proteins *in vivo* (Wang, Kahane *et al.* 2011). As a result, this technique may be useful for increasing our understanding of the roles of various *Chlamydia* proteins.

1.4 Bacterial phosphorylation systems

Intracellular phosphorylation is a crucial form of post-translational modification that is common to many cellular organisms and integral to signal transduction pathways. Bacterial phosphorylation signalling is involved in several cell processes including virulence, chemotaxis, nitrogen assimilation, protein expression, cellular localization, and sporulation (Bourret, Borkovich *et al.* 1991). Stock *et al.*, have suggested that *E.coli* have approximately thirty histidine kinases and over one hundred phosphorylated proteins (Stock, Robinson *et al.* 2000; Ge and Shan 2011). The transfer of a high-energy phosphate group from one protein to another is a reversible covalent protein modification involved in signal transduction and protein recruitment and has been investigated in

human cells since the early 1950s. The first published enzymatic protein phosphorylation event in 1954, by *Burnett and Kennedy*, identified the transfer of phosphate to a serine residue on the protein casein from the mitochondrial samples of Ehrlich ascites tumors (Burnett and Kennedy 1954). Using radiolabelled ATP, the authors surmised that casein acts as a model substrate for the protein phosphokinase of the liver (Burnett and Kennedy 1954). The first evidence of protein kinase signalling was identified in 1978 in *Salmonella typhimurium* using the *in vivo* incorporation of radiolabelled phosphate and thin-layer chromatography (Wang and Koshland 1978). Over the last thirty years, hundreds of prokaryotic protein kinases have been well characterized.

The transfer of a phosphate group to another protein is catalyzed by protein kinases. Protein kinases strip the gamma phosphate from a nucleoside triphosphate (such as ATP) using enzymatic hydrolysis and facilitate esterification by creating a covalent bond between phosphate and an adjacent protein substrate. The formation of a protein-phosphate bond is fuelled by the exergonic release (ΔG= -36.8 kJ/mol) of a high-energy γ-phosphate molecule from ATP. The five subclasses of protein kinases (cAMP-dependent, cGMP-dependent, Ca^{2+}- dependent, RNA-dependent, and non-specific protein kinases) represent the majority of protein kinases found in both eukaryotic and prokaryotic cells and generally fall into three broad systems (Krebs and Beavo 1979). In prokaryotes, the most common protein kinase-mediated signalling networks create covalently bonded *N*-phosphoramidates, phosphate anhydrides, or *O*-phosphomonoesters on specific amino acids (Cozzone 1988). *N*-phosphoramidates are created in the phosphorylation of basic amino acids (such as arginine, histidine, and lysine) by a protein

kinase. These covalent amide post-translational modifications are commonly found in two-component signal transduction pathways, such as the autophosphorylation of histidine kinases on histidine residues. Phosphate anhydrides are also formed in two-component signalling when a phosphate is covalently bound to an acidic amino acid (such as aspartic or glutamic acid). In this instance, a phosphate molecule is transferred from the histidine kinase to a conserved aspartic acid residue in a regulatory region of the substrate. *O*-phosphomonoesters are covalent esters formed with the phosphorylation of hydroxyamino acids (such as serine, threonine, or tyrosine), often by serine/threonine kinases.

Eukaryotic-like serine/threonine and tyrosine protein kinases (STPK and TPK) are a prominent family of prokaryotic proteins involved in signal transduction. The first prokaryotic STPK, Pkn1, was identified in the species *Myxoccocus xanthus* and was shown to autophosphorylate serine residues in autoradiographs with radiolabelled ATP (Munoz-Dorado, Inouye *et al.* 1993). Initially, these prokaryotic protein kinases were classified as 'eukaryotic-like' due to their structural similarities to eukaryotic kinases (twelve Hanks domains) which form part of the active site for phosphorylation (Hanks, Quinn *et al.* 1988). Genomic sequencing-based investigations have disputed their classification and reorganized their taxonomy based on sequence alignment and phylogeny (Tyagi, Anamika *et al.* 2010). Recent studies in *Pseudomonas aeruginosa* have reported that Gram-negative bacterial virulence mechanisms are regulated by serine/threonine phosphorylation (Mougous, Gifford *et al.* 2007). For example, Mougous *et al.* discovered a STPK, PpkA, and a corresponding phosphatase, which phosphorylated

the forkhead-associated (FHA) domain of a type VI secretion component, Fha1 (Mougous, Gifford *et al.* 2007). The phosphorylation state of the Fha1 protein regulated the secretion of effector proteins, such as Hcp1 (Mougous, Gifford *et al.* 2007). This study provided the first evidence of phosphorylation events directly involved in bacterial secretion.

In addition to protein kinases and phosphorylated substrates, phosphate-binding proteins are important components associated with the modulation and regulation of signal transduction pathways. There are a variety of protein domains which interact and dock with phosphorylated residues. For instance, the FHA domain, first referenced in 1995, consists of approximately eighty to one hundred amino acids folded into a sandwich of eleven β-strands (Sadowski, Stone *et al.* 1986). This domain is found in at least 700 eukaryotic and over 500 prokaryotic proteins and is believed to act as a phospho-threonine/serine recognition domain involved in DNA repair, vesicular transport, protein stability, and various signalling pathways (Liang and Van Doren 2008; Pennell, Westcott *et al.* 2010). Furthermore, conserved residues between the β-sheets, such as arginine of the 3-4 loop, serine of the 4-5 loop, and asparagine of the 6-7 loop, are involved in bridging the phosphate, stabilizing the binding site, and hydrogen bonding to the peptide ligand (Liang and Van Doren 2008). Amongst other phosphate-binding domains, FHA domains play a crucial role in signal transduction.

1.5 Evidence of phosphorylation events in *Chlamydia*

Chlamydia spp. contain several phosphorylated proteins that may be involved in amino acid metabolism, folate biosynthesis, cell division, carbohydrate transport, and virulence mechanisms. Phosphorylated proteins and kinases can been classified into three generic mechanisms; namely, the two-component, STPK, and PEP-dependent phosphotransferase (PTS) systems (Koo and Stephens 2003). In 2003, Koo and Stephens provided the first evidence of a two-component signalling system in *Chlamydia* (Koo and Stephens 2003). CtcB, a sensor kinase, is autophosphorylated in the presence of divalent cations and transfers its phosphate molecule to its response regulator, CtcC, which is likely responsible for transcriptional regulation (Koo and Stephens 2003). Secondly, in addition to the two-component regulatory system, PTS is another major prokaryotic signalling mechanism that uses phosphorylation modifications. A large number of orthologous PTS-associated proteins have been identified in *Chlamydia*, such as PtsH, PtsI, and PtsN, which are predicted to be responsible for bacterial carbohydrate transport. Currently, little is known about these *Chlamydia* proteins. Thirdly, two STPKs were characterized in *C. trachomatis* in 2003 by Verma and Maurelli (Verma and Maurelli 2003). Pkn1 and PknD are hypothetical STPKs that were capable of autophosphorylation and contain twelve conserved Hanks domains and corresponding residues typical of eukaryotic STPK. More specifically, these two STPKs contain a GxGxxGxV motif in domain I, lysine residue in domain II, glutamic acid residue in domain III, and an arginine residue in domain XI which are highly conserved regions involved in anchoring the α and β phosphate molecules of ATP, the catalytic loop region, and the substrate binding site.

These two putative kinases were capable of phosphorylating maltose binding protein (MBP), a model substrate for eukaryotic STPK (Verma and Maurelli 2003). In 2007, the Mahony laboratory demonstrated that the functional ortholog of PknD in *C. pneumoniae, Cpn0095*, was capable of phosphorylating the FHA domains of a T3SS component, CdsD (Johnson and Mahony 2007). More specifically, PknD phosphorylated both serine and tyrosine residues in the FHA2 domain of CdsD making it the first dual-specificity STPK identified in prokaryotes (Johnson and Mahony 2007). These studies provide a link between phosphorylation events by STPK and the T3S system in *Chlamydia*.

1.6 Bacterial secretion systems

Gram-negative bacteria utilize a wide range of mechanisms for exporting proteins across the inner and outer membranes. There are currently six known groups of bacterial protein secretion pathways which are used for a variety of cellular functions including nutrient acquisition, organelle biogenesis, and virulence (Thanabalu, Koronakis *et al.* 1998). Essentially, all of these secretion systems transport proteins across the outer membrane where they are either expelled into the extracellular environment or remain attached to the outer membrane. Most of the systems require energy in the form of ATP to transport large proteins through the membrane and most proteins require chaperones to prevent premature folding in the cytoplasm. A basic description of the six general secretion types is important to understand the survival and pathogenesis of *Chlamydia* (see Figure 1.3).

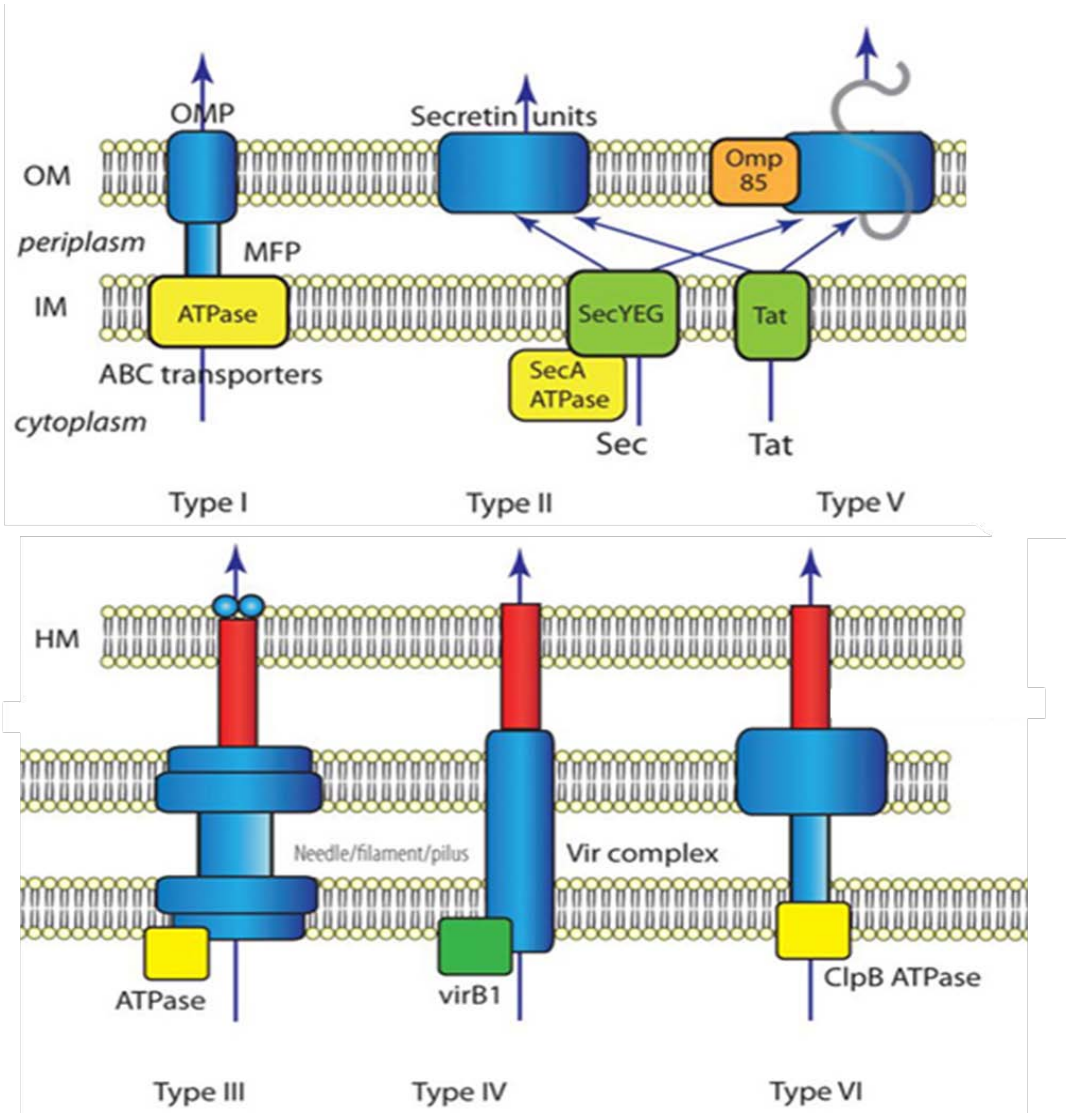

Figure 1.3 (adapted from (Tseng, Tyler *et al.* 2009)) – The six types of Gram-negative bacterial secretion systems. A conceptual schematic diagram which displays the general signalling components of each Gram-negative bacterial secretion system. Type I, II, IV, and V secretion are dependent on the SEC pathway for delivering proteins into the periplasmic space. Type III secretion is SEC independent and forms a complex of approximately twenty proteins spanning the inner and outer membranes. Type III, IV, V, and VI secretion are all contact dependent secretion mechanisms. Type VI secretion is similar in structure to that of phage T4 in its base plate formation and contact-dependent separation of the needle-tip complex. (HM=Host membrane; IM=inner membrane; OM=outer membrane; OMP=outer membrane protein; MFP=membrane fusion protein; Tat=twin arginine translocation)

Type I secretion uses an ATP-binding cassette (ABC) transporter, membrane fusion protein, and an outer membrane protein channel, exemplified by TolC, which spans both the inner and outer membrane in gram-negative bacteria (Thanabalu, Koronakis *et al.* 1998). This system is used primarily to secrete toxins, proteases, and lipases in a variety of gram-negative bacteria, such as the α-hemolysin secretion system produced by *Escherichia coli* (Desvaux, Parham *et al.* 2004). The ABC transporter hydrolyzes ATP in order to provide energy to fuel the translocation event and the type I secretion pathway secretes proteins directly across the periplasm usually without any intermediate proteins (Thanabalu, Koronakis *et al.* 1998; Desvaux, Parham *et al.* 2004). Although the localization of the substrate to the inner membrane transporter is secretion (Sec) protein independent, Sec signalling is involved occasionally in facilitating the translocation of proteins across the outer membrane (Desvaux, Parham *et al.* 2004).

Type II secretion operates in a combination of two steps and is responsible for the secretion of extracellular enzymes and bacterial toxins (Thanabalu, Koronakis *et al.* 1998). First, the substrate protein is secreted by a translocase either in the secretin pathway, the twin arginine translocation (TAT) pathway, or the Sec-dependent pathway (Desvaux, Parham *et al.* 2004). Once in the periplasm, the signal sequence is cleaved and the protein is prepared for export (Thanabalu, Koronakis *et al.* 1998). Second, an outer membrane complex composed of twelve to sixteen accessory proteins, known as the secretin, is responsible for protein translocation across the outer membrane (Thanabalu, Koronakis *et al.* 1998).

Similar to type I and II secretion systems, the inner membrane translocation of type IV secretion is Sec dependent (Desvaux, Parham *et al.* 2004). This is a pilus-based system which exports multi-subunit bacterial toxins, such as the pertussis toxin, nucleoprotein DNA conjugation intermediates, and monomeric proteins into the extracellular environment or another cell (Thanabalu, Koronakis *et al.* 1998; Desvaux, Parham *et al.* 2004). Like T3S, this system can be contact-dependent which helps initiate bacterial survival and growth at the expense of another cell (Hayes, Aoki *et al.* 2010). The general structure of this pathway is composed of a Type IV coupling protein located at the entrance to the secretion channel, a secretion channel which enables the movement of the substrate, and cell surface adhesins or pili that mediate cellular interactions (Hayes, Aoki *et al.* 2010). This system is clinically significant for its role in exotoxin delivery and the facilitative horizontal transfer of antibiotic resistance genes (Hayes, Aoki *et al.* 2010).

The Type V secretion system is the largest family of all systems and is typically composed of either one protein, an autotransporter, or two proteins, known as two-partner secretion (Desvaux, Parham *et al.* 2004). Secreted proteins first require either the use of the Sec pathway or signal-recognition particle pathway to shuttle into the periplasm (Desvaux, Parham *et al.* 2004). The autotransporters contain an internal β-barrel structure which forms a hole in the outer membrane known as a porin (Desvaux, Parham *et al.* 2004). The porin enables the translocation of the remaining protein into the extracellular space where it undergoes proteolytic cleavage and becomes activated (Hayes, Aoki *et al.* 2010).

The Type VI secretion system is very similar to T3S because it involves the formation of a multisubunit complex, is a contact-dependent mechanism, and is a Sec independent pathway (Desvaux, Parham *et al.* 2004; Hayes, Aoki *et al.* 2010). The mechanism seems to be structurally similar to that of a phage because it contains a cell-puncturing device and baseplate similar to that of phage T4 (Hayes, Aoki *et al.* 2010). This recently identified mechanism of secretion is regulated by a threonine phosphorylation signalling cascade which is essential for signalling events during secretion (Bingle, Bailey *et al.* 2008). Mougous *et al.* have reported that PpkA, a serine threonine kinase, is responsible for the post-transcriptional phosphorylation of Fha1 and is thought to trigger type VI secretion (Mougous, Gifford *et al.* 2007).

1.7 Type III secretion in Gram-negative bacteria

The T3S apparatus is composed of a complex of about twenty proteins that extends from the bacterial cytoplasm, reaches across both the inner and outer membrane, and attaches directly to the eukaryotic cell membrane (see Figure 1.4) (Thanabalu, Koronakis *et al.* 1998). Type III secretion is Sec independent and is primarily used to secrete anti-host effector proteins into the cytosol of target eukaryotic cells (Thanabalu, Koronakis *et al.* 1998). One of the important features of the T3S 'injectisome' is that it creates a direct route from the bacterial cytoplasm to the eukaryotic cytoplasm allowing the secretion of effector proteins into host cells (Desvaux, Parham *et al.* 2004). These effector proteins aid in the pathogenicity of the bacteria by diverting host cell immune responses and supporting the survival of the bacteria (Desvaux, Parham *et al.* 2004). The

basal body, located at the base of the injectisome, is believed to contain several proteins involved in needle formation, ATP hydrolysis, and effector/chaperone recruitment (Thanabalu, Koronakis *et al*. 1998). The completed basal body complex resembles the shape of a needle syringe and is segmented into an outer membrane ring

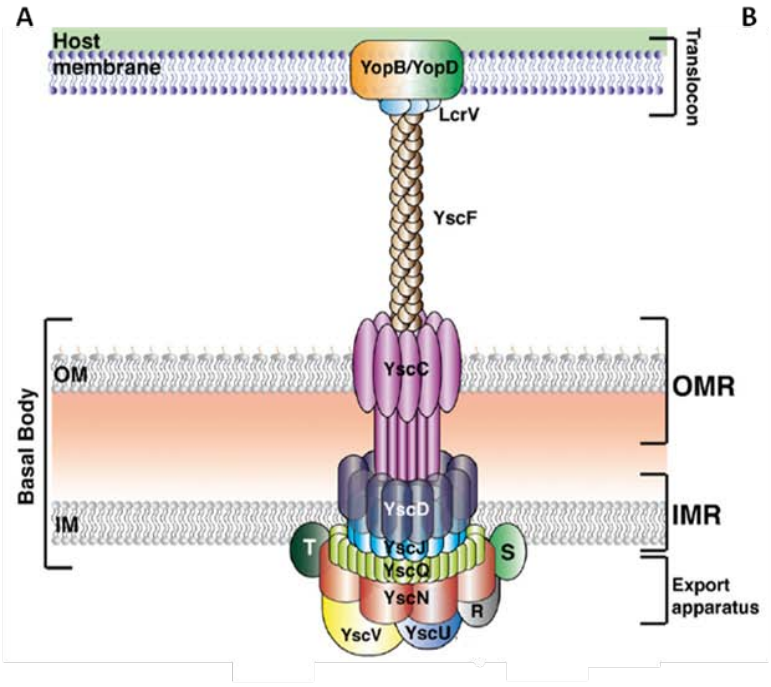

B

Yersinia	*Salmonella*	*Shigella*
YopB	SipB	IpaB
YopD	SipC	IpaC
YscF	PrgI	MxiH
YscC	InvG	MxiD
YscD	PrgH	MxiG
YscJ	PrgK	MxiJ
YscQ	SpaO	Spa33
YscN	InvC	Spa47
YscV	InvA	MxiA
YscU	SpaS	Spa40
YscR	SpaP	Spa24
YscS	SpaQ	Spa9
YscT	SpaR	Spa29

Figure 1.4 (adapted from (Izore, Job *et al.* 2011)) - A generic diagram of the T3S apparatus in Gram-negative bacteria. (A) The hypothetical structure of the *Yersinia* T3S apparatus displays fourteen distinct proteins inserted in the inner membrane (IM), outer membrane (OM) and host cell membrane. The translocator proteins (YopB/YopD) and needle-tip protein (LcrV) comprise the translocon located in the host cell membrane. The filament protein (YscF) is located in the extracellular space and connects the translocon to the basal body apparatus. The basal body apparatus is composed of a variety of proteins in the outer and inner membranes, including components of the C-ring export apparatus. (OMR=outer membrane ring; IMR=inner membrane ring) **(B)** A table presenting the annotation of orthologous T3S-associated proteins(read horizontally) in the *Yersinia* (Ysc), *Salmonella* (SPI-1), and *Shigella* (Mxi/Spa) injectisomes. Within these protein families, sequence similarity and functional orthology has been demonstrated in a variety of studies in these three systems. A more detailed list of the T3S-associated components annotation can be found in Appendix A.

(secretin), inner membrane ring, and export apparatus (cytoplasmic (C)-ring) (Thanabalu, Koronakis *et al.* 1998).

1.7.1 Basal body components of the IMR and OMR

Proteins in the basal body are believed to anchor the structural and functional components of the injectisome. Since Chlamydia have not been genetically manipulated, models of the basal body in Chlamydia have been proposed based on structural orthology to T3S apparatuses in *Yersinia, Salmonella, Shigella* and *Escherichia.* The IMR is composed of approximately seven proteins that are thought to stabilize proteins in the C-ring export apparatus at the base of the injectisome and anchor OMR and needle filament components in the periplasm. As a result, seven IM proteins are expected to interact with a wide range of T3S-associated components.

Studies describing two proteins in the IMR of *Yersinia,* YscD and YscJ, suggest that IM components are essential for T3S apparatus assembly. First, using recombinant immunofluorescent proteins, Diepold *et al.* demonstrated that EGFP-YscD is inserted into the inner membrane following the insertion of only the outer membrane secretin (Diepold, Amstutz *et al.* 2010). Next, the co-purification of YscD with YscC and YscJ and the lack of co-purification in the absence of YscC suggested that YscD required only YscC to insert into the inner membrane (Diepold, Amstutz *et al.* 2010). These authors hypothesize that YscD creates a bridge between the inner and outer membranes in the T3S apparatus. The recombinant lipoprotein EGFP-YscJ may then be incorporated into the inner membrane, where it is believed to form a oligomeric ring with an amino (N)-

terminal lipid-binding region and a C-terminal transmembrane region (Silva-Herzog, Ferracci *et al.* 2008). As two of the initial proteins inserted into the membrane, YscD and YscJ may be crucial for the recruitment of other IMR or C-ring components to the membrane.

The remainder of the inner membrane proteins in the IMR are mostly hydrophobic possibly due to the high number of predicted transmembrane regions. The only hydrophobic component of this IMR studied extensively is YscU, an autoproteolytic protein which is required to aid in the secretion of effectors by the T3S apparatus (Bjornfot, Lavander *et al.* 2009). Lavander *et al.* have shown that YscU may mimic the function of its flagellar homolog FlhB by increasing effector secretion at low concentrations and decreasing secretion at higher levels (Lavander, Sundberg *et al.* 2002). As a result of these findings, these authors hypothesize that YscU plays a substrate switching role in the inner membrane at the base of the T3S apparatus. A more recent study by Diepold *et al.*, suggests that YscU requires the oligomerization and shuttling of YscV in order to insert into the inner membrane (Diepold, Wiesand *et al.* 2011). The result of a large compilation of co-immunoprecipitations amongst YscV, YscU, YscR, YscS, and YscT provided evidence that a platform of three proteins inserts into the membrane independently of the YscC and YscD proteins (Diepold, Wiesand *et al.* 2011). These three inner membrane proteins (YscR, YscS, and YscT) aid in the oligomerization of YscV and the subsequent recruitment of YscU to the base of the platform (Diepold, Wiesand *et al.* 2011). As a result, YscJ is responsible for connecting the two complexes

in the inner membrane, thereby completing the putative structure of the basal body in the T3S apparatus.

1.7.2 Cytoplasmic (C)-ring components and secretion hierarchy

Contrary to the scaffolding role of the IMR and OMR in the basal body, the C-ring export apparatus is expected to play a functional role in effector secretion. C-ring components enable the recruitment of chaperone/effector complexes to the base of the apparatus, regulate the timed secretion of multiple T3S components and effectors, and provide the energy required to shuttle proteins through the injectisome. The recruitment of effectors to the base of the T3S apparatus involves specific chaperones which dock effector/chaperone pairs to the C-ring. Unlike molecular chaperones, T3S-associated chaperones are not believed to assist in protein folding and do not require ATP (Fattori, Prando *et al.* 2011). Class IA and IB chaperones are responsible for associating with either a single or multiple effector proteins, respectively (Wattiau, Bernier *et al.* 1994). There are a large number of characterized T3S-associated chaperone/effector complexes which form in the bacterial cytoplasm (Bennett and Hughes 2000; Page and Parsot 2002). For instance, CesT, a class IB chaperone, has previously been shown to require a C-terminal domain to recruit bacterial effectors (such as Tir and Map) to EscN in the basal body (Thomas, Deng *et al.* 2005). Class II chaperones, like SycD in *Yersinia,* interact with and shuttle the putative hydrophobic translocator proteins, such as YopD, and are characterized by a tetratricopeptide repeat region (Schreiner and Niemann 2012). Class III chaperones stabilize and prevent the premature polymerization of needle filament

proteins (Page and Parsot 2002). Yip *et al.* have shown that the *Escherichia* chaperone CesA stabilizes the filament protein, EspA, in its monomeric state and is capable of inhibiting polymerization (Yip, Finlay *et al.* 2005). Even though there are three classifications of chaperones, all T3S-associated chaperones have common physical characteristics, such as a molecular weight of less than 15 kilodaltons (kDa) and an acidic pI (Page and Parsot 2002). The coordinated transcription and translation of these specific classes of chaperones enables the controlled recruitment of a wide variety of substrates to the base of the injectisome.

Bacterial proteins must be translocated through the apparatus in a particular order to ensure that the needle assembly precedes the secretion of effectors. This sorting process, called the 'secretion hierarchy', involves chaperones and components at the base of the injectisome which are believed to form the C-ring complex. Lara-Tejero *et al.* have shown that SpaO, a shuttling component of the C-ring in *Salmonella spp.*, is capable of forming complexes with the needle filament, translocases, and IM proteins, such as the tethering protein InvJ (Lara-Tejero, Kato *et al.* 2011). In the absence of InvJ, SpaO is not localized to the membrane and the T3S apparatus is locked in a mode that secretes needle filament proteins and not translocases (Lara-Tejero, Kato *et al.* 2011). These authors have also shown that chaperones are essential to recruit translocator and effector proteins to the C-ring at the base of the apparatus (Lara-Tejero, Kato *et al.* 2011). As a result of these findings, these authors propose that SpaO, OrgA, and OrgB form a sorting platform that exists on the cytoplasmic face of the basal body apparatus and is responsible for arranging chaperone/effector complexes. The molecular mechanisms responsible for

mediating this process have yet to be determined. Stamm and Goldberg proposed that loading of chaperone/effector complexes in the sorting platform may reflect the varying affinities of chaperone/effector complexes for the sorting platform (Stamm and Goldberg 2011).

Energy is necessary to power the process of effector protein delivery and secretion though the T3S apparatus. Within the C-ring, an ATPase is predicted to drive the unfolding of secreted substrates and the dissociation of chaperone/effector complexes by ATP hydrolysis (Blaylock, Riordan *et al.* 2006). T3S ATPases have shown significant structural similarity to the β subunit of the F_oF_1ATPase and exhibit ATP-dependent protein unfolding (Sauer, Bolon *et al.* 2004). Co-purifications of YscN, the ATPase of the T3S apparatus in *Yersinia,* have displayed evidence that it binds to the eleven residue, N-terminal degradation signal of an effector, YopR, and can be blocked *in vivo* with the addition of a large recombinant tag to the substrate (Sorg, Blaylock *et al.* 2006). Furthermore, Blaylock *et al.* indicate that YscN plays an important role in chaperone/effector complex recognition and is tethered to the apparatus by YscL, an ATPase regulator protein (Blaylock, Riordan *et al.* 2006). YscL, along with the putative plug protein YopN, possibly regulate the secretion of proteins through the injectisome by regulating the ATPase function and preventing the premature release of effectors (Cheng, Kay *et al.* 2001; Ghosh 2004). All together, these functional components of the C-ring antechamber enable the coordinated assembly and secretion of T3S-associated components and effectors.

1.7.3 Type III secretion inhibitors

The T3S virulence factor is a target for bacterial inhibition due to its highly conserved nature in most Gram-negative bacteria. Recent studies have shown that the secretion of a large majority of effectors by the T3S apparatus can be blocked *in vitro* by the addition of a recombinant protein tag, such as glutathione-s-transferase (GST), to the carboxy (C)-terminus of effector proteins (Sorg, Blaylock *et al.* 2006; Riordan, Sorg *et al.* 2008). In addition, small molecule inhibitors of the T3S apparatus have also been identified. In 2005, Nordfelth *et al.* demonstrated that a group of small molecules, acylated hydrazones, are capable of blocking effector secretion in *Yersinia* (Nordfelth, Kauppi *et al.* 2005). Confirmation studies in *Chlamydia, Salmonella,* and *Shigella* have shown that these small molecules also inhibit epithelial cell invasion and the activation of macrophage apoptosis by these Gram-negative pathogens (Nordfelth, Kauppi *et al.* 2005). In a recent study, the application of small molecules *in vitro* considerably reduced the activity of the T3S ATPase in *Yersinia*, YscN, at concentrations (IC_{50}) lower than 20 uM (Swietnicki, Carmany *et al.* 2011). These lead compounds were also capable of inhibiting Yop secretion in bacterial cell secretion inhibition assays (Swietnicki, Carmany *et al.* 2011). The T3S apparatus remains an important target for bacterial inhibition in Gram-negative bacteria.

1.8 Type III secretion in *Chlamydia*

Due to the lack of a genetic manipulation technique, a functional T3S apparatus in *Chlamydia* has only recently been identified by sequence similarities to other Gram-

negative pathogenicity islands, the expression profile of *Chlamydia*, and established T3S-associated effector secretion. The first evidence of a *Chlamydia* T3SS was proposed in 1997 from a set of genomic studies which analyzed the sequence homology of four *Chlamydia* genes (*cdsV*, *cdsU*, *copN*, and *scc1*) in *C. psittaci* (Hsia, Pannekoek *et al.* 1997). One of the protein products of these four genes, CopN (*Cpn0324*), displayed almost fifty percent sequence similarity and over twenty-three percent identity to a T3SS gene product of Yersinia, YopN (Hsia, Pannekoek *et al.* 1997). An entire repertoire of T3SS genes was confirmed in *C. pneumoniae* after Kalman *et al.* revealed the conservation of the T3SS virulence mechanism genes from *C. trachomatis* (Kalman, Mitchell *et al.* 1999). Reverse transcriptase-polymerase chain reaction (RT-PCR) has further demonstrated that the expression of these genes occurs *in vivo* (Lugert, Kuhns *et al.* 2004). A functioning *Chlamydia* T3SS is supported by the presence of non-Sec dependent proteins located within the host cell cytoplasm prior to bacterial entry and in the inclusion membrane (Subtil, Parsot *et al.* 2001). In summary, this evidence has sparked a rapid increase in research interests exploring the structural and functional role of T3S proteins in *Chlamydia*.

The T3S system in *C. pneumoniae* is believed to be composed of approximately twenty proteins, whose corresponding genes are dispersed throughout the *Chlamydia* genome in ten short operons (Hefty and Stephens 2007). The nomenclature ‘Cds’ of secretion components was initially proposed by Hsia *et al.* and represents the contact dependent secretion (Cds) apparatus components (Hsia, Pannekoek *et al.* 1997). Our knowledge of the structure of the T3S injectisome in *C. pneumoniae* is based on the

structural and functional orthology of the *Yersinia* T3SS (Betts-Hampikian and Fields 2010). A hypothetical model predicts that the T3SS consists of a C-ring export apparatus composed of a putative ATPase, CdsN (*Cpn0707*), an ATPase regulator, CdsL (*Cpn0826*), a plug protein, CopN (*Cpn0324*), and a chaperone/effector shuttle, CdsQ (*Cpn0704*) (see Figure 1.5). The Mahony laboratory demonstrated that CdsN possessed ATPase activity and this T3S ATPase is regulated by the addition of recombinant CdsL (Stone, Johnson *et al.* 2008; Stone, Bulir *et al.* 2011). Both CdsL and CdsN are hypothesized to interact with the shuttling protein, CdsQ, and the plug protein, CopN, at the base of the apparatus. GST-pull down data have indicated that CdsQ may deliver chaperone/effector complexes to the base of the apparatus as it interacts with both structural components and chaperone/effector complexes associated with the T3S apparatus (Toor, Stone *et al.* 2012). CopN, the putative plug protein of the T3S apparatus in *Chlamydia*, has been shown to interact with a wide variety of recombinant proteins including the C-ring components CdsN and CdsQ and the chaperone proteins Scc1 and Scc4 (Stone, Johnson *et al.* 2008; Silva-Herzog, Joseph *et al.* 2011; Toor, Stone *et al.* 2012). However, the role of CopN as the putative plug protein remains to be characterized. These four proteins in the C-ring export apparatus are thought to be crucial for regulating secretion throughout the *Chlamydia* developmental cycle.

A

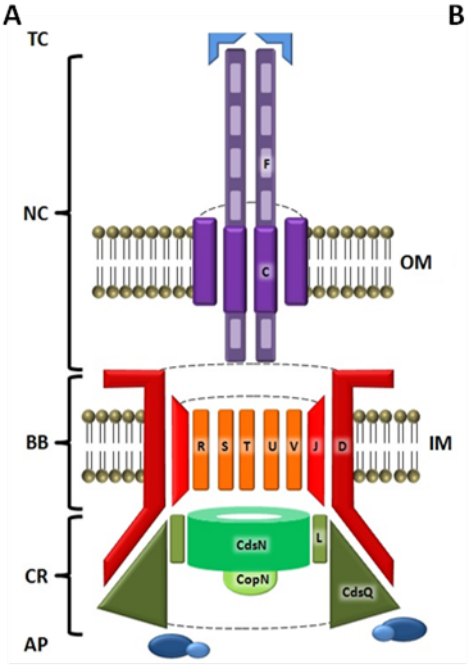

B

T3S Component	*C. pneumoniae*	*C. trachomatis*	Location
CdsF	*Cpn0710*	*CT666*	NC
CdsC	*Cpn0702*	*CT674*	OM
CdsD	*Cpn0712*	*CT664*	IM/BB
CdsJ	*Cpn0828*	*CT559*	IM/BB
CdsQ	*Cpn0704*	*CT672*	CR
CdsN	*Cpn0707*	*CT669*	CR
CdsL	*Cpn0826*	*CT561*	CR
CdsV	*Cpn0323*	*CT090*	IM/BB
CdsU	*Cpn0322*	*CT091*	IM/BB
CdsR	*Cpn0825*	*CT562*	IM/BB
CdsS	*Cpn0824*	*CT563*	IM/BB
CdsT	*Cpn0823*	*CT564*	IM/BB
CopN	*Cpn0324*	*CT089*	CR

Figure 1.5 (adapted from (Betts-Hampikian and Fields 2010)) – A structural representation of the T3S apparatus in *Chlamydia*. (A) The hypothetical model of the T3S apparatus in *Chlamydia* indicates the various structural components of the injectisome including the basal body (BB), needle complex (NC), tip complex (TC), ancillary proteins (AP), and the C-ring (CR). The secretin, CdsC, is located in the outer membrane (OM) and is thought to interact with both the needle filament (CdsF) and components of the basal body located in the inner membrane (IM). The basal body is believed to be composed of CdsD, CdsJ, CdsR, CdsS, CdsT, CdsU, and CdsV. The C-ring is proposed to accumulate at the base of the basal body and is thought to be composed of CdsQ, CdsN, CdsL, and the putative plug protein, CopN. Ancillary proteins would represent chaperone effector complexes that form in the cytoplasm and are shuttled to the base of the apparatus. This model is not to scale and does not accurately represent the multimeric structure of the T3S components. Translocator proteins CopB, CopB2, CopD, and CopD2 (not shown) are believed to insert into the host cell membrane, thereby forming a translocon pore with the unidentified tip protein. In addition, the ruler protein, CdsP, is presumed to be associated with the apparatus, however its localization has not been determined experimentally in *Chlamydia*. **(B)** A table that denotes the protein names and genetic ID of the T3S-associated components of both *C. pneumoniae* and *C. trachomatis*. The table also mentions the putative location of each component in the hypothetical diagram.

Results of GST pull-down experiments in the Mahony laboratory suggest that components of the C-ring interact with proteins of the inner membrane. These proteins

include CdsD (*Cpn0712*), CdsJ (*Cpn0828*), CdsR (*Cpn0825*), CdsS (*Cpn0824*), CdsT (*Cpn0823*), CdsU (*Cpn0322*), and CdsV (*Cpn0323*), which are all associated with the basal body apparatus. The assembly of the inner membrane proteins and the C-ring proteins at the base of the inner membrane ring constitutes the majority of the basal body. Very few studies have characterized the role of the inner membrane proteins of the T3S apparatus of *Chlamydia*. Similar to studies in *Yersinia*, CdsU from *C. pneumoniae* has been shown to undergo auto-cleavage events *in vitro* (Gilchrist 2010, unpublished). With regards to other components of the basal body, Johnson *et al.* have shown by co-purification that CdsD interacts directly with CdsQ and CdsL in *C. pneumoniae* (Johnson, Stone *et al.* 2008). In a separate study, Johnson *et al.* provided evidence that CdsD is phosphorylated *in vitro* by PknD (*Cpn0095*) (Johnson and Mahony 2007). These authors hypothesize that phosphorylation events involving PknD may play a key role in the developmental cycle of *Chlamydia* (Johnson, Stone *et al.* 2009). Recent evidence indicates that the oxidation status of membrane components may contribute to the formation of oligomeric rings and the coordinated assembly of the basal body structure of the T3S apparatus (Betts-Hampikian and Fields 2011). At this point, the order of assembly and the precise role of each basal body component remain relatively unknown.

Secretion of the filament protein, CdsF, is believed to follow basal body formation and its polymerization is proposed to be regulated by the molecular ruler protein, CdsP (*Cpn0705*). The needle tip protein, translocator proteins (CopD (*Cpn0808*), CopB (*Cpn0809*), CopD2 (*Cpn1019*), and CopD2 (*Cpn1020*)), and effectors are suspected to be secreted following the completion of needle assembly. Chellas-Gery *et al.* determined,

using ectopic expression, that the paralogous *Chlamydia* translocator proteins, CopB and CopB2, colocalize with host and inclusion membrane fractions, respectively (Chellas-Gery, Wolf *et al.* 2011). These authors hypothesize that CopB acts as a integral membrane translocon protein in host cell membranes and that CopB2 associates peripherally with the inclusion membrane (Chellas-Gery, Wolf *et al.* 2011). In addition, various effector proteins have been crystallized and characterized. For instance, Stone *et al.* have shown that *Cpn0803* may form a hexameric structure in solution and interacts with the shuttling protein CdsQ, the putative ATPase CdsN, and the filament protein CdsF (Stone, Sugiman-Marangos *et al.* 2012). *Cpn0803* also binds phospholipids suggesting that it may be involved with host cell recognition, secretion activation, or host cell signalling (Stone, Sugiman-Marangos *et al.* 2012).

1.9 Foreword

With respect to CdsD, only the membrane localization, phosphorylation, and three interactions with other T3S-associated proteins have been explored. The localization of CdsD in the membrane of *C. pneumoniae* has been debated as it has been experimentally found in the outer membrane, inner membrane, and cytoplasm by a variety of methods. The Mahony laboratory has proposed that CdsD localizes to the inner membrane as a peripheral membrane protein (Johnson, Stone *et al.* 2008). For example, indirect immunofluorescence with anti-CdsD FHA2 uniformly stained whole *Chlamydia* inclusions 48 hours post infection, suggesting the presence of CdsD in the membrane of RBs (Johnson, Stone *et al.* 2008). The characterization of binding partners of CdsD has

been limited to GST pull-downs and co-purifications from EB lysates. Furthermore, the kinase domain of PknD has been shown to autophosphorylate and phosphorylates CdsD in both FHA domains *in vitro* (Johnson and Mahony 2007). These findings suggest that CdsD may play both a functional and structural role in injectisome assembly. Using GST pull-downs, immunoprecipitations, *in vitro* kinase and phosphatase assays, and native gel electrophoresis, I have attempted to characterize the structural and functional roles of CdsD as a member of the T3S apparatus in *C. pneumoniae.* The following two chapters discuss the methods and results of these experiments and the final chapter discusses a framework for understanding and interpreting the results of these experiments.

CHAPTER TWO

MATERIALS AND METHODS

2.1 Recombinant protein cloning

Full-length T3S-associated *Chlamydia* genes were cloned using the Gateway Cloning Kit (Invitrogen) in order to create cell lines that can express recombinant proteins for *in vitro* experimentation. Briefly, gene sequences from *C. pneumoniae* genomic DNA were amplified using primers designed with the attB recombination site included in the forward primer upstream gene's start codon (see primer sequences in Appendix B). Each gene fragment amplified with a Polymerase Chain Reaction (PCR) on a PTS thermal cycler (MJ Research) was completed with an annealing temperature of 55°C and an extension time of one minute per thousand base pairs. In some cases, the annealing temperature was lowered to decrease the specificity of primer annealing. The *attB*-gene product was then gel purified and run in a BP reaction along with the pDONR201 vector, which contains the *attB* recombination site, and recombination enzyme (BP Clonase II). Reactions were stopped with 1 µL of Proteinase K after one hour at 37°C, transformed into *E.coli* XL-1, and plated on Luria Bertani (LB) and kanamycin agar plates overnight. Colonies were picked off a plate, grown in LB at 37°C overnight and lysed with a BioBasic Plasmid DNA Kit to extract plasmids. After the plasmid concentration was measured with a Nanodrop spectrophotometer, plasmids were electrophoresed along with pDONR201 on a 0.6% (m/v) agarose gel to visualize a shift in plasmid size. Once the proper shift was viewed, the plasmids were sequenced and compared to gene sequences found on STDGEN (see http://stdgen.northwestern.edu/). These plasmids were then recombined in a LR reaction along with the appropriate destination vector (pDEST15,

pDEST17, pDESTperiHisMBP or pDEST544) in order to introduce protein tag sequences (GST, Polyhistidine (His), His-MBP and His-NusA, respectively) upstream from the gene of interest. Highly hydrophobic proteins, such as CdsC and CdsJ, had low solubility upon protein expression and they were re-cloned into pDEST544. pDEST544 encodes a NusA tag which has been shown to considerably increase the solubility of recombinant proteins (Harrison 1999). After one hour at room temperature, the reaction was stopped with 1 µL of Proteinase K at 37°C, the plasmids were transformed into *E.coli* XL-1 cells, and then plated on LB and ampicillin agar plates. Once again plasmids were harvested from overnight cultures inoculated with a bacterial colony from the plate. These expression vectors were digested with specific restriction enzymes (as in section 2.2) to identify the expected altered migration on an agarose gel and then transformed into *E. coli* BL21 (DE3) cells for inducible protein expression.

2.2 Restriction enzyme digestion

Restriction enzyme digestion was completed in order to demonstrate that the cloned gene of interest was successfully inserted into the destination vector and was visualized by a shift in molecular size on an agarose gel. Each restriction enzyme was chosen to excise the recombinant plasmid at a single, unique site. This was an important step that would enable each plasmid to migrate as a single band in the final agarose gel. Plasmid sequences were obtained from Addgene (http://www.addgene.org/) and genetic sequences were obtained from CMR (http://cmr.jcvi.org/). A restriction enzyme was chosen by identifying the unique restriction sites located on the plasmid of interest and by

ensuring that there were no identical restriction sites within the gene of interest using Nebcutter2.0 (NEB). Once the restriction enzyme was chosen, a reaction mixture containing 14µL of ddH_2O, 2.5µL of NEB Reaction Buffer, 1µL of restriction enzyme and 7.5µL of plasmid DNA was created. The reaction was placed in a 55°C water bath for one hour, then stopped with the addition of loading buffer and electrophoresed on a 0.6% (m/v) agarose gel. Agarose gels were viewed using a GelDoc (Biorad).

2.3 Agarose gel electrophoresis

Agarose gel electrophoresis was used to estimate the size of DNA fragments. An agarose buffer solution (0.6%-2.0% (m/v)) was heated in a microwave and poured into a plastic mould with a ten or fifteen well comb. The gels were left at room temperature for twenty minutes to solidify and were submerged into a gel apparatus filled with TAE buffer. DNA samples were aliquoted into 15µL fractions and diluted 1:2 with loading dye before loading approximately 20µL into the wells. The gel was electrophoresed at 140 mV for forty-five minutes and visualized using the GelDoc (Biorad).

2.4 Expression of recombinant proteins

Recombinant cell lines created using the Gateway Cloning Kit (Invitrogen) were propagated in large batches of LB broth in order to obtain large quantities of recombinant protein for use in *in vitro* kinase assays and Far-Western blotting. *E. coli* BL21 (DE3) cells containing the plasmid of interest were incubated in a 100 mL mixture of LB broth and ampicillin overnight at 37°C. Ten millilitres of overnight culture were added to each

flask containing a 1 L mixture of LB broth and Ampicillin (thereby creating a 1:1,000 dilution). These flasks were incubated and shaken at 37°C until they reached an optical density of at least 0.6 at a wavelength of 600 nm. At this point, the cells were induced at room temperature with 0.1 mM isopropyl-B-D-thiogalactopyranoside (IPTG) for two hours. With the kPknD-pEX15 and CdsD-pEX17 constructs, the cells were cooled to 20°C on ice and induced overnight at room temperature with 0.1 mM IPTG to obtain proper folding of the protein. Cells were then pelleted in a Sorvall RC-5B centrifuge at 7,000 rpm and resuspended in ice-cold Nickel A Buffer for Histidine tagged proteins or Phosphate Buffered Saline (PBS) for Glutathione-S-transferase (GST)-tagged proteins along with 1X Complete Ethylenediaminetetraacetic acid (EDTA)-free Protease Inhibitor cocktail (Roche). The resuspended cells were then sonicated using a Fischer Scientific Sonic Dismembrator Model 100 and centrifuged at 20,000 rpm for forty minutes. The supernatant was collected and filtered through a 0.45 µm PES Bottle Top filter (Nalgene). The His-tagged proteins were then purified by Fast Protein Liquid Chromatography (FPLC) using a nickel-nitrilotriacetic acid (Ni-NTA) column (see Section 2.3) with an increasing concentration of imidazole and eluted with a final imidazole concentration of 300 mM. The GST-tagged proteins were also purified by FPLC utilizing a glutathione agarose column and eluted with a reduced glutathione solution. All proteins were washed with 5 mM EDTA and dialyzed against enzyme activity buffer.

2.5 Purification of polyhistidine-tagged proteins

His-tagged recombinant protein preparations were purified to remove protein contaminants from the lysate and isolate the desired protein for use in *in vitro* kinase assays and Far-Western blotting. An *E. coli* cell lysate obtained from the large scale propagation of recombinant cell lines and expressing a polyhistidine-tagged protein of interest was filtered with a 0.2 µm PES Bottle Top filter (Nalgene) on ice and then loaded into a 50 mL superloop column (GE Lifesciences). A 1 mL HiTrap Ni-NTA affinity column (GE Lifesciences) was prepared by washing the column consecutively with 20 mL of 0.05M EDTA, ddH_2O, and 0.1 M $NiCl_2$ at 100 mL/hour. The column was placed on an AKTA FPLC and washed with approximately 15 mL of Nickel A buffer at 1.5 mL/minute. The filtered cell lysate was then injected into the Ni-NTA column at a rate of 1.00 mL/minute. Once the entire sample was injected into the column, the column was washed with Nickel A buffer to elute unbound protein. Weakly associated protein was eluted with consecutive 10 mL fractions of 5% (v/v), 10% (v/v), and 15% (v/v) Nickel B buffer in Nickel A buffer. Finally, the polyhistidine-tagged protein of interest was eluted with 100% Nickel B buffer and collected on ice in a 15 mL conical Falcon tube. All of the purified protein (about 10 mL in Nickel B buffer) was reloaded into the 50 mL superloop column and a 26/10 HiPrep Desalting Column (GE Lifesciences) was attached to the FPLC. The desalting column was washed with approximately 100 mL of new buffer (activity buffer or PBS) at 4.00 mL/minute and followed by injection of the purified protein sample at a rate of 1.00 mL/minute. After the entire protein sample was injected, the new buffer was once again loaded at a rate of 4.00 mL/minute. Protein

elution was observed by a sharp increase in ultra-violet (UV) absorbance (about 13 mL post-injection) and collected on ice in a 50 mL Millipore concentrating tube. The purified protein was concentrated by centrifugation for 30 minutes at 3,000 rpm.

2.6 Purification of Glutathione-S-Transferase (GST)-tagged proteins

Similar to His-tagged protein purification, GST-tagged recombinant protein preparations were purified to remove protein contaminants from the lysate and isolate the desired protein for use in *in vitro* kinase assays and Far-Western blotting. An *E. coli* lysate expressing a GST-tagged protein of interest was filtered with a 0.2 µm PES Bottle Top filter (Nalgene) on ice and then loaded into a 50 mL superloop column (GE Lifesciences). A 1mL GSTrap Glutathione-sepharose column (GE Lifesciences) was prewashed with 15 mL of PBS at 1.5 mL/minute on the AKTA FPLC machine. The filtered cell lysate was then injected into the GSTrap column at a rate of 0.30 mL/minute. Once the entire sample was injected into the GSTrap column, the column was washed with PBS at 0.50 mL/minute to elute unbound protein. Lastly, a solution of reduced glutathione was washed through the column at a rate of 1.00 mL/minute to elute the protein of interest and collect it on ice in a 15 mL conical Falcon tube. All of the purified protein (about 10 mL in reduced glutathione solution) was reloaded into the 50 mL superloop column and a 26/10 HiPrep Desalting Column (GE lifesciences) was attached to the FPLC. The desalting column was washed with approximately 100 mL of new buffer (activity buffer or PBS) at 4.00 mL/minute and followed by injection of the purified protein sample at a rate of 1.00 mL/minute. After the entire protein sample was

injected, the new buffer was once again loaded at a rate of 4 mL/minute. Protein elution was observed by a sharp increase in UV (about 13 mL post-injection) and collected on ice in a 50 mL Millipore concentrating tube. The purified protein was concentrated by centrifugation for 30 minutes at 3,000 rpm.

2.7 Sodium dodecyl sulphate-polyacrylamide gel electrophoresis (SDS-PAGE)

A polyacrylamide gel was cast and assembled using two glass slides, a slide holder and a casting stand. Briefly, a resolving gel solution was created with a mixture composed of 30% (v/v) acrylamide:bis solution (Biorad), resolving gel buffer, ddH_20, 20% (v/v) SDS, 0.15% (m/v) ammonium persulfate (APS), and tetramethylethylenediamine (TEMED). The resolving gel was loaded up to approximately one centimeter below the top of the glass slide and 1 mL of isopropanol was added across the top of the resolving gel. After fifteen minutes, the isopropanol was removed and the resolving gel was washed and dried with ddH_2O. Finally, a stacking gel mixture was created (30% (v/v) acrylamide:bis solution (Biorad), stacking gel buffer, ddH_20, 20% (v/v) SDS, 0.15% (m/v) APS, and TEMED) and added to the top of the resolving gel. A 15-well comb was inserted into the stacking gel and the gel was allowed to solidify over one hour at room temperature. An electrophoresis apparatus was used to hold the gel and was loaded with approximately 250 mL of electrophoresis running buffer. Protein samples were resuspended in sample loading buffer and heated for five-ten minutes at A Powerpac was connected to the electrophoresis apparatus and run at 80 V for 20 minutes followed by 120 V for 80 minutes. Finally, the gels were either

transferred to a nitrocellulose membrane using the iBlot gel transfer apparatus at 20 V for 7 minutes or stained with Coomassie Brilliant Blue.

2.8 Native SDS-PAGE

A non-denaturing native polyacrylamide gel was created as previously described in section 2.7, with a few modifications. First, when making and loading acrylamide gels, non-denaturing resolving buffer (see List of Buffers), stacking gel buffer, sample loading buffer and electrophoresis buffer were used instead of denaturing SDS buffers (discussed previously in section 2.7). Second, the gel electrophoresis was run at 4°C instead of room temperature to ensure that the heat generated by the apparatus would not affect protein structure and electrophoretic mobility.

2.9 Phos-tag SDS-PAGE

Phos-tag SDS-PAGE was used to identify and separate phosphorylated proteins from unphosphorylated proteins. Briefly, approximately 42 µL of Phos-tag acrylamide and 42 µL of 10 mM $MnCl_2$ were added to the resolving gel solution before the addition of TEMED and APS. The phos-tag resolving gel solution was used to cast acrylamide gels ranging from 8-12% (v/v) acrylamide. The gels were electrophoresed at 80 mV for 20 minutes and subsequently at 120 mV for 80 minutes. Before transferring the proteins to a nitrocellulose membrane, the phos-tag acrylamide gels were soaked in 10 mM EDTA-transfer buffer and EDTA-free transfer buffer for ten minutes each. Finally, the

gels were transferred to a nitrocellulose membrane using the iBlot gel transfer apparatus (Invitrogen) at 25 V for 10 minutes.

2.10 GST pull-down assay

The purpose of the GST-pull down assay is to elucidate strong interactions between two recombinant proteins. Briefly, glutathione agarose beads were swollen in 2 M NaCl overnight and washed in 1X Phosphate-buffered Saline (PBS) solution twice. Approximately 500 µL of agarose beads were added to the cell lysate of the Glutathione-S-Transferase tagged fusion protein, CdsD-GST. The solution of beads was shaken for one hour at 4°C, centrifuged at 1,000 rpm for five minutes, and the supernatant was discarded. The pellet was blocked overnight with Tris-Buffered Saline + Triton X-100 (TBST) and 4% (m/v) BSA. Tubes containing the agarose beads were centrifuged at 1,000 rpm for five minutes and the supernatant was carefully removed. The bait protein beads were then resuspended in 1XPBS and stored at 4°C. A cell lysate of the prey protein (polyhistidine-tagged protein) was aliquoted into 700 µL fractions and kept at 4°C. Approximately 50 µL of bait protein beads were added to the prey protein fraction and shaken at 4°C for at least one hour. The aliquots were centrifuged for seven seconds and the supernatant was carefully discarded. The beads were resuspended in high salt wash buffer (see List of Buffers), centrifuged for seven seconds, and the supernatant was discarded. After repeating the wash seven times, the final wash was stored for TCA precipitation and the final pellet was resuspended in 10 µL of 5X sample loading dye with β-mercaptoethanol. GST alone was used as a negative control for confounding

interactions between GST and the prey protein. The published interaction between GST-CdsD and His-CdsQ was used as a positive control (Johnson, Stone *et al.* 2008).

2.11 TCA precipitation

Trichloroacetic acid (TCA) precipitation was used, in combination with Western blotting, to analyze the last wash and ensure that the positive results of the pull-down were not due to non-specific trapping of proteins. Briefly, approximately 100 µL 100% TCA (10% (v/v) final concentration) was added to each final wash supernatant and they were rocked gently at 4°C overnight. Precipitated proteins were pelleted by centrifugation at 13,200 rpm for forty minutes in an Eppendorf 5415R microcentrifuge. The supernatants were aspirated and removed from the Eppendorf tubes. Each pellet was then washed with 1 mL of 100% acetone and centrifuged again at 13,200 rpm for 20 minutes. After the acetone was removed, the pellets were dried at room temperature for twenty minutes and then resuspended in loading buffer for use in an SDS-PAGE.

2.12 *In vitro* kinase assay

An *in vitro* kinase assay was used to phosphorylate CdsD and additional T3S protein components. First, the his-tagged kinase domain of PknD and the substrate protein (usually His-CdsD or His-CdsQ) were grown at 37°C and cooled to 20°C before induction at room temperature. Proteins were purified with a Ni-NTA column and aliquots of approximately 50 to 100 ng of His-kPknD and His-tagged substrate were incubated at 34°C for two hours in 30 µL fractions containing 10 mM HEPES, pH 7.3, 20

mM β-glycerophosphate, 10 mM $MnCl_2$, 1 x complete EDTA-free protease inhibitors, and 4 mM ATP. The reactions were terminated with the addition of 5x SDS loading buffer and loaded on Phos-tag acrylamide SDS-PAGE. Phos-tag acrylamide impedes the migration of phosphorylated proteins through the gel by attracting anion groups, like phosphate, and allowing unphosphorylated proteins to migrate freely through the gel (Kinoshita, Takahashi *et al.* 2004). The acrylamide gels were then transferred onto a nitrocellulose membrane using the Invitrogen iBlot dry blotting system at twenty-five volts for ten minutes. The nitrocellulose membranes were blotted using a mouse monoclonal anti-His antibody (Sigma) at a dilution of 1:4,000 and followed by HRP-conjugated goat anti-mouse antibody at a 1:4,000 dilution for detection of the loaded protein.

2.13 *In vitro* phosphatase assay

An *in vitro* lambda phosphatase assay was used to dephosphorylate recombinant protein for use as a control in experiments involving phosphorylated His-CdsD. Briefly, a master mix of protein (about 5 ug/µL), 10x $MnCl_2$ buffer, and 10x reaction buffer (500 mM Tris-HCl, pH 7.5, 1 mM Na_2EDTA, 50 mM DTT, and 0.1% (m/v) BRIJ 35) were combined, vortexed, and aliquoted into 4 µL fractions. One microliter of lambda phosphatase was added to each reaction mixture and incubated at 30°C. After one hour, the reaction was stopped with the addition of 60 mM EDTA at 65°C for one hour. The protein samples were resuspended in sample loading buffer and run on a Phos-tag acrylamide gel for phosphorylation detection.

2.14 Far-Western blotting

Far-Western blotting was used in combination with phos-tag acrylamide gels to detect phosphorylation-dependent recombinant protein interactions. Fractions of recombinant His-kPknD and His-CdsQ (approximately 5-20 µg) were electrophoresed on an 8% (v/v) phos-tag acrylamide gel, to separate the phosphorylated and unphosphorylated proteins, and then transferred to a nitrocellulose membrane. Purified His-CdsD was added to the membrane at a concentration of approximately 5 ng/µL and incubated overnight at 4°C. The membrane was washed with phosphate buffered saline (PBS) + 1% (v/v) TWEEN-20 and probed at room temperature using a monoclonal mouse anti-His or rabbit anti-CdsD antibody at a dilution of 1:4,000 for one hour. The membrane was then washed with PBS+1% TWEEN-20 and probed for one hour with HRP-conjugated goat anti-mouse or goat anti-rabbit antibody at a 1:4,000 dilution. Mouse anti-His and anti-GST antibodies were purchased from Sigma-Aldrich and *Chlamydia*-specific antibodies were developed by Colcalico Biologicals Inc. (Reamstown, PA) and affinity purified as per Johnson *et al.* (Johnson, Stone *et al.* 2008). Bands on the membrane were visualized using ECL reagent (Pierce).

2.15 *C. pneumoniae* strains and eukaryotic cell lines

C. pneumoniae was propagated in HeLa or HEC-1B eukaryotic cell lines for immunofluorescent staining and immunoprecipitation. HeLa 229, HEC-1B, and *C. pneumoniae* CWL209 were obtained from ATCC (Manassas) (catalog # CCL-2.1, HTB-

113, and VR1310, respectively). Aliquots of these cell lines were flash frozen in liquid nitrogen and stored at -80°C for use in propagating cell monolayers (see section 2.16).

2.16 Propagating eukaryotic cells (HeLa and HEC-1B)

Aliquots of cells were thawed at room temperature in order to propagate eukaryotic cells in T75 flasks. These confluent monolayers were subsequently used for propogating *Chlamydia.* The HeLa or HEC-1B cells were pelleted by centrifugation in sterile 2 mL Eppendorf tubes at 4,000 rpm for two minutes and the supernatant was aspirated and discarded. HeLa cells were resuspended in 2 mL of minimal essential media (MEM) containing Earle's salts and L-glutamine (Invitrogen, Burlington) supplemented with 10% (v/v) fetal bovine serum (FBS). HEC-1B cells were resuspended in 2 mL of MEM containing Hank's salts and L-glutamine (Invitrogen, Burlington) supplemented with 15% (v/v) FBS. The cellular resuspension was pipetted into a T25 flask containing 8 mL of fresh MEM+FBS and incubated at 37°C and 5% CO_2 until 90% confluent.

At a confluency of 90% (approximately 72 hours), the old media was discarded by aspiration and 2 mL of trypsin was added to the T25 flask for approximately thirty seconds with gentle agitation. The trypsin was then aspirated and discarded and 2 mL of fresh trypsin was added to the T25 flask and incubated for five minutes at 37°C and 5% CO_2. After five minutes, 2 mL of fresh MEM+FBS was added to the trypsinized cells and the 4 mL solution was pipetted against the wall of the flask to ensure the separation of aggregated cells. Finally, the cells were added to 8 mL of fresh MEM+FBS in a T75

flask. Passaging was repeated as per this protocol every three days (or at a confluency of at least 90%) and generally split one T75 flask into five new T75 flasks per passage.

2.17 Propagating and harvesting *C. pneumoniae* in T75 flasks

Four HeLa cell-confluent T75 flasks were aspirated to discard old media and 7 mL of fresh MEM+FBS spiked with 500 µL of *C. pneumoniae* seed (approximately $1x10^6$ ifu (infection forming units)/mL and a multiplicity of infection (MOI) of 1) was added to each T75 flask. These flasks were centrifuged at 2,500 rpm for one hour and then incubated at 37°C and 5% CO_2. After one hour of incubation, the old media was aspirated from the four flasks and 10 mL of fresh MEM+FBS containing 20 ug of cyclohexamide was added. The T75 flasks were incubated at 37°C and 5% CO_2 for 72 hours. After 72 hours, the cells were detached from the base of the flask using a cell scraper. These suspended cells were then pipetted into a 50 mL Falcon tube containing sterile glass beads and cycled four times between vortexing for 25 seconds and placing in ice for thirty seconds. The Falcon tubes were then centrifuged at 1,500 rpm for ten minutes to pellet cellular debris and then the supernatant was removed and placed in another sterile centrifuge tube. The supernatant was centrifuged at 18,000 rpm for forty minutes and the pellet was resuspended in 1 mL of MEM+FBS and 1 mL of 2x SPG freeze/thaw buffer, pipetted into a 2 mL cryovial tube, and placed in the -20°C freezer for one hour. The cryovial tube containing *C. pneumoniae* EBs was then placed in a -80°C freezer until required for further propagation

2.18 Propagating *C. pneumoniae* in bead culture

In order to propagate a large batch of *C. pneumoniae*, four T75 flasks of HEC-1B cells were incubated at 37°C and 5% CO_2 until 90% confluent (approximately 72 hours). Sterile microcarrier beads were preincubated in MEM (with Hank's salts) + 10% (v/v) FBS (Hanks media) for thirty minutes at 22°C and then the media was replaced with fresh Hanks media and incubated at 37°C and 5% CO_2 for two hours. The four T75 flasks of HEC-1B cells were trypsinized and pelleted by centrifugation at 1500 rpm for 5 minutes. The old media was aspirated off of the pelleted cells and the cells were resuspended in 10 mL of fresh Hanks media. Fresh Hanks media was added to the microcarrier beads (20 mL total) and then both beads and cells were added to a 500 mL Proculture glass spinner flask (Corning) and placed at 37°C and 5% CO_2 for three hours. Approximately 120 mL of fresh Hanks media was added to the spinner flask and incubated at 37°C and 5% CO_2 overnight on a magnetic stir platform.

After 24 hours, 90 mL of spent media was removed from the spinner flask after the beads had settled and approximately 1 mL of *C. pneumoniae* seed was added to the spinner flask. The flask was incubated at 37°C and 5% CO_2 for two hours. Finally, 90 mL of fresh Hanks media and 400 ug of cycloheximide was added to the spinner flask and incubated at 37°C and 5% CO_2 for 72 hours. *C. pneumoniae* EBs were harvested by bead lysis as described in section 2.17.

2.19 Purifying EBs and RBs from HeLa cell lysates

To purify EBs or RBs from harvested *C. pneumoniae*-infected flasks, the cells from eight T75 HeLa cell flasks, infected at an MOI of 1, were aspirated to remove old media and detached from the flask with a cell scraper in 2.5 mL of ice-cold PBS containing complete EDTA-free protease inhibitors (Roche). Approximately 10-12 mL of resuspended cells were added to a dounce homogenizer and homogenized with forty strokes of the pestle. The lysate was then transferred to a new 50 mL Falcon tube and centrifuged at 1,000 rpm and 4°C for 10 minutes. The supernatant was collected and centrifuged in a 30 mL polypropylene tube through 15 mL of 30% (v/v) gastrografin in PBS using the Beckman ultracentrifuge (SW-28 rotor) at 19,000 rpm and 4°C for one hour (low brake). Prior to the completion of the spin, a discontinuous gradient was prepared from 5 mL of 59% (v/v) gastrografin, 8 mL of 44% (v/v) gastrografin, and 12 mL of 35% (v/v) gastrografin in PBS on ice. The supernatant from the spin was discarded and the pellet was resuspended in 2 mL of ice-cold PBS using a 10 mL pipette and then a 25 gauge needle. The resuspended cells were then added slowly to the top of the discontinuous gradient and centrifuged once again at 19,000 rpm and 4°C for one hour (no brake). A foggy-white band located at the 35/44% interface was collected (RB fraction) and the sharper white band located at the 44/59% interface was collected (EB fraction). Each fraction was pipetted into two sterile polypropylene tubes on ice, 25 mL of ice-cold SPG buffer was added to each solution, and then each tube was centrifuged at 13,000 rpm and 4°C for 25 minutes (low brake). The supernatants were discarded and each pellet was resuspended in 500 µL of PBS at stored at -80°C.

2.20 Titering *C. pneumoniae* seed using immunofluorescent staining

Serial dilutions of *C. pneumoniae* seed were added to confluent monolayers of HeLa cells in shell vials and stained in order to determine inclusion forming units. To measure the infectivity of *C. pneumoniae*, infected HeLa cell shell vials were stained with a fluorescein isothiocyanate (FITC)-conjugated anti-LPS antibody within the Pathfinder reagent (Bio-rad, Mississauga). The titer of *C. pneumoniae* corresponded to the greatest dilution factor that yielded a fluorescent inclusion. Briefly, sterile shell vials with cover slips were inoculated with $1x10^5$ HeLa cells (estimated with a hemocytometer) and 2 mL of fresh MEM+10% FBS and incubated overnight at 37°C and 5% CO_2. In the morning, at a confluency of approximately 90%, the HeLa cell monolayers were infected with 500 µL serial dilutions of *C. pneumoniae* seed (1 to $1x10^{-8}$ mL per vial, diluted in fresh MEM+10% FBS). After 72 hours, the old media was aspirated off of the monolayer and the vials were rinsed once with sterile PBS. Approximately 1 mL of ice-cold 100% methanol was added to each shell vial for 10 minutes at room temperature and then aspirated off. The monolayers were then rinsed twice with sterile PBS, removed from the shell vial, and placed cell –layer up on top of a rectangular slide. Two drops of the Pathfinder monoclonal antibody were added to the circular cover slips, which were placed in a covered, humidified petri dish, at 37°C and 5% CO_2 for 35 minutes. The slides were then removed from the dish and rinsed with PBS five times. Finally, the slides were inverted, placed on top of 8 µL of mounting media, and visualized using an Olympus fluorescent microscope.

2.21 Immunoprecipitation of proteins from *C. pneumoniae*

In order to precipitate native CdsD from purified EB lysates, six cryovials containing approximately $1x10^7$ ifu/mL of *C. pneumoniae* each were thawed, resuspended, and transferred to sterile 2 mL microcentrifuge tubes. The cells were pelleted by centrifugation at 13,200 rpm for twenty minutes and the supernatant was removed and replaced with 500 µL of fresh ice-cold lysis buffer. Each resuspended pellet was pipetted into a 14 mL conical tube and nutated at 4°C. After three hours, the lysis solution was centrifuged at 13,200 rpm for fifteen minutes and the supernatant was collected in a new 14 mL conical tube. Excess amounts of anti-CdsD antibody were added to the supernatant to a final dilution of 1:100. Once again, *Chlamydia*-specific rabbit anti-CdsD antibodies were produced and affinity purified by Colcalico Biologicals Inc. (Reamstown, PA) as per Johnson *et al.* (Johnson, Stone *et al.* 2008). The supernatant containing primary antibody was rocked overnight at 4°C. The next morning, approximately 100 µL of Protein A/G beads (Roche) were added to the supernatant/antibody solution and nutated again at 4°C for one hour. Finally, the solution was centrifuged at 3,000 rpm for two minutes, the supernatant was removed and the beads were resuspended in 50 µL of sample loading buffer. The samples were boiled at 95°C for five minutes and loaded into an appropriate acrylamide gel.

CHAPTER THREE

3.1 Forward and contributions

All of the work presented in this thesis was completed by the author with the exception of the preparation of the affinity purified antibody to CdsD (rabbit anti-CdsD FHA2) and six of the entry vectors used in cloning recombinant proteins. Entry vectors encoding *Cpn0707*, *Cpn0705*, *Cpn0704*, *Cpn0095*, *Cpn0826* and *Cpn0702* were obtained from Dr. Christopher Stone in the Mahony laboratory and sequenced to confirm the proper insertion of the gene of interest. These vectors were cloned into the appropriate destination vectors for transformation in *E. coli*. Affinity purified rabbit anti-CdsD FHA2 antibody was also obtained from the Mahony laboratory (Colcalico Biologicals Inc.) and prepared by Dr. Dustin Johnson as per his protocol (Johnson, Stone *et al.* 2008).

RESULTS

3.2 Domain prediction and analysis of CdsD

CdsD (*Cpn0712*) is an 845 amino acid (93.2 kDa) protein that may play a similar role to basal body proteins of other Gram-negative bacteria, including PrgH (in *Salmonella*), YscD (in *Yersinia*), MxiG (in *Shigella*), EscD (in *Escherichia*), and CT664 (in *C. trachomatis*). A Basic Local Alignment Search Tool (BLAST) comparison of the sequences of these five putative orthologous proteins suggests that CdsD may be significantly different from its counterparts in other Gram-negative bacteria (see Figure 3.1). Even though CdsD has a 444 amino acid C-terminus which is significantly similar to YscD (expected value = $1e^{-04}$), it also contains two FHA domains within the unique N-terminal 500 amino acids (Schultz, Copley *et al.* 2000). Using BLAST, the 500 N-

terminal amino acids show no sequence similarity to Gram-negative T3S components. The most similar sequence from *C. trachomatis (G/9768),* CT664, contains 829 amino acids and has an expected value of approximately zero (maximum sequence identity of 55%). The maximum sequence alignment between the C-terminal 445 amino acids of *Cpn0712* and other putative orthologs in *Yersinia* (28%), *Salmonella* (22%), *Escherichia* (13%), and *Shigella* (8%) were significantly lower. The TMpred server predicts one transmembrane region spanning from residues 546 to 568 (Hofmann and Stoffel 1993). The Phyre and SMART servers predict FHA domains between residues 25-90 and 422-488 (e value = $1.25e^{-01}$ and $1.03e^{-11}$, respectively) and one BON domain (e value =$1.30e^{-04}$) (Schultz, Copley *et al.* 2000; Kelley and Sternberg 2009).

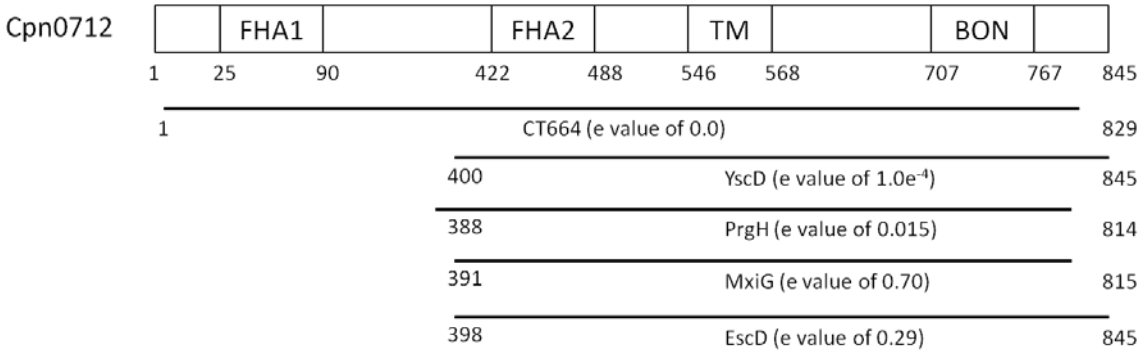

Figure 3.1 – Domain mapping of CdsD shows some sequence similarity to orthologous T3S proteins. The domain structure of CdsD in *C. pneumoniae* and alignment with orthologous proteins in *C. trachomatis* (CT664), *Y. pestis* (YscD), *S. typhimurium* (PrgH), *S. flexneri* (MxiG), and *E. coli* (EscD). The N-terminus (labelled 1 in the *Cpn0712* line of the diagram) 400 amino acids are unique to CdsD (*Cpn0712*) in *Chlamydia spp.* and do not show any appreciable sequence similarity to other T3S components in other Gram-negative bacteria. The SMART and TMpred servers predict two FHA domains, one transmembrane domain, and one BON domain. The FHA domains are putative phospho-threonine binding domains and the BON domain is a putative phospholipid binding domain.

3.3 Interaction of CdsD with T3SS components

The GST pull-down assay was used to assess the possible interactions of T3S components with CdsD *in vitro*. CdsD could interact with many proteins in the apparatus as it is a large, IMR protein of the T3S injectisome that partially resides in both the cytoplasm and the periplasmic space. Briefly, a GST tag sequence was cloned upstream of *cdsD* and GST-CdsD was expressed and immobilized on glutathione beads. These beads were incubated with *E. coli* cell lysates containing each potential binding partner in the T3S apparatus. The potential binding partners that were tested included CdsQ, CdsL, CdsD, PknD, CdsC, CdsJ, CdsS, CdsT, CdsF, CdsP, CopN, SycH, and IncC. Of these proteins, CdsQ, CdsL, CdsD, PknD, and CdsF co-purified with GST-CdsD under high salt conditions (500 mM NaCl) (see Figure 3.2). The remainder of the recombinant proteins showed no interaction with CdsD under high salt conditions. GST alone was immobilized on glutathione agarose beads and used as a negative control adjacent to all pull-downs. None of the proteins co-purified with GST. Also, the final washes of each pull-down were TCA precipitated in order to demonstrate the absence of nonspecific trapping of His-tagged proteins resulting from centrifugation. No protein was found after the TCA precipitations were pelleted, loaded on an acrylamide gel, transferred to a nitrocellulose membrane, blotted with HRP-conjugated anti-His antibody and visualized with ECL reagents. The results of these TCA precipitations confirm that the interactions were not the result of residual protein contaminants.

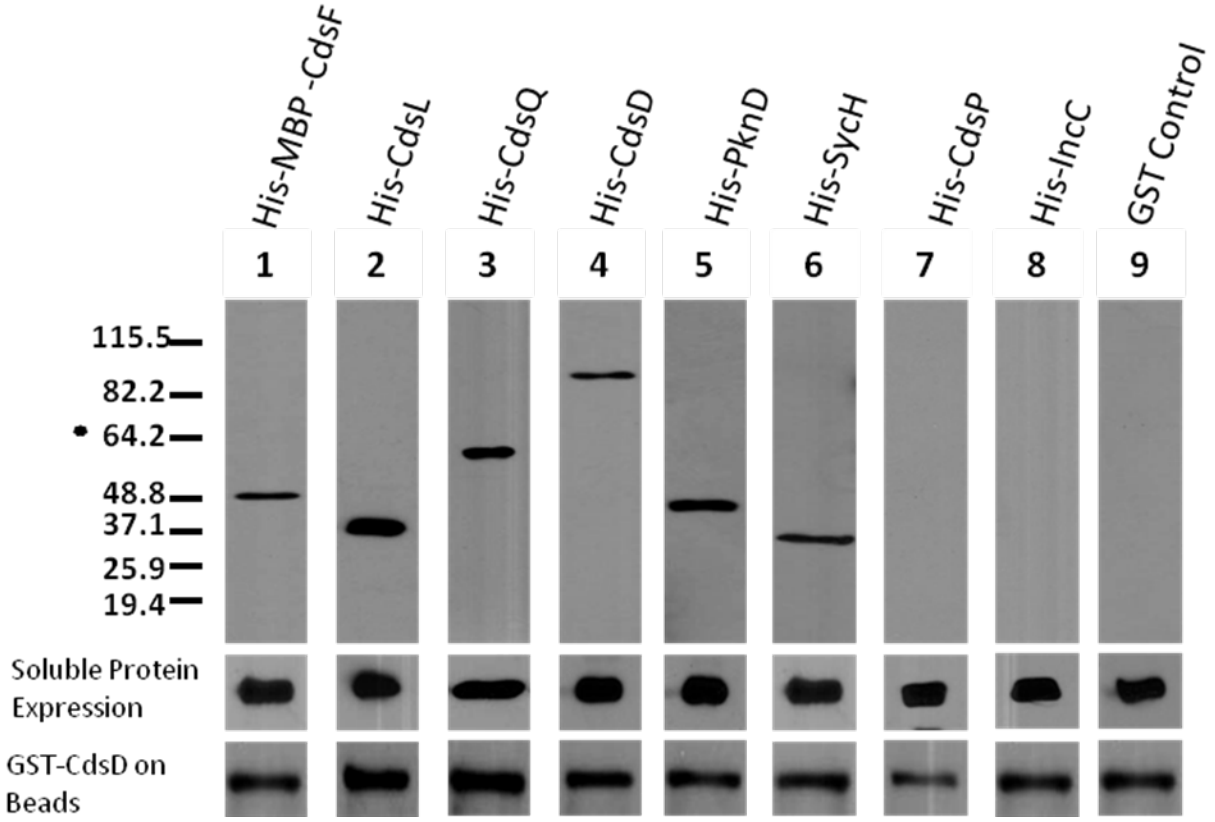

Figure 3.2 - Full-length GST-CdsD pull-down of type III secretion-associated proteins displayed interactions with recombinant CdsF, CdsL, CdsQ, CdsD, PknD, and SycH. Full-length CdsD was cloned and expressed as a GST-fusion recombinant protein and mixed with filtered lysates of T3S-associated recombinant His-tagged proteins of interest. Under 500 mM NaCl conditions, lanes 1-6 display that recombinant His-MBP-CdsF, His-CdsL, His-CdsQ, His-CdsD, His-kPknD, and His-SycH co-purified with GST-CdsD, as visualized using the ECL reagent (Pierce). Recombinant His-CdsP and His-IncC did not display an interaction under high salt conditions with full-length GST-CdsD (see lanes 7 and 8). In addition, recombinant His-CdsR, His-CdsS, His-CdsT, His-CopN, His-CdsC, and His-CdsJ did not display interactions under high salt conditions (data not shown). Soluble expression of each His-tagged protein and expression of GST-CdsD (displayed horizontally beneath lanes 1-8) were detected by western blot (WB) with mouse anti-His and anti-GST antibody (Sigma). GST alone was tested against each His-tagged protein lysate as a negative control to detect spurious interactions with the protein tag (lane 9). No proteins displayed an interaction with GST alone under high salt conditions.

In addition, the same five proteins that gave positive results with full length GST-CdsD were tested against the FHA1, FHA2 and BON domain fragments of CdsD (see Figure 3.3). In these cases, GST-FHA1, GST-FHA2, and GST-BON were all immobilized on glutathione agarose and the previous experiments were repeated and visualized. The results of the first two proteins showed that both the FHA1 and FHA2 fragments interacted with His-CdsD and His-CdsQ however they both did not interact with the negative control, His-CdsP. In addition, GST-FHA1 had a strong interaction with His-SycH, a putative chaperone protein immediately upstream of *cdsD* in the *C. pneumoniae* genome. The GST-BON fragment interacted with His-MBP-CdsF and not with other membrane proteins (His-NusA-CdsJ and His-NusA-CdsC) or the negative control, His-CdsP.

3.4 The phosphorylation of CdsD using PknD and visualized with phos-tag acrylamide electrophoresis

The *in vitro* phosphorylation of CdsD by PknD was first detected by Johnson *et al.* using P^{32} autoradiography (Johnson and Mahony 2007). An *in vitro* kinase assay was designed to phosphorylate CdsD with PknD and the results were visualized with phos-tag acrylamide gel electrophoresis. To validate the use of the phos-tag acrylamide gel system to distinguish phosphorylated from unphosphorylated CdsD, the *in vitro* phosphorylation method was repeated using autophosphorylated recombinant PknD and its substrate, CdsD, following the protocol of Johnson *et al.* (Johnson and Mahony 2007). Briefly, the kinase domain of PknD (kPknD) and full-length CdsD were expressed with His-tags at

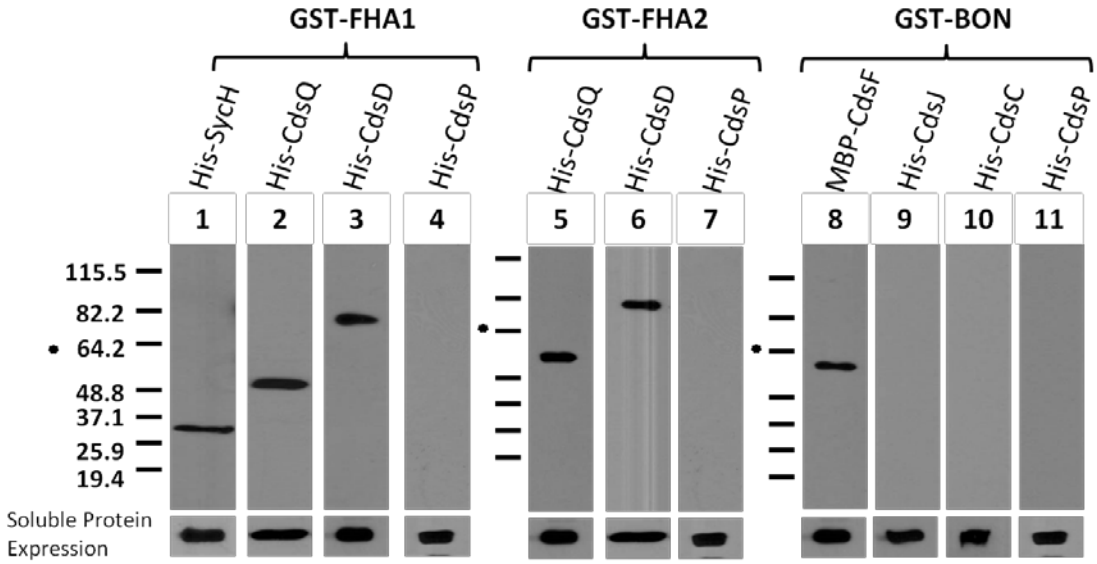

Figure 3.3 – Interactions of GST-FHA1, GST-FHA2, and GST-BON domains of CdsD with T3S proteins using GST pull-down assay. To determine if specific domains were involved in the interactions of specific T3S-associated components, GST-tagged fragments of CdsD (FHA1 (residues 25-90), FHA2 (residues 422-488), and BON (residues 645-845)) were expressed and immobilized on glutathione agarose beads. The high-affinity interactions established in Figure 3.2 were re-probed with each of the three GST-fusion fragments of CdsD. Lanes 1-4 display interactions between GST-FHA1 and His-tagged recombinant proteins. Under high salt conditions, His-SycH, His-CdsQ, and His-CdsD co-purified with GST-FHA1 (see lanes 1-3). Lanes 5-7 show interactions between GST-FHA2 and the same His-tagged recombinant proteins. Under high salt conditions, His-CdsQ and His-CdsD co-purified with GST-FHA2 (see lanes 5 and 6). Lanes 8-11 display interactions between GST-BON and His-tagged recombinant proteins. Under high salt conditions, only His-MBP-CdsF co-purified with GST-BON (see lane 8). Soluble expression of each His-tagged protein (displayed horizontally beneath lanes 1-11) was detected by WB with mouse anti-His (Sigma). GST was expressed alone (without the additional *Chlamydia* genetic component) and tested against each His-tagged protein lysate as a negative control to detect spurious interactions with the protein tag. No proteins displayed an interaction with GST alone under high salt conditions.

20°C and purified using a Ni-NTA column using FPLC. The two proteins were incubated as described above for two hours at 34°C and run on an 8% phos-tag acrylamide gel along with purified kPknD and CdsD (see Figure 3.4). This detection method is the only variation from the original *in vitro* kinase assay protocol developed previously (Johnson and Mahony 2007). The His-kPknD and His-CdsD were also electrophoresed simultaneously on a normal 8% SDS-PAGE for comparison with the kinase assay phos-tag acrylamide results. Prestained protein ladders were not used in conjunction with phos-tag acrylamide gels due to the fact that the ladder distorts the adjacent lanes and does not separate correctly in the presence of the phos-tag compound. Instead known recombinant proteins were used as markers of protein size.

We expected that the phos-tag acrylamide gel would separate phosphorylated kPknD and CdsD from their unphosphorylated counterparts. This technique would enable the identification of phosphorylated proteins *in vitro*. The results shown in Figure 3.4 display a distinct separation of two kPknD bands in the fourth lane and signify the presence of both unphosphorylated and phosphorylated kPknD in the purified sample. Also, both unphosphorylated and phosphorylated CdsD were detected in the purified sample (lane 3) and in the kinase assay (lane 5). As expected, the normal SDS-PAGE results show that both purified His-kPknD and His-CdsD migrate as one single band (lane 1 and 2, respectively). Unfortunately, due to the low sensitivity for detecting phosphorylated proteins in the mass spectrometry facility at McMaster University, were not able to confirm the identity of these phosphorylated proteins or identify the sites of phosphorylation by mass spectrometry.

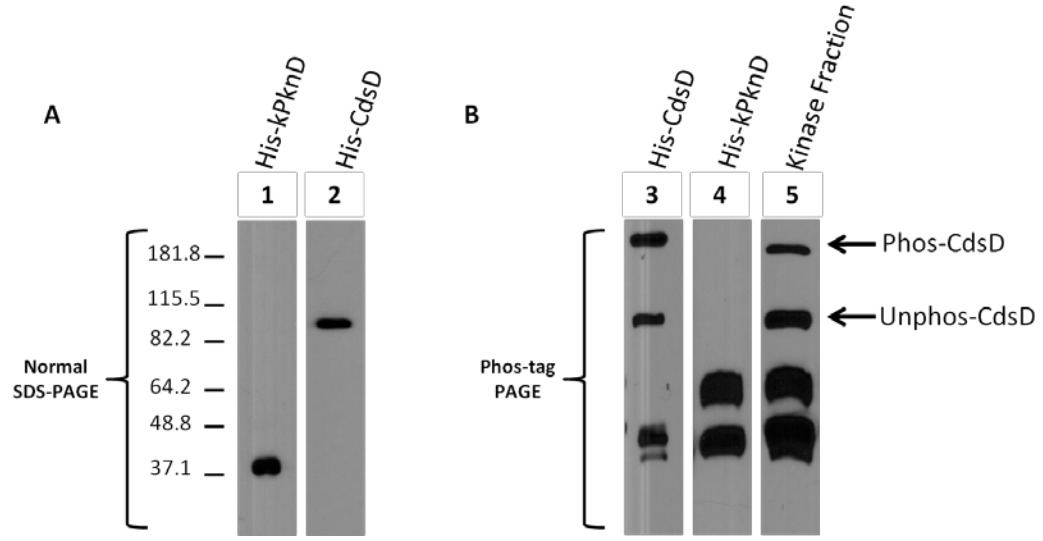

Figure 3.4 – Separation of phosphorylated and unphosphorylated CdsD and kPknD as identified by a phos-tag acrylamide gel. (A) A normal acrylamide gel (8%) shows the migration of the recombinant purified kinase domain of PknD (His-kPknD) and full length recombinant His-CdsD. Both proteins migrated at their predicted sizes(see lane 1 and 2, respectively). **(B)** A phos-tag acrylamide gel displays the migration of the same samples of purified His-kPknD and His-CdsD (see lanes 3 and 4). Lane 3 displays the migration of purified His-CdsD into two distinct bands. In addition, lane 4 displays the migration of purified His-kPknD into two distinct bands. Lane 5 indicates the presence of all four bands after both purified proteins were combined in an *in vitro* kinase assay. The kinase fraction (lane 5) consists of recombinant PknD and CdsD. Since the protein migration in a phos-tag gel is affected by the phosphorylation status in addition to its size, recombinant proteins of established sizes were run instead of a prestained protein ladder, which ran poorly and distorted the gel.

3.5 Detection of phosphorylated CdsD during the *Chlamydia* replication cycle

We attempted to detect phosphorylated CdsD by precipitating CdsD with anti-CdsD FHA2 antibody and electrophoresed the immunoprecipitated samples on phos-tag acrylamide gels in order to separate phosphorylated CdsD from unphosphorylated CdsD. Briefly, at 72 hpi, HeLa cells, infected with *C. pneumoniae* at an MOI of approximately

one, were harvested by bead lysis and purified on a discontinuous gastrografin gradient. Purified EBs located in the 44/59% gastrografin layer interface were lysed with ice-cold cell lysis buffer and mixed overnight with rabbit anti-CdsD FHA2 antibody (Colcalico Biologicals Inc.) attached to Protein A/G beads. The beads were centrifuged, washed and boiled in SDS sample loading buffer. Samples from the pellet, supernatant, beads, and recombinant protein preparations were run on an 8% phos-tag acrylamide gel and probed with high-sensitivity ECL reagents for five minutes. A lane of recombinant His-CdsD was electrophoresed alongside the immunoprecipitated fractions to gauge the appropriate molecular weight of the unphosphorylated CdsD.

The same experiment was repeated with RBs in order to detect phosphorylated CdsD mid cycle. Once again, CdsD was precipitated with rabbit anti-CdsD FHA2 antibody and then electrophoresed on a phos-tag acrylamide gel. Briefly, HeLa cells infected with *C. pneumoniae* at an MOI of approximately five were harvested at 40 hpi using a dounce homogenizer and purified on a discontinuous gastrografin gradient. Purified RBs located at the 35/55% gastrografin layer interface were lysed with ice-cold cell lysis buffer and mixed overnight with rabbit anti-CdsD FHA2 antibody (Colcalcio Biologicals Inc.) attached to Protein A/G beads. Once again, the beads were centrifuged, washed and boiled in sample loading buffer and electrophoresed on an 8% phos-tag acrylamide gel.

The results in Figure 3.5 show that phosphorylated CdsD was not detected by immunoprecipitation with anti-CdsD FHA2 antibody in purified EBs at 72 hours post infection (hpi) (see Figure 3.5). In the precipitated fraction (lane 5) only one band at

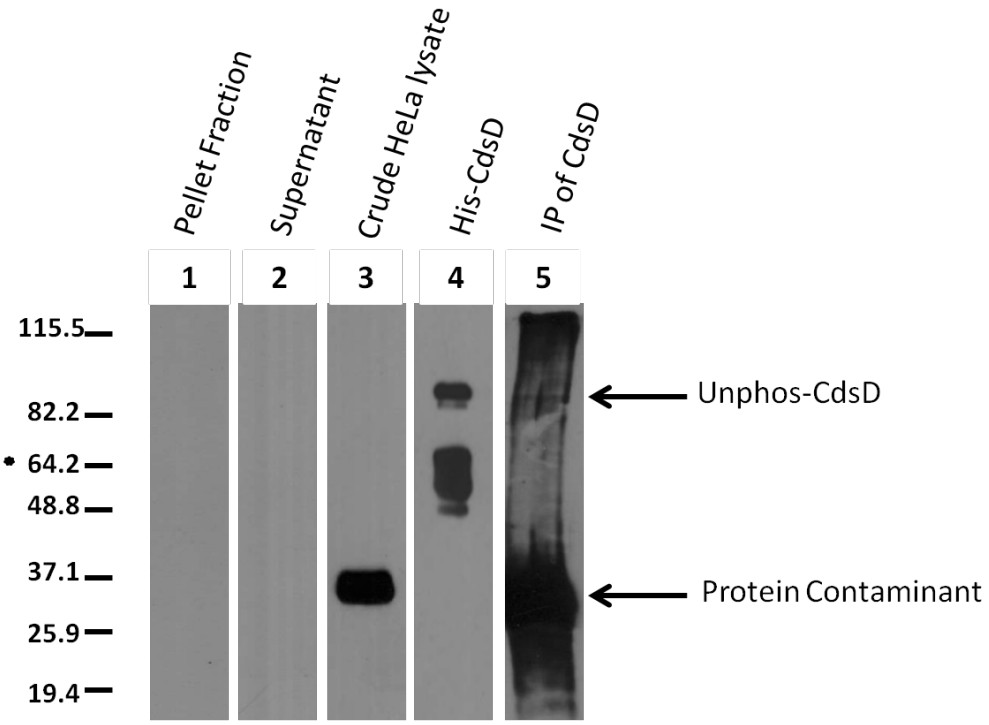

Figure 3.5 – Detection of unphosphorylated CdsD in purified *C. pneumoniae* EBs (72 hpi) using affinity purified rabbit anti-CdsD FHA2 antibody. Three fractions of *C. pneumoniae* lysates and one non-infected HeLa lysate were run on an 8% Phos-tag acrylamide gel and blotted with primary rabbit anti-CdsD FHA2 antibody (1:500) in order to detect CdsD. No bands were present in the pellet and supernatant fractions (see lane 1 and 2), however unphosphorylated CdsD was detected in the immunoprecipitation fraction, which was repeated in triplicate (see lane 5). Recombinant His-CdsD was run adjacent to the immunoprecipitation fraction to confirm the size of the desired protein (see lane 4). A low molecular weight band was detected in both the immunoprecipitated fraction and a non-infected HeLa cell lysate (see lanes 3 and 5). This band may represent a cross-reactive protein present in eukaryotic cells that was precipitated using rabbit-anti-CdsD FHA2 antibody (Colcalico Biologicals Inc.).

approximately 93 kDa was visualized by high-sensitivity ECL reagents. When comparing the electrophoretic mobility of this band to that of recombinant CdsD (lane 4), only unphosphorylated CdsD was precipitated in the lysed cells. The molecular weight of this band was measured by comparing the precipitated protein fraction to recombinant

CdsD (lane 4). This experiment was repeated at 40 hours post infection and by purifying RBs using a discontinuous gastrografin gradient, however CdsD was not detected in these fractions. Cross-reactivity with another protein of approximately 35 kDa was present as evident in the crude cell lysate (non-purified *C. pneumoniae* infected HeLa cells). This protein contaminant was also precipitated by the rabbit anti-CdsD FHA2 antibody in the purified immunoprecipitated *C. pneumoniae* infected sample. No protein was detected by anti-CdsD FHA2 western blotting in the pellet or precipitated supernatant fractions.

3.6 The phosphorylation of CdsD by PknD may promote CdsD oligomerization

The phosphorylation of CdsD by PknD may enable the formation of high-order complexes in the IMR of *C. pneumoniae.* Native gel electrophoresis was used in combination with the *in vitro* kinase assay to determine if the phosphorylation of CdsD is related to the formation of oligomers. Recombinant His-CdsD and GST-kPknD were expressed and purified in *E. coli*, run in an *in vitro* kinase assay, and electrophoresed simultaneously on 8% phos-tag and native acrylamide gels. The presence of phosphorylated CdsD in each reaction mixture was demonstrated using the phos-tag acrylamide gel and WB to separate and visualize unphosphorylated from phosphorylated CdsD. The results in Figure 3.6 show that high molecular weight compounds were found in the non-denaturing gel at approximately 180 kDa, which is consistent with the size of a dimeric complex (see lane A2). The high molecular weight bandswere absent on the native gel after the addition of lambda phosphatase to recombinant His-kPknD and His-

CdsD (see lane A3). Only unphosphorylated CdsD was present in the phosphatase-treated sample, as indicated by the phos-tag acrylamide gel in lane B3. The non-

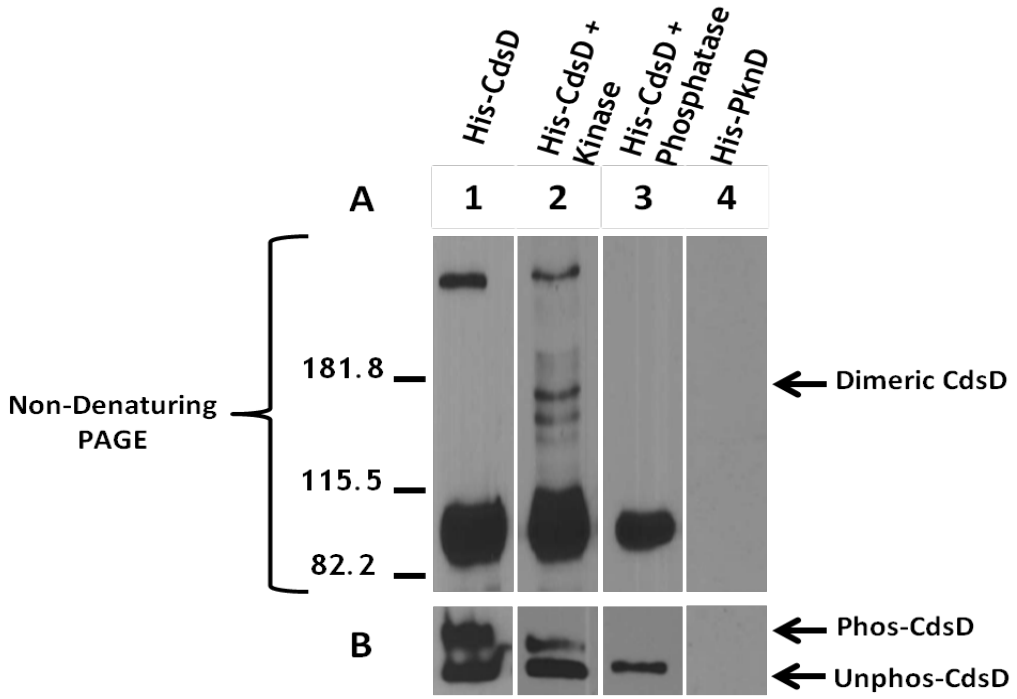

Figure 3.6 – Phosphorylation-dependent oligomerization of CdsD. After performing simultaneous *in vitro* kinase and phosphatase assays, one half of each reaction volume (approximately 15 µL) was loaded into a non-denaturing native gel (A) and the other half was loaded into a phos-tag acrylamide gel (B). **(A)** After probing for CdsD using rabbit anti-CdsD FHA2 antibody, high molecular weight complexes were identified (see lanes A1 and A2)only in the presence of phosphorylated CdsD (confirmed in lanes B1 and B2). These multimeric complexes were not visualized by WB in the presence of a generic phosphatase (see lane A3). After stripping the membrane and re-probing with rabbit anti-kPknD, there was a lack of kPknD present in the high molecular weight complexes (see lane A4). **(B)** Phos-tag acrylamide gel electrophoresis was used to confirm the presence of phosphorylated protein products. Lane B1 and B2 show a distinct separation of two bands representing phosphorylated and unphosphorylated His-CdsD, whereas lane 3 shows only one His-CdsD band present in the phosphatase reaction.

denaturing gel was stripped and re-probed with rabbit anti-PknD to detect high molecular weight complexes involving PknD, however no bands were visualized above 80 kDa (see

lanes A4 and B4). Multiple bands have been consistently present between approximately 60 and 75 kDa (see lane 4 in Figure 3.5 for example) in each protein preparation and predict that they are degradation products of CdsD (as they are detected by anti-CdsD Western blotting). The proteins in these gels were expressed and induced under the same conditions as previous protein preparations used in kinase assays (such as in Figure 3.4). Recombinant purified His-CdsD prepared in kinase activity buffer was also capable of forming a high molecular weight complex, however without the addition of His-kPknD, ATP, HEPES, $MnCl_2$, and β-glycerophosphate the dimeric complex was not present.

3.7 CdsD FHA2 contains conserved residues that may form a phospho-threonine binding pocket

FHA domains in eukaryotic and prokaryotic proteins have been shown to interact specifically with phosphorylated threonine residues. In contrast to the phosphorylation-dependent oligomerization hypothesis presented previously, the two FHA domains of CdsD may bind to other phosphorylated proteins associated with the T3S apparatus. To identify the potential for phosphate binding, the sequence similarity of well-characterized FHA domain-containing proteins, including Rad53, Rv0020c, Chk2, CT664, and YscD, were compared along with both predicted FHA domains of CdsD and analyzed for the conserved regions and residues of the FHA domains (see Figure 3.7). The FHA1 domain of CdsD falls between amino acids 25 and 79 and the FHA2 domain of CdsD is predicted to range from amino acid 417 to 466. Figure 3.7 displays the six conserved residues from

these FHA domain-containing proteins (glycine, arginine, serine, histidine, asparagine, and a second glycine residue). Five of the six conserved glycine, arginine, serine,

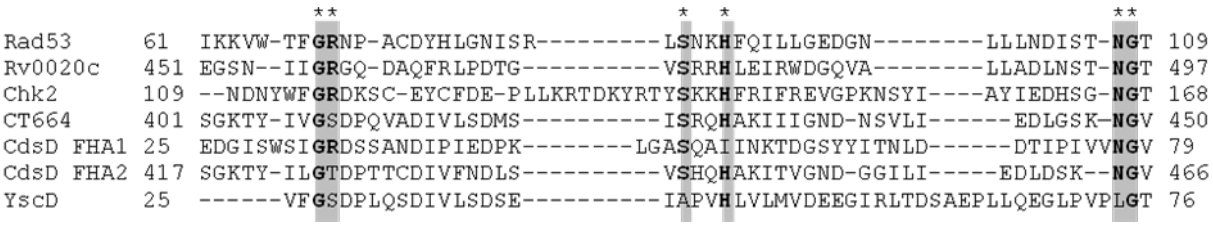

Figure 3.7 – Sequence alignment of FHA domains in various prokaryotic and eukaryotic proteins displays the presence of conserved amino acids. A comparison of seven putative FHA domain sequences from human cells (Rad53 and Chk2), *C. trachomatis* (CT664), *C. pneumoniae* (CdsD FHA1 and FHA2), *Y. pestis* (YscD), and *Mycobacterium tuberculosis* (Rv0020c). FHA domains are predicted to have six conserved residues within a predicted beta sandwich motif. Five of these conserved residues are present within the FHA1 domain of CdsD (G33, R34, S51, N76, and G77) and within the FHA2 domain of CdsD (G424, S441, H444, N464, and G465). Among these seven sequences, all seven protein contained at least three conserved residues.

histidine, and asparagine residues are present in both the FHA1 and FHA2 domains of CdsD.

Furthermore, to ensure that these residues would contribute collaboratively to a single binding pocket, the Phyre server was used to model the structure of the FHA2 domain of CdsD and mark conserved residues that may form a binding pocket (see Figure 3.8). These residues were highlighted and visualized using Pymol software. Four of these conserved residues (S441, H444, N464, and G465) were found in close proximity and localized to one section of the FHA domain between loops 3-4 and loops 5-6. This highlighted region was consistent with the phosphate-binding regions of other FHA domains (Liang and Van Doren 2008).

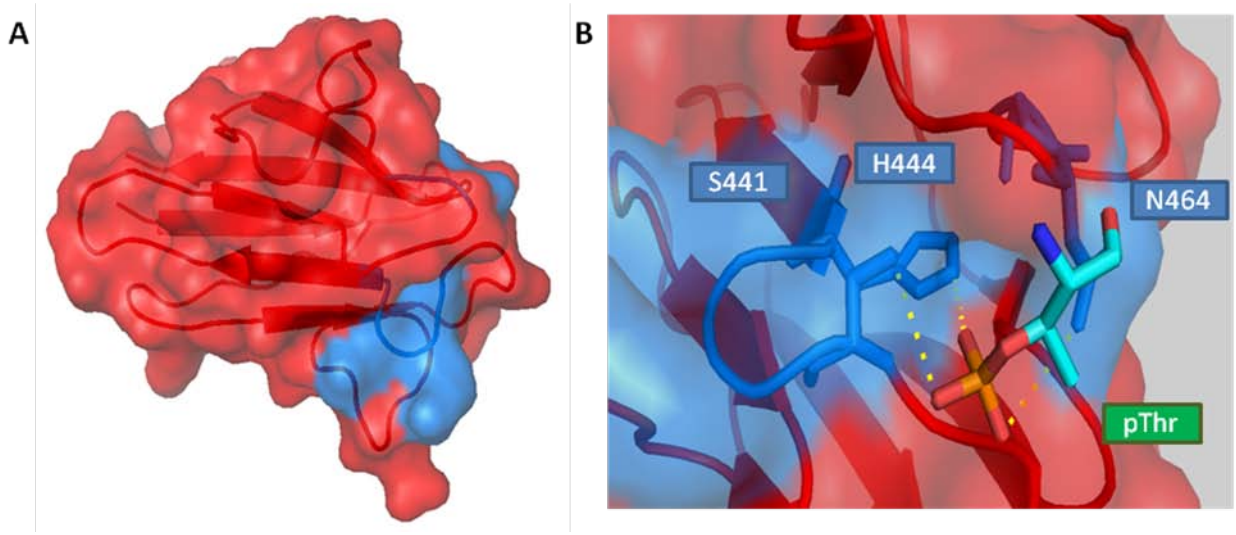

Figure 3.8 – Model of key amino acids involved in phospho-threonine binding based on the structure of the FHA2 domain of CT664 (A) A predicted structure of the FHA2 domain (residues 422-488) of CdsD (developed by the Phyre server) shows a predicted hydrophilic phosphate binding pocket (blue) between loops 3-4 and 5-6. **(B)** The conserved serine (S441), histidine (H444), and asparagine (N464) residues form the phosphate binding pocket and coordinate the interaction with phosphothreonine residues. This is a hypothetical diagram based on the structural information provided by the Phyre server. The FHA domain tertiary structure was developed based on the unpublished crystal structure of the FHA2 domain of CT664 on the protein data bank.

3.8 CdsD interacts specifically with phosphorylated PknD

Information gathered in section 3.7 revealed a model of a phosphate-binding pocket composed of four conserved phospho-threonine binding residues located in the FHA2 domain of CdsD. To explore the possible interaction between CdsD and other phosphorylated proteins *in vitro*, recombinant GST-CdsD was expressed in *E. coli* (BL21) and purified along with the recombinant His-CdsQ and His-kPknD, which displayed positive results in previously reported GST pull-down experiments. His-kPknD was electrophoresed along with a positive control, His-CdsQ, on an 8% phos-tag acrylamide gel, transferred to nitrocellulose membranes, and probed with approximately 500 ug of recombinant purified GST-CdsD. Rabbit anti-CdsD FHA2 and goat anti-rabbit

antibodies were added in successive blocking steps in order to probe for GST-CdsD bound to immobilized His-CdsQ and His-kPknD on the membrane. After detection with ECL reagents, the membrane was stripped and re-probed for His-tagged protein detection.

PknD may need to be phosphorylated in order to interact with CdsD. The Far-Western blot results in Figure 3.9 show that recombinant GST-CdsD binds to the higher molecular weight band of His-kPknD (see Figure 3.9, lane 2). Also, recombinant CdsD did not bind to unphosphorylated kPknD, as observed in lane two. Moreover, after expressing and purifying the recombinant GST-FHA2 and GST-FHA1 domains of CdsD, the FHA2 domain of CdsD interacted solely with the immobilized phosphorylated kPknD (see lane 3). GST-FHA1 did not bind to either the unphosphorylated or phosphorylated band of His-kPknD (see lane 4). CdsD bound to a single band of immobilized His-CdsQ, which was used as a positive control to ensure that the overlay of CdsD on the membrane was successful (data not shown). The negative control, GST alone, was incapable of binding to either His-kPknD or His-CdsQ bands.

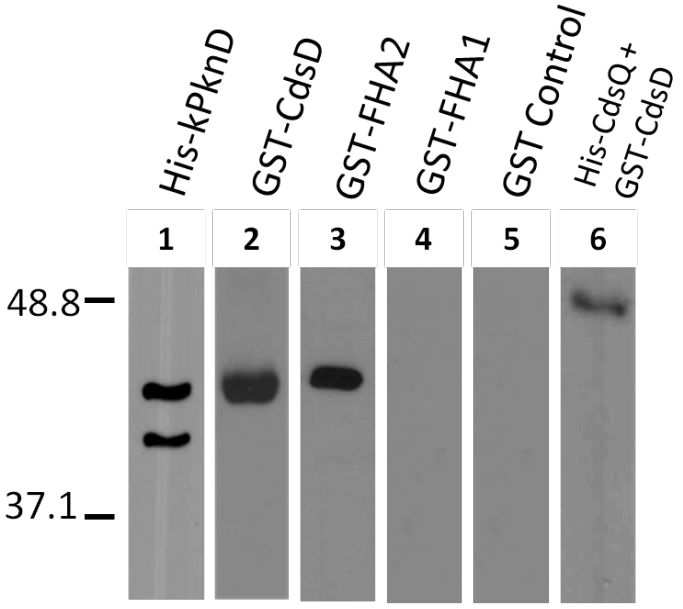

Figure 3.9 – Far-Western blotting indicates that GST-CdsD and GST-FHA2 bind specifically to phosphorylated PknD. Purified Recombinant His-kPknD electrophoresed on a Phos-tag gel and probed with GST-CdsD, GST-FHA2, or GST (1.25 ng/µL), with secondary mouse anti-GST antibody, and finally with tertiary goat anti-mouse antibody conjugated to HRP for detection with ECL reagents. Recombinant GST-CdsD and GST-FHA2 interacted with only the phosphorylated form of His-kPknD (see lanes 2 and 3). GST alone did not interact with His-kPknD (see lane 4) and the kPknD positive control was positive for both phosphorylated and unphosphorylated kPknD (see lane 1). The positive control in lane 6 demonstrates that recombinant CdsD interacted with His-CdsQ by Far-Western blot, which was consistent with GST pull-down data.

CHAPTER FOUR

GENERAL DISCUSSION

4.1 Structural role of CdsD in the T3S apparatus

PrgH, the IMR protein of *Salmonella* is possibly the best studied ortholog of CdsD and is thought to be essential for T3S. The gene encoding the ortholog of CdsD in *Salmonella*, *prgH*, exists on an operon along with three other T3SS genes *prgI*, *prgJ*, and *prgK*, which encode two needle proteins and another inner membrane protein (Pegues, Hantman *et al.* 1995). A genetic knockout of *prgH*, created by Miller *et al.* was shown to prevent bacterial-mediated endocytosis of *S. typhimurium*; however, complementation with a plasmid encoding the *prgH* gene reverted the phenotype to enable secretion (Pegues, Hantman *et al.* 1995). The assembly of the base structure of the injectisome is thought to be independent of effector proteins and membrane components; however the insertion of PrgH and PrgK into the membrane has been demonstrated to be dependent upon intact peptidoglycan layers (Pucciarelli and Garcia-del Portillo 2003). The interaction between peptidoglycan and PrgH may facilitate the formation of the inner membrane ring (Pucciarelli and Garcia-del Portillo 2003). Many molecular models of the injectisome in *Salmonella*, *Yersinia*, and *Shigella* have been published regarding the precise location of CdsD orthologs in the inner membrane (Marlovits, Kubori *et al.* 2004). In addition, multiple orthologs of CdsD, such as PrgH and YscD from *Salmonella* and *Yersinia*, have also been shown to interact with the outer membrane secretin ring, InvG and YscC, and the inner membrane proteins PrgK and YscJ, respectively (Diepold, Amstutz *et al.* 2010; Sanowar, Singh *et al.* 2010). Collectively, these data, together with

a high homology score, suggest that CdsD may play a structural role in the T3S apparatus similar to those of PrgH and YscD.

4.1.1 Interactions of CdsD in the basal body of the T3S apparatus

The basal body component of the T3S apparatus in *C. pneumoniae* is believed to be composed of multiple structural and functional proteins. Previous studies in *Salmonella* and *Yersinia* have shown that CdsD is one of the first T3S-associated proteins inserted into the membrane. It is believed that CdsD provides structure to the apparatus by stabilizing the other membrane components in the inner and outer bacterial membranes. We performed GST pull-downs using recombinant full length GST-CdsD with other T3S-associated membrane components to characterize the interactions with other T3S-associated membrane components. We cloned and expressed His-tagged recombinant proteins of predicted inner membrane (CdsU, CdsR, CdsS, CdsT, and CdsJ) and outer membrane (CdsC) components. His-tagged recombinant CdsS, CdsR, CdsT and CdsU and His-NusA-tagged CdsC and CdsJ were all soluble and expressed in *E. coli* (BL21) for use in GST pull-down assays.

Diepold *et al.* reported that YscJ, the ortholog of CdsJ, is essential for mediating the interactions between YscD and the inner membrane components. Consistent with this hypothesis, the inner membrane components CdsS, CdsR, CdsT, and CdsU did not interact directly with recombinant CdsD *in vitro* in the GST pull-down assay (see Figure 4.1 for summary of interactions). With the exception of a NusA-His-CdsJ interacting under low salt conditions, none of the proteins formed stable interactions under high salt

conditions. These results suggest that the inner membrane components likely aggregate and form a protein complex independent of CdsD. From the published results with orthologous proteins in *Yersinia*, we hypothesized that there would be an interaction between CdsD and CdsC, the outer membrane secretin, under high salt conditions. However, this GST pull-down experiment was also negative. The relatively large NusA protein tag may have interfered with the interacting domains of native CdsJ and CdsC, which was added initially to increase solubility of the recombinant proteins. This is a valid assumption considering that CdsJ is a relatively small protein compared to the size of the tag and that the predicted interaction with the C-terminus of CdsC may be hindered by the presence of a large C-terminal protein tag. Future experiments that use C-terminal NusA protein tag may help detect the predicted interaction between these membrane components *in vitro*.

4.1.2 Interactions of CdsD with cytoplasmic components of the T3S apparatus

At the base of the T3S apparatus, CdsD is believed to stabilize components of the cytoplasmic ring. Our laboratory has shown, with Triton X-114 phase partitioning, that CdsD resides in the cytoplasm and TMpred predicts one transmembrane region between residues 546 and 568 (Johnson, Stone *et al.* 2008). This evidence suggests that cytoplasmic portions of CdsD may interact with cytoplasmic components of the T3S apparatus. In the past, Johnson *et al.* have shown that recombinant CdsD interacts with two cytoplasmic components of the C-ring antechamber (Johnson, Stone *et al.* 2008). In addition, Stone *et al.* have provided *in vitro* evidence that CdsD also interacts with the

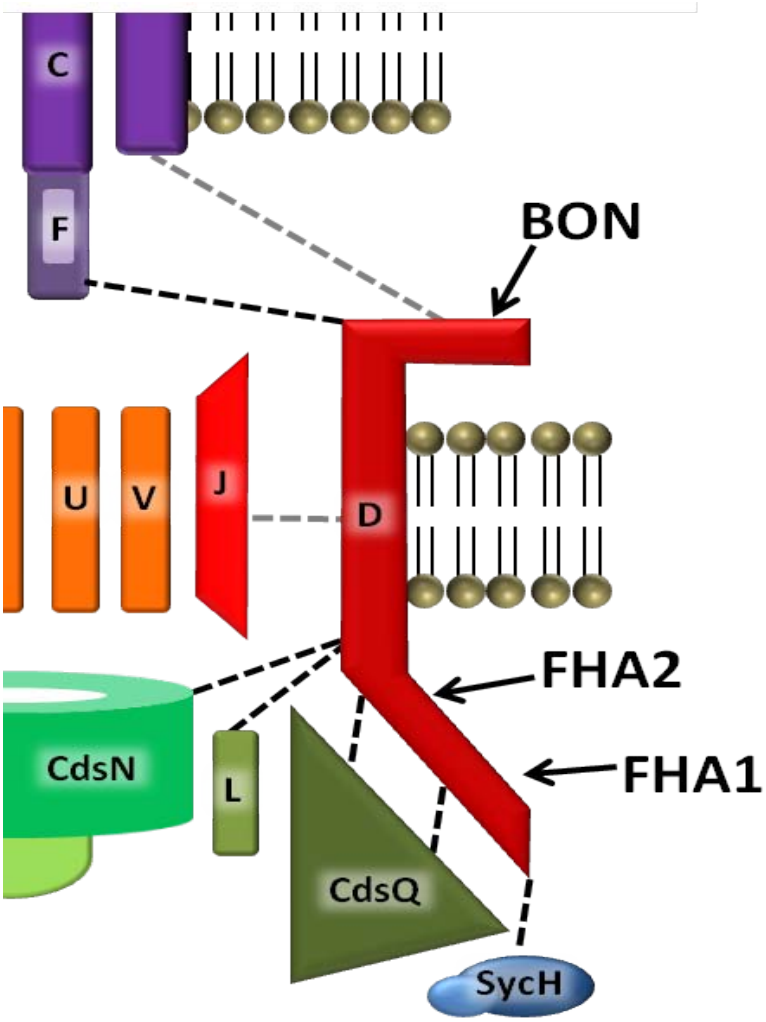

Figure 4.1 – Summary of proposed interactions in the T3S apparatus. A schematic diagram of the interactions predicted by GST pull-down results (indicated in black) and the hypothetical interactions predicted in orthologs (indicated in grey) that have yet to be confirmed by GST pull-down. It is possible that the interactions of CdsC and CdsJ with CdsD may have been sterically hindered by the large, soluble N-terminal NusA protein tag.

putative ATPase, CdsN (Stone, Johnson *et al.* 2008). As a result, we hypothesize that

CdsD stabilizes and interacts with cytoplasmic proteins at the base of the T3S apparatus.

Lara-Tegjero *et al.* suggested that the formation of a sorting platform at the base of the injectisome may involve stabilization by inner membrane components. The sorting platform, composed of C-ring proteins and some IMR components, is thought to regulate the recruitment of chaperone/effector complexes and timed secretion of specific T3S effectors. With the relatively large N-terminal cytoplasmic domain, CdsD may represent one of the proteins involved in stabilizing the functional C-ring proteins. We performed GST pull-downs with recombinant GST-CdsD and His-CdsQ, His-CdsL, His-CdsD, His-SycH (*Cpn0713*) and His-kPknD. His-CdsN was not recloned into a pDEST544 vector because an interaction with GST-CdsD had already been confirmed by Stone *et al.* (Stone, Bulir *et al.* 2011). The positive results of these GST pull-downs with His-CdsQ and His-CdsL confirm the results of previous studies and were used primarily as positive controls for detecting novel interactions. These predicted cytoplasmic proteins likely form a complex, along with the cytoplasmic portion of CdsD, at the base of the apparatus that is involved in localizing chaperone/effector complexes to the membrane. The *in vitro* evidence of interactions between CdsD and CdsQ, CdsL, and CdsN indicates a possible connection between basal body components and C-ring components at the base of the apparatus. As expected, the interaction between GST-CdsD and His-CdsD is consistent with the formation of CdsD oligomers that has been reported in orthologs of CdsD, which form higher-order ring complexes in the inner membrane. In addition, novel interactions with the putative kinase PknD and the upstream chaperone SycH indicate additional roles of CdsD in the base of the injectisome. The interaction between CdsD and the putative class IA chaperone, SycH, may indicate a role for CdsD orthologs in the sorting platform.

This is the first evidence of a chaperone-binding ability of CdsD and future experiments should explore interactions with other chaperone classes in order to elucidate the role of CdsD in the sorting process.

PknD is one of three putative serine/threonine kinases in *C. pneumoniae* and has been shown to phosphorylate MBP and CdsD *in vitro* (Verma and Maurelli 2003; Johnson and Mahony 2007). Our laboratory has shown previously that PknD is an integral inner membrane protein which has a catalytic domain in the cytoplasm (Johnson and Mahony 2007). The *in vitro* interaction between CdsD and PknD may suggest a role for phosphorylation signalling at the base of the T3S apparatus. Johnson *et al.* were capable of phosphorylating CdsD with kPknD *in vitro*; however, at this point, there is no evidence of phosphorylated T3S-associated structural components. Therefore, it is more likely that this interaction is based on the strong affinity of the FHA domain of CdsD for the phosphorylated threonine residues of PknD. These two hypotheses are explored further in section 4.2 and 4.3 of this thesis.

4.1.3 Interactions of CdsD with predicted periplasmic components of the T3S apparatus

Based on the research in *Yersinia* by Ross and Plano, orthologs of CdsD are believed to contain periplasmic domains that interact with components of the outer membrane (Ross and Plano 2011). The C-terminal 300 amino acids are believed to form a ring-building motif and a bacterial OmpY and nodulation (BON) domain, which binds phospholipids. We predicted that CdsD may also interact with other T3S-associated

periplasmic proteins such as the putative filament protein, CdsF, and ruler protein, CdsP. We cloned *cdsF* and *cdsP* into pDESTperiHisMBP and pDEST17, respectively, to create His-MBP-CdsF and His-CdsP recombinant fusion proteins. CdsF required a larger protein tag because it was too small (approximately 9 kDa) for purification and may have been degraded during protein preparation. We showed that GST-CdsD interacts with His-MBP-CdsF and this interaction was stable under high salt conditions. This result suggests that CdsD may play a role in the construction, localization, or stabilization of the needle complex thereby anchoring the filament in the periplasm. The interaction between the needle filament and the basal body may be unique to *C. pneumoniae* as it has not been reported in other Gram-negative T3S systems. Conversely, there was no interaction between GST-CdsD and His-CdsP. This is consistent with the ruler protein, Spa32, in *Shigella*, which may be anchored to an ortholog of CdsU in the cytoplasmic ring and not the inner membrane components.

4.1.4 Cytoplasmic and periplasmic domains interact with T3S-associated components

The SMART server predicts that CdsD contains two FHA domains (e value = $1.25e^{-01}$ and $1.03e^{-11}$, respectively) and one BON domain (e value = $1.30e^{-04}$). With one predicted transmembrane domain (TMpred and SMART), we hypothesized that CdsD inserts into the membrane and interacts with proteins in both the cytoplasm and periplasm. Using full-length GST-CdsD pull-downs, we found that CdsD interacts with both cytoplasmic and periplasmic components associated with the T3S apparatus. To

further characterize these interactions, we cloned the two cytoplasmic domains of CdsD, FHA1 (amino acids 25-90) and FHA2 (amino acids 422-488), and the periplasmic BON domain (amino acids 707-767) and used them to perform GST pull-downs with the previous interactions with full-length GST-CdsD. Based on the topology of CdsD orthologs, we predicted that the FHA1 and FHA2 domains are localized to the cytoplasm. The cytoplasmic proteins CdsQ, PknD and SycH might interact with the FHA1 and FHA2 domains of CdsD. Under high salt conditions, GST-FHA1 interacted with the class I chaperone, SycH, the shuttling protein, CdsQ, and His-CdsD. GST-FHA2 also interacted with CdsQ and CdsD and GST-BON interacted with the filament protein CdsF.

The interaction between the FHA1 domain of CdsD and the chaperone SycH is novel. Previous studies in *Yersinia*, report that the stability of YopN, another T3S-associated component, is reduced in the absence of its chaperones SycH and YscB (Day and Plano 1998). Similarly, the interaction between CdsD and SycH in *Chlamydia* may increase the stability of the cytoplasmic domains of CdsD. The *Chlamydia* gene encoding this chaperone, *sycH*, is immediately upstream of *cdsD* in the same operon and it is probable that these genes are expressed at the same time point (approximately 20 hours post infection) in the developmental cycle (Belland, Zhong *et al.* 2003). This hypothesis is supported by our observation of a large amount of degradation products upon ectopic expression of His-CdsD in *E. coli* (BL21) in the absence of this chaperone.

CdsD also interacted with the cytoplasmic protein, CdsQ, via the FHA1 and FHA2 domains. Orthologs of CdsQ in *Shigella* and *Salmonella* are associated with inner membrane components and are involved in docking chaperone/effector complexes in the

C-ring sorting platform (Stamm and Goldberg 2011). With the relatively large cytoplasmic domain of CdsD, it is possible that the CdsD interacts with multiple C-ring components. We predict that the cytoplasmic portion of CdsD may form part of the sorting platform in the base of the T3S apparatus. At the very least, these results suggest that the N-terminal domain of CdsD resides in the cytoplasm and provides a scaffolding function for C-ring components of the T3S apparatus.

Orthologs of CdsD in *Salmonella* and *Shigella* form oligomeric rings in the inner membrane. The interactions between the cytoplasmic FHA1 and FHA2 domains of CdsD and full-length CdsD indicate that the oligomerization domain may reside in the cytoplasm. This result contrasts the research by Spreter *et al.*, which identified a ring building motif in the periplasmic domain of PrgH (Spreter, Yip *et al.* 2009). This atypical oligomerization domain could be the result of the additional 400 amino acids at the N-terminus of CdsD, which share limited sequence similarity with any T3S-associated Gram-negative component.

The role of the periplasmic portion of CdsD is not known. The predicted periplasmic portion, GST-BON, had a strong interaction with the filament protein CdsF, suggesting that the periplasmic portion of CdsD may play a role in anchoring the base of the needle complex. Consistent with the hypothesis that CdsD stabilizes CdsF in the periplasm, neither the FHA1 nor the FHA2 domain interacted with CdsF. These results imply that CdsD does not directly interact with CdsF in the cytoplasm or at the base of the apparatus. In addition, the lack of an interaction between the BON domain and the ruler protein, CdsP, supports that control of the needle length may not involve the

periplasmic domain of CdsD. As a result, we predict that CdsD anchors the base of the needle filament in the periplasm and is not involved in the recruitment and secretion of filament proteins during the assembly of the apparatus.

4.2 Phosphorylation of CdsD in *C. pneumoniae*

In 2007, the Mahony laboratory identified that recombinant PknD phosphorylated CdsD *in vitro* (Johnson and Mahony 2007). Although this result was not demonstrated *in vivo,* this was the first published evidence of a phosphorylated structural component of the T3S apparatus in Gram-negative bacteria. We hypothesized that CdsD may be phosphorylated in *C. pneumoniae* either to aid in the assembly of the apparatus or to contribute to its functional activity. To detect phosphorylated protein we performed immunoprecipitations of CdsD in *C. pneumoniae* at 48 and 72 hours post infection. Since we were adapting the protocol of the *in vitro* kinase assay to exclude the use of radioisotopes, we corroborated the *in vitro* kinase results using phos-tag gel acrylamide electrophoresis. The results demonstrated that PknD was capable of autophosphorylation in enzyme activity buffer, thereby supporting the previously published data in *C. trachomatis* by Verma and Maurelli (Verma and Maurelli 2003).

Surprisingly, recombinant CdsD was also phosphorylated in *E. coli* without PknD. With the presence of multiple hypothetical serine/threonine protein kinases in *E. coli*, recombinant His-CdsD may be phosphorylated by a generic kinase prior to purification with a Ni-NTA column. Regardless, the *in vitro* kinase assay conditions showed both autophosphorylated PknD and phosphorylated CdsD. This evidence supported the results

presented in previous studies and confirmed the utility of phos-tag acrylamide gel electrophoresis for visualizing phosphorylated proteins (Johnson and Mahony 2007).

4.2.1 The phosphorylation status of CdsD in *C. pneumoniae*

Post-translational protein phosphorylation is an important mechanism for regulating a variety of prokaryotic cell processes. Although no evidence of protein phosphorylation in the virulence mechanisms of *C. pneumoniae* currently exists, we speculated that the *in vitro* evidence of the phosphorylation of CdsD may represent a novel regulatory mechanism for T3S in *C. pneumoniae*. Our initial hypothesis was that the phosphorylation status of CdsD was important for the structural assembly of the apparatus, implying that the phosphorylation of CdsD may regulate the assembly of the injectisome *in vivo*. Therefore, at 72 hpi a fully formed apparatus would be expected to contain phosphorylated CdsD. We performed an immunoprecipitation, using an affinity purified anti-CdsD antibody, to detect phosphorylated CdsD in *C. pneumoniae*. The precipitated protein sample was run on an acrylamide gel and a phos-tag acrylamide gel to separate phosphorylated from unphosphorylated precipitated protein. We were, however, unable to detect phosphorylated CdsD at 72 hpi. At 72 hpi, CdsD was detected weakly in the precipitated fraction and no phosphorylated products were detected by WB. This experiment was performed in triplicate and there was no detectable CdsD in the negative control fractions. Additionally, we tested for the phosphorylation of CdsD at 48 hpi in purified RBs and were unable to detect CdsD by WB, indicating a low level of CdsD expression in RBs. Due to the relatively weak WB signal, the antibody may not

have been able to precipitate a sufficient quantity of CdsD for detection of phosphorylated protein. According to Cozzone, the total amount of phosphorylated protein in prokaryotes was much lower than that of eukaryotic proteins, which makes them far more difficult to detect by conventional immunoprecipitations (Cozzone 1988). An even smaller percentage of prokaryotic proteins are phosphorylated on tyrosine residues, as was suggested by Johnson *et al.* using thin-layer chromatography (Johnson and Mahony 2007). In the future, a more sensitive detection method, such as autoradiography, combined with a pulse-chase time-course experiment could perhaps be used to detect phosphorylated CdsD *in vivo*.

Alternatively, since post-translational phosphorylation events are reversible and transient, we cannot definitively rule out the occurrence of phosphorylated CdsD in *Chlamydia* at stages in the developmental cycle other than at 40 and 72 hpi. If the phosphorylation of CdsD does not occur at 72 hpi, then the phosphorylation of CdsD may not be involved in stabilizing the multimeric inner membrane ring in EBs. Phosphorylation of CdsD could be involved in other aspects of protein activity, such as its degradation. However, the immunofluorescent detection of CdsD in *C. pneumoniae*-infected HeLa cells at 72 hpi by our laboratory indicates that it is unlikely that phosphorylation triggers protein degradation (Johnson, Stone *et al.* 2008). The remainder of these hypothetical events will require extensive experimentation as discussed further in section 4.4 and in the future experiments section of this thesis.

4.2.2 Role for CdsD phosphorylation in the phosphorylation-dependent oligomerization of CdsD

Phosphorylated FHA domains exist in a small number of eukaryotic and prokaryotic protein systems, while the phosphorylation of residues adjacent to phospho-peptide binding domains, such as the MH2 and SH2 domains, is not rare (Xu, Tsvetkov *et al.* 2002). Phosphorylation-dependent oligomerization is one mechanism which requires both of these features and has been demonstrated previously in eukaryotic systems. In the past, Chk2, a eukaryotic checkpoint kinase, has demonstrated a phosphorylation-dependent oligomerization event wherein a phosphorylated residue within one FHA domain acts as the binding partner for the FHA domain on another monomer (Xu, Tsvetkov *et al.* 2002). CdsD orthologs, such as PrgH and MxiG, have been shown to form multimeric ring-like structures in the inner membrane of *Salmonella* and *Shigella* (McDowell, Johnson *et al.* 2011). Stemming from the involvement of FHA domains in phosphorylation-dependent oligomerization of eukaryotic proteins, we hypothesized that the oligomerization of CdsD may be dependent on its phosphorylation state. To test this hypothesis, we used phos-tag acrylamide gel electrophoresis and lambda phosphatase to examine the phosphorylation state of CdsD in monomers and oligomers of CdsD. We found that CdsD oligomers contained phosphorylated CdsD while phosphatase-treated CdsD failed to form oligomers. Collectively, these results indicate that phosphorylation events could be involved in the formation of oligomeric CdsD in the inner membrane of *C. pneumoniae*. The high-molecular weight complexes observed were at a size of approximately 180 kDa, which represents the predicted size of a dimeric complex of

CdsD. Two predicted orthologs of CdsD, PrgH and MxiG, however, have demonstrated the ability to form rings with 24-fold and 20-fold symmetry, respectively (Sanowar, Singh *et al.* 2010). Therefore, even though the phosphorylation of CdsD *in vitro* may permit the formation of a dimeric complex, the formation of high-order complexes of CdsD may not require a phosphorylation event. The relevance of this *in vitro* phosphorylation-dependent dimerization will need confirmation *in vivo.* Future experiments could confirm the size of high-order complexes of CdsD in native gels using a high molecular weight markers and a longer electrophoresis time.

4.3 The role of the CdsD FHA domains

In the GST pull-down experiments described previously, we observed a strong interaction between the kinase domain of PknD and full-length CdsD. Although we determined that CdsD may interact with PknD resulting in CdsD phosphorylation, we did not expect to be able to see a high affinity interaction between the enzyme and its substrate. In the past, both Johnson *et al.* and Verma and Maurelli have shown that PknD is putatively autophosphorylated on threonine residues using thin-layer chromatography (Verma and Maurelli 2003; Johnson and Mahony 2007). We hypothesized that the interaction between CdsD and PknD may be based on the high affinity of the FHA domains for phosphorylated threonine residues. As a result, it was important to characterize the possible roles of the CdsD FHA domain in relation to the context of other T3S proteins.

4.3.1 CdsD binds specifically to phosphorylated threonine residues

The FHA domain of eukaryotic and prokaryotic proteins contains six conserved residues that form a binding pocket for phosphorylated threonine residues. The two FHA domains in CdsD are predicted to form a beta sandwich, a fold of eleven beta strands characteristic to all FHA domains (Liang and Van Doren 2008). Five conserved residues are present in both the FHA1 and FHA2 domains of CdsD suggesting that these domains may be capable of binding phosphorylated threonine residues on other proteins. Together with predicted structural data (Phyre server) from the crystal structure of CT664, four of these residues could form a phosphate-binding pocket. The results of the Far-Western blots show that CdsD interacts specifically with phosphorylated PknD, but not with unphosphorylated PknD. This suggests that CdsD may bind specifically to phosphorylated components of the T3S apparatus.

CdsD is unique amongst its orthologs in that it contains an additional 400 amino acids that may contain two FHA domains. To further characterize this phospho-specific interaction, we cloned and expressed GST-FHA1 and GST-FHA2 and repeated the Far-Western blot. We found that the GST-FHA2 domain bound specifically to phosphorylated PknD band and not to the unphosphorylated protein. The FHA2 domain may require a specific sequence in order to bind with high affinity to the phosphorylated PknD. Liang and Doren provide evidence with eukaryotic proteins that the phospho-threonine motif on the substrate determines the specificity of the interaction with the FHA domain, such as the phospho-threonine motif on Rad9 and its interaction with the FHA domain of Rad53 (Liang and Van Doren 2008). This specificity depends on the sequence

variation within each binding pocket. Crystallization of CdsD FHA domains may aid in the understanding of the binding roles of these FHA domains.

4.3.2 Additional phosphorylated T3S-associated components

A recent study by Barison *et al.* demonstrated that a phosphorylated peptide from the T3S-associated protein Spa33 bound with high affinity to the CdsD ortholog, MxiG (Barison, Lambers *et al.* 2012). This was the first evidence of a phosphorylated T3S-associated C-ring component. Since CdsQ, the ortholog of Spa33 in *Chlamydia spp.*, has two predicted phosphorylated threonine motifs (TxxI/L/D), we hypothesized that CdsQ may be phosphorylated in *C. pneumoniae* (Barison, Lambers *et al.* 2012). We prepared recombinant His-CdsQ, GST-PknD and GST-Pkn5 (*Cpn0703*), which is the serine/threonine kinase encoded by the gene immediately upstream of *cdsQ*, and tested PknD and Pkn5 for their ability to phosphorylate CdsQ. The results of *in vitro* kinase assays indicated that PknD does not phosphorylate His-CdsQ *in vitro*. It has been difficult to obtain active Pkn5 for an *in vitro* kinase assay so it is not yet known if Pkn5 phosphorylates CdsQ. Further characterization of phosphorylated T3S proteins *in vivo* would be necessary to provide evidence of the role of phosphorylation in the T3S apparatus.

4.4 A model for the role of CdsD in T3S

The T3S system of *C. pneumoniae* secretes effector proteins into the host cytoplasm for both host cell invasion and to provide an intracellular niche for replication.

The T3S apparatus is believed to actively secrete effectors into the host cell throughout the *Chlamydia* developmental cycle. In some bacterial genera, such as *Salmonella, Escherichia,* and *Yersinia,* multiple T3S apparatuses are encoded by genes on separate pathogenicity islands (Shea, Hensel *et al.* 1996; Foultier, Troisfontaines *et al.* 2002). A series of flagellar-like proteins have been annotated in *C. pneumoniae* that share sequence paralogy with T3S-associated components, such as FliI which shares sequence similarity, regulatory mechanisms, and enzymatic activity with the putative ATPase CdsN (Stone, Bulir *et al.* 2010). Only three flagellar-like proteins have been predicted thus far and these proteins are believed to represent paralogs of basal body components CdsV, CdsJ, and CdsN. Quantitative RT-PCR data indicates that these flagellar-like proteins are expressed early-mid cycle in *C. trachomatis* (Belland, Zhong *et al.* 2003). This expression profile contrasts that of CdsV, CdsJ, and CdsN, which appear to be expressed later in the developmental cycle (Belland, Zhong *et al.* 2003). The interaction between these flagellar-like paralogs and the T3S apparatus may indicate novel regulatory mechanism for basal body assembly of the T3S apparatus.

Following the assembly of the basal body and the needle filament, the secretion of effectors in *C. pneumoniae* is believed to be controlled by proteins at basal body. Establishing a secretion hierarchy that controls the order of secretion of early and late effectors is an essential regulatory mechanism that has yet to be elucidated in *Chlamydia spp*. The autocleavage of YscU is thought to control the transition from filament protein secretion to early effector secretion in *Yersinia* (Bjornfot, Lavander *et al.* 2009). We speculate that the existence of paralogous basal body proteins that are expressed at

different times in the developmental cycle may implicate that the sorting platform at the base of the apparatus is involved in the transition from middle to late effectors. Based on the research presented in this thesis, post-translational phosphorylation events may play a role in either the assembly of the basal body or contribute to the hierarchical secretion of effectors. We propose a model where the phosphorylation of CdsD, and perhaps other T3S proteins, plays a role in regulating the sorting platform in the basal body of the apparatus.

The role of the unique cytoplasmic domain of CdsD in the T3S apparatus has yet to be elucidated. In addition to its putative role as a scaffolding protein that anchors components in the cytoplasm and periplasm, previous studies in the Mahony laboratory have suggested that CdsD is phosphorylated by a putative *Chlamydia* kinase (Johnson and Mahony 2007). The i*n vitro* oligomerization data presented in this thesis suggests that the basal body protein may form phosphorylation-dependent oligomers. If the phosphorylation-dependent oligomerization of CdsD occurs in *Chlamydia*, we would expect that intact T3S apparatuses at 72 hpi could contain phosphorylated CdsD. The failure to detect phosphorylated CdsD at 72 hpi could indicate that a transient and reversible phosphorylation and subsequent conformational change in CdsD may occur during basal body assembly. Assuming that this conformational change occurs mid-cycle, phosphorylation of CdsD may lead to the release of mid-cycle components of the C-ring (FliI, FliF, and FlhA) and the reassembly of late-cycle paralogous proteins (CdsN, CdsJ, and CdsV). If the two putative ATPases FliI and CdsN have different affinities for subsets of chaperone/effector complexes, the re-assortment of C-ring components could

result in effector selection required for the secretion hierarchy. This model is speculative and would require substantial experimentation to confirm that the annotated flagellar-like proteins assemble with other T3S components forming the T3S apparatus in *Chlamydia.*

In addition, we predict that the unusual existence of two FHA domains within the N-terminal 500 amino acids of CdsD implies that phosphate signalling may play an important role in the positioning of proteins at the sorting platform in the basal body. Barison *et al.* recently identified a phosphorylated peptide of the CdsQ ortholog, Spa33, that bound with increased affinity to the ortholog of CdsD, compared to unphosphorylated Spa33 (Barison, Lambers *et al.* 2012). Similarly, data presented in this thesis have shown that CdsD interacts preferentially with autophosphorylated PknD as opposed to unphosphorylated PknD. In the absence of *in vivo* data confirming the presence of phosphorylated T3S-associated proteins, the role of Pkn5 remains obscure. The mid-cycle expression of Pkn5 in *C. trachomatis,* which is encoded in the same operon as CdsQ, CdsN, CdsD, CdsF, and CdsC, indicates that phosphorylation may play a unique role in the function of these T3S-associated components. If CdsQ is indeed phosphorylated and recruited to the base of the apparatus, we hypothesize that it interacts with CdsD in two capacities. First, CdsQ may sequentially shuttle chaperone/effectors to the base of the apparatus and present them to the putative ATPases. Second, phosphorylated CdsQ may act as a cytoplasmic 'cap' at the base of the cytoplasmic ring preventing the premature dissociation of C-ring components. In this second role, upon a hypothetical conformational change to CdsD, the CdsQ 'cap' is released from the sorting platform and re-recruited at a later time period once the paralogous components of the C-

ring are assembled. This model of the role of CdsD phosphorylation in the basal body assembly is speculative and requires the support of numerous *in vitro* and *in vivo* studies.

Regardless, CdsD is a large 93 kDa protein of *C. pneumoniae* that anchors peripheral membrane proteins in the cytoplasm against the inner bacterial membrane and is likely one of the earliest T3S-associated proteins to be inserted into the inner membrane. We have indicated that the FHA domains of CdsD interact with T3S proteins in the cytoplasm and the BON domain anchors the filament protein in the periplasmic space. The predicted structural role of CdsD and hypothetical transmembrane region indicate indirectly that CdsD is an integral bacterial inner membrane protein that spans from the cytoplasm, across the inner membrane, and into the periplasmic space. CdsD likely provides structural support for the T3S apparatus and facilitates assembly of other T3S proteins into the basal body of the apparatus.

FUTURE EXPERIMENTS

The results of GST pull-downs presented in this thesis indicate that six proteins interact with CdsD *in vitro*; however these interactions have not been confirmed *in vivo.* A significant limitation of the work presented in this thesis is that the majority of experiments were completed under non-native conditions. For instance, the concentration of each protein, the buffer conditions, and the number of proteins involved in each reaction were artificially combined to measure interactions with GST-CdsD. Co-precipitations of protein complexes involving CdsD with or without chemical cross-linkers may aid in the identification of actual interactions in the apparatus. The strength of these interactions can be assessed by dissociation constants obtained using surface plasmon resonance. These and other experiments would help corroborate the *in vitro* data collected thus far.

Future experiments should clarify the role of the FHA domains in phosphate signalling and attempt to confirm the existence of CdsD phosphorylation *in vivo*. Phosphoproteomic studies characterizing the incorporation of radiolabelled phosphate into components of the T3S apparatus would help determine the role of phosphorylation in the T3S secretion assembly and function. Alternatively, the sequential elution from immobilized metal affinity chromatography (SIMAC) methodology, which has a stronger ability to detect lower concentrations of phosphorylated proteins, may aid in the recovery of greater numbers of low concentration T3S-associated proteins. Theoretically, this may enable the detection of phosphorylated CdsD in *C. pneumoniae* or the identification of

additional phosphorylated T3S components. A phosphorylation-dependent conformational change of CdsD can also be analyzed using nuclear magnetic resonance.

The recently described genetic transformation protocol developed for *C. trachomatis* could add to our current understanding of the T3S system in *Chlamydia*. The identification of important residues involved in post-translational signalling could contribute to the mechanistic understanding of molecular models of the apparatus. Using this system, genetic knockouts or fluorescent recombinant probes may elucidate the roles and localization of individual proteins in the apparatus. These techniques would also be useful for identifying the roles of the annotated flagellar-like proteins in *Chlamydia.* Together, these future experiments should aid in the understanding of the apparatus and explore the novel role of phosphorylation in T3S of *C. pneumoniae.*

CONCLUDING REMARKS

CdsD, the basal body protein associated with the T3S apparatus in *C. pneumoniae*, may have important roles in both the assembly and regulation of secretion hierarchy. However, the current lack of a genetic transformation system for *C. pneumoniae* has made the study of T3S challenging. This thesis suggests that this large inner membrane protein has multiple binding partners in the inner membrane, cytoplasm, and periplasmic space of the bacterial cell. In addition, it addresses the possible roles of the cytoplasmic FHA domains and phosphorylation in the sorting platform at the base of the injectisome. The results presented thus far do not unambiguously demonstrate the presence of T3S protein phosphorylation events in *C. pneumoniae.* Future research using more sensitive methods of phosphorylated protein detection will undoubtedly clarify the ideas put forth in this thesis. New techniques, including the recent advent of a transformation protocol for *C. trachomatis* will also pave the way for future discoveries in the *Chlamydia* field. The discovery of novel post-translational mechanisms, such as phosphorylation, for regulating the T3S apparatus may lead to the development of new therapeutics to prevent the increasing incidence of antibiotic-resistant *Chlamydia spp.*.

REFERENCES

Abdelrahman, Y. M. and R. J. Belland (2005). "The chlamydial developmental cycle." FEMS Microbiol Rev. **29**(5): 949-959.

Al-Younes, H. M., T. Rudel, et al. (2001). "Low iron availability modulates the course of Chlamydia pneumoniae infection." Cell Microbiol. **3**(6): 427-437.

Bannantine, J. P., R. S. Griffiths, et al. (2000). "A secondary structure motif predictive of protein localization to the chlamydial inclusion membrane." Cell Microbiol. **2**(1): 35-47.

Barison, N., J. Lambers, et al. (2012). "Interaction of MxiG with the cytosolic complex of the type III secretion system controls Shigella virulence." Faseb J. **26**(4): 1717-1726. Epub 2012 Jan 1712.

Bavoil, P. M., R. Hsia, et al. (2000). "Closing in on Chlamydia and its intracellular bag of tricks." Microbiology. **146**(Pt 11): 2723-2731.

Belland, R. J., G. Zhong, et al. (2003). "Genomic transcriptional profiling of the developmental cycle of Chlamydia trachomatis." Proc Natl Acad Sci U S A **100**(14): 8478-8483.

Bennett, J. C. Q. and C. Hughes (2000). "From flagellum assembly to virulence: the extended family of type III export chaperones." Trends in Microbiology **8**(5): 202-204.

Betts-Hampikian, H. J. and K. A. Fields (2010). "The Chlamydial Type III Secretion Mechanism: Revealing Cracks in a Tough Nut." Front Microbiol. **1**: 114. Epub 2010 Oct 2019.

Betts-Hampikian, H. J. and K. A. Fields (2011). "Disulfide bonding within components of the Chlamydia type III secretion apparatus correlates with development." J Bacteriol. **193**(24): 6950-6959. Epub 2011 Oct 6914.

Bingle, L. E., C. M. Bailey, et al. (2008). "Type VI secretion: a beginner's guide." Curr Opin Microbiol. **11**(1): 3-8. Epub 2008 Mar 2004.

Bjornfot, A. C., M. Lavander, et al. (2009). "Autoproteolysis of YscU of Yersinia pseudotuberculosis is important for regulation of expression and secretion of Yop proteins." J Bacteriol. **191**(13): 4259-4267. Epub 2009 Apr 4224.

Blaylock, B., K. E. Riordan, et al. (2006). "Characterization of the Yersinia enterocolitica type III secretion ATPase YscN and its regulator, YscL." J Bacteriol. **188**(10): 3525-3534.

Bourret, R. B., K. A. Borkovich, et al. (1991). "Signal transduction pathways involving protein phosphorylation in prokaryotes." Annu Rev Biochem. **60**: 401-441.

Brade, L., K. Zych, et al. (1997). "Structural requirements of synthetic oligosaccharides to bind monoclonal antibodies against Chlamydia lipopolysaccharide." Glycobiology. **7**(6): 819-827.

Brickman, T. J., C. E. Barry, 3rd, et al. (1993). "Molecular cloning and expression of hctB encoding a strain-variant chlamydial histone-like protein with DNA-binding activity." J Bacteriol. **175**(14): 4274-4281.

Burnett, G. and E. P. Kennedy (1954). "The enzymatic phosphorylation of proteins." J Biol Chem. **211**(2): 969-980.

Byrne, G. I. and J. W. Moulder (1978). "Parasite-specified phagocytosis of Chlamydia psittaci and Chlamydia trachomatis by L and HeLa cells." Infect Immun. **19**(2): 598-606.

Carabeo, R. A., D. J. Mead, et al. (2003). "Golgi-dependent transport of cholesterol to the Chlamydia trachomatis inclusion." Proc Natl Acad Sci U S A. **100**(11): 6771-6776. Epub 2003 May 6712.

Chellas-Gery, B., K. Wolf, et al. (2011). "Biochemical and localization analyses of putative type III secretion translocator proteins CopB and CopB2 of Chlamydia trachomatis reveal significant distinctions." Infect Immun. **79**(8): 3036-3045. Epub 2011 May 3023.

Cheng, L. W., O. Kay, et al. (2001). "Regulated secretion of YopN by the type III machinery of Yersinia enterocolitica." J Bacteriol. **183**(18): 5293-5301.

Chopra, I., C. Storey, et al. (1998). "Antibiotics, peptidoglycan synthesis and genomics: the chlamydial anomaly revisited." Microbiology. **144**(Pt 10): 2673-2678.

Clifton, D. R., K. A. Fields, et al. (2004). "A chlamydial type III translocated protein is tyrosine-phosphorylated at the site of entry and associated with recruitment of actin." Proc Natl Acad Sci U S A. **101**(27): 10166-10171. Epub 12004 Jun 10115.

Coombes, B. K. and J. B. Mahony (2002). "Identification of MEK- and phosphoinositide 3-kinase-dependent signalling as essential events during Chlamydia pneumoniae invasion of HEp2 cells." Cell Microbiol. **4**(7): 447-460.

Cozzone, A. J. (1988). "Protein phosphorylation in prokaryotes." Annu Rev Microbiol. **42**: 97-125.

Day, J. B. and G. V. Plano (1998). "A complex composed of SycN and YscB functions as a specific chaperone for YopN in Yersinia pestis." Mol Microbiol. **30**(4): 777-788.

Desvaux, M., N. J. Parham, et al. (2004). "The general secretory pathway: a general misnomer?" Trends Microbiol. **12**(7): 306-309.

Diepold, A., M. Amstutz, et al. (2010). "Deciphering the assembly of the Yersinia type III secretion injectisome." EMBO J **29**(11): 1928-1940.

Diepold, A., U. Wiesand, et al. (2011). "The assembly of the export apparatus (YscR,S,T,U,V) of the Yersinia type III secretion apparatus occurs independently of other structural components and involves the formation of an YscV oligomer." Mol Microbiol **82**(2): 502-514.

Everett, K. D. (2000). "Chlamydia and Chlamydiales: more than meets the eye." Vet Microbiol. **75**(2): 109-126.

Everett, K. D. E., R. M. Bush, et al. (1999). "Emended description of the order Chlamydiales, proposal of Parachlamydiaceae fam. nov. and Simkaniaceae fam. nov., each containing one monotypic genus, revised taxonomy of the family Chlamydiaceae, including a new genus and five new species, and standards for the identification of organisms." International Journal of Systematic Bacteriology **49**(2): 415-440.

Fattori, J., A. Prando, et al. (2011). "Bacterial secretion chaperones." Protein Pept Lett. **18**(2): 158-166.

Fields, K. A. and T. Hackstadt (2002). "The chlamydial inclusion: escape from the endocytic pathway." Annu Rev Cell Dev Biol. **18**: 221-245. Epub 2002 Apr 2002.

Foultier, B., P. Troisfontaines, et al. (2002). "Characterization of the ysa pathogenicity locus in the chromosome of Yersinia enterocolitica and phylogeny analysis of type III secretion systems." J Mol Evol. **55**(1): 37-51.

Gabel, B. R., C. Elwell, et al. (2004). "Lipid raft-mediated entry is not required for Chlamydia trachomatis infection of cultured epithelial cells." Infect Immun. **72**(12): 7367-7373.

Ge, R. and W. Shan (2011). "Bacterial phosphoproteomic analysis reveals the correlation between protein phosphorylation and bacterial pathogenicity." Genomics Proteomics Bioinformatics. **9**(4-5): 119-127.

Ghosh, P. (2004). "Process of protein transport by the type III secretion system." Microbiol Mol Biol Rev. **68**(4): 771-795.

Ghuysen, J. M. and C. Goffin (1999). "Lack of cell wall peptidoglycan versus penicillin sensitivity: new insights into the chlamydial anomaly." Antimicrob Agents Chemother. **43**(10): 2339-2344.

Grayston, J. T. (1968). "[Immunization against trachoma]." Bol Oficina Sanit Panam. **65**(3): 220-237.

Grayston, J. T., C. C. Kuo, et al. (1989). "Chlamydia pneumoniae sp. nov. lbr Chlamydia strain TWAR. ." International Journal of Systematic Bacteriology **39**: 88-90.

Grayston, J. T., C. C. Kuo, et al. (1986). "A new Chlamydia psittaci strain, TWAR, isolated in acute respiratory tract infections." N Engl J Med. **315**(3): 161-168.

Hackstadt, T., D. D. Rockey, et al. (1996). "Chlamydia trachomatis interrupts an exocytic pathway to acquire endogenously synthesized sphingomyelin in transit from the Golgi apparatus to the plasma membrane." Embo J. **15**(5): 964-977.

Hackstadt, T., M. A. Scidmore-Carlson, et al. (1999). "The Chlamydia trachomatis IncA protein is required for homotypic vesicle fusion." Cell Microbiol. **1**(2): 119-130.

Hafner, L., K. Beagley, et al. (2008). "Chlamydia trachomatis infection: host immune responses and potential vaccines." Mucosal Immunol. **1**(2): 116-130. Epub 2008 Jan 2009.

Hahn, D. L., Anttila, T., and Saikku, P. (1999). "Chlamydia pneumoniae, asthma, and COPD: what is the evidence?" Annals of Allergy, Asthma, and Immunology **83**: 271-291.

Hahn, D. L., A. Schure, et al. (2012). "Chlamydia pneumoniae-specific IgE is prevalent in asthma and is associated with disease severity." PLoS One. **7**(4): e35945. Epub 32012 Apr 35924.

Hammerschlag, M. R. (2002). "The intracellular life of chlamydiae." Semin Pediatr Infect Dis. **13**(4): 239-248.

Hanks, S. K., A. M. Quinn, et al. (1988). "The protein kinase family: conserved features and deduced phylogeny of the catalytic domains." Science. **241**(4861): 42-52.

Harrison, R. G. (1999). "Expression of soluble heterologus proteins via fusion with NusA protein " Innovations: 4-7.

Hayes, C. S., S. K. Aoki, et al. (2010). "Bacterial contact-dependent delivery systems." Annu Rev Genet. **44**: 71-90.

Hefty, P. S. and R. S. Stephens (2007). "Chlamydial type III secretion system is encoded on ten operons preceded by sigma 70-like promoter elements." J Bacteriol. **189**(1): 198-206. Epub 2006 Oct 2020.

Heinzen, R. A. and T. Hackstadt (1997). "The Chlamydia trachomatis parasitophorous vacuolar membrane is not passively permeable to low-molecular-weight compounds." Infect Immun. **65**(3): 1088-1094.

Heuer, D., C. Kneip, et al. (2007). "Tackling the intractable - approaching the genetics of Chlamydiales." Int J Med Microbiol. **297**(7-8): 569-576. Epub 2007 Apr 2030.

Hofmann, K. and W. Stoffel (1993). "TMbase - A database of membrane spanning proteins segments." Biol. Chem. Hoppe-Seyler **374**(166).

Hogan, R. J., S. A. Mathews, et al. (2004). "Chlamydial persistence: beyond the biphasic paradigm." Infect Immun. **72**(4): 1843-1855.

Hsia, R. C., Y. Pannekoek, et al. (1997). "Type III secretion genes identify a putative virulence locus of Chlamydia." Mol Microbiol. **25**(2): 351-359.

Hybiske, K. and R. S. Stephens (2007). "Mechanisms of host cell exit by the intracellular bacterium Chlamydia." Proc Natl Acad Sci U S A. **104**(27): 11430-11435. Epub 12007 Jun 11425.

Izore, T., V. Job, et al. (2011). "Biogenesis, regulation, and targeting of the type III secretion system." Structure **19**(5): 603-612.

Johnson, D. L. and J. B. Mahony (2007). "Chlamydophila pneumoniae PknD exhibits dual amino acid specificity and phosphorylates Cpn0712, a putative type III secretion YscD homolog." J Bacteriol. **189**(21): 7549-7555. Epub 2007 Aug 7531.

Johnson, D. L., C. B. Stone, et al. (2009). "A novel inhibitor of Chlamydophila pneumoniae protein kinase D (PknD) inhibits phosphorylation of CdsD and suppresses bacterial replication." BMC Microbiol. **9**: 218.

Johnson, D. L., C. B. Stone, et al. (2008). "Interactions between CdsD, CdsQ, and CdsL, three putative Chlamydophila pneumoniae type III secretion proteins." J Bacteriol. **190**(8): 2972-2980. Epub 2008 Feb 2915.

Kalman, S., W. Mitchell, et al. (1999). "Comparative genomes of Chlamydia pneumoniae and C. trachomatis." Nat Genet. **21**(4): 385-389.

Kelley, L. A. and M. J. Sternberg (2009). "Protein structure prediction on the Web: a case study using the Phyre server." Nat Protoc. **4**(3): 363-371.

Kinoshita, E., M. Takahashi, et al. (2004). "Recognition of phosphate monoester dianion by an alkoxide-bridged dinuclear zinc(II) complex." Dalton Trans.(8): 1189-1193. Epub 2004 Mar 1122.

Klos, A., J. Thalmann, et al. (2009). "The transcript profile of persistent Chlamydophila (Chlamydia) pneumoniae in vitro depends on the means by which persistence is induced." FEMS Microbiol Lett. **291**(1): 120-126. Epub 2008 Dec 2009.

Kol, A., G. K. Sukhova, et al. (1998). "Chlamydial Heat Shock Protein 60 Localizes in Human Atheroma and Regulates Macrophage Tumor Necrosis Factor- and Matrix Metalloproteinase Expression." Circulation **98**(4): 300-307.

Koo, I. C. and R. S. Stephens (2003). "A developmentally regulated two-component signal transduction system in Chlamydia." J Biol Chem **278**(19): 17314-17319.

Krebs, E. G. and J. A. Beavo (1979). "Phosphorylation-dephosphorylation of enzymes." Annu Rev Biochem. **48**: 923-959.

Kuo, C. C., H. H. Chen, et al. (1986). "Identification of a new group of Chlamydia psittaci strains called TWAR." J Clin Microbiol. **24**(6): 1034-1037.

Kuo, C. C., A. M. Gown, et al. (1993). "Detection of Chlamydia pneumoniae in aortic lesions of atherosclerosis by immunocytochemical stain." Arterioscler Thromb. **13**(10): 1501-1504.

Kuo, C. C., L. A. Jackson, et al. (1995). "Chlamydia pneumoniae (TWAR)." Clin Microbiol Rev. **8**(4): 451-461.

Kuo, C. C., A. Lee, et al. (2004). "Cleavage of the N-linked oligosaccharide from the surfaces of Chlamydia species affects attachment and infectivity of the organisms in human epithelial and endothelial cells." Infect Immun. **72**(11): 6699-6701.

Lara-Tejero, M., J. Kato, et al. (2011). "A sorting platform determines the order of protein secretion in bacterial type III systems." Science. **331**(6021): 1188-1191. Epub 2011 Feb 1183.

Lavander, M., L. Sundberg, et al. (2002). "Proteolytic cleavage of the FlhB homologue YscU of Yersinia pseudotuberculosis is essential for bacterial survival but not for type III secretion." J Bacteriol. **184**(16): 4500-4509.

Liang, X. and S. R. Van Doren (2008). "Mechanistic insights into phosphoprotein-binding FHA domains." Acc Chem Res **41**(8): 991-999.

Loomis, W. P. and M. N. Starnbach (2002). "T cell responses to Chlamydia trachomatis." Curr Opin Microbiol. **5**(1): 87-91.

Lugert, R., M. Kuhns, et al. (2004). "Expression and localization of type III secretion-related proteins of Chlamydia pneumoniae." Med Microbiol Immunol. **193**(4): 163-171. Epub 2003 Oct 2031.

Marlovits, T. C., T. Kubori, et al. (2004). "Structural insights into the assembly of the type III secretion needle complex." Science. **306**(5698): 1040-1042.

Marrie, T. J., N. Costain, et al. (2012). "The role of atypical pathogens in community-acquired pneumonia." Semin Respir Crit Care Med. **33**(3): 244-256. Epub 2012 Jun 2020.

Matsumoto, A. (1982). "Surface projections of Chlamydia psittaci elementary bodies as revealed by freeze-deep-etching." J Bacteriol. **151**(2): 1040-1042.

Matsumoto, A. and G. P. Manire (1970). "Electron microscopic observations on the effects of penicillin on the morphology of Chlamydia psittaci." J Bacteriol. **101**(1): 278-285.

McDowell, M. A., S. Johnson, et al. (2011). "Structural and functional studies on the N-terminal domain of the Shigella type III secretion protein MxiG." J Biol Chem. **286**(35): 30606-30614. Epub 32011 Jul 30605.

Mougous, J. D., C. A. Gifford, et al. (2007). "Threonine phosphorylation post-translationally regulates protein secretion in Pseudomonas aeruginosa." Nat Cell Biol. **9**(7): 797-803. Epub 2007 Jun 2010.

Moulder, J. W. (1993). "Why is Chlamydia sensitive to penicillin in the absence of peptidoglycan?" Infect Agents Dis. **2**(2): 87-99.

Munoz-Dorado, J., S. Inouye, et al. (1993). "Eukaryotic-like protein serine/threonine kinases in Myxococcus xanthus, a developmental bacterium exhibiting social behavior." J Cell Biochem. **51**(1): 29-33.

Nordfelth, R., A. M. Kauppi, et al. (2005). "Small-molecule inhibitors specifically targeting type III secretion." Infect Immun. **73**(5): 3104-3114.

Page, A. L. and C. Parsot (2002). "Chaperones of the type III secretion pathway: jacks of all trades." Mol Microbiol. **46**(1): 1-11.

Pantoja, L. G., R. D. Miller, et al. (2001). "Characterization of Chlamydia pneumoniae persistence in HEp-2 cells treated with gamma interferon." Infect Immun. **69**(12): 7927-7932.

Paradowski, B., M. Jaremko, et al. (2007). "Evaluation of CSF-Chlamydia pneumoniae, CSF-tau, and CSF-Abeta42 in Alzheimer's disease and vascular dementia." J Neurol. **254**(2): 154-159. Epub 2007 Feb 2021.

Pegues, D. A., M. J. Hantman, et al. (1995). "PhoP/PhoQ transcriptional repression of Salmonella typhimurium invasion genes: evidence for a role in protein secretion." Mol Microbiol. **17**(1): 169-181.

Pennell, S., S. Westcott, et al. (2010). "Structural and functional analysis of phosphothreonine-dependent FHA domain interactions." Structure **18**(12): 1587-1595.

Peschel, G., L. Kernschmidt, et al. (2010). "Chlamydophila pneumoniae downregulates MHC-class II expression by two cell type-specific mechanisms." Mol Microbiol. **76**(3): 648-661. Epub 2010 Mar 2010.

Peterson, E. M., L. M. de la Maza, et al. (1998). "Characterization of a neutralizing monoclonal antibody directed at the lipopolysaccharide of Chlamydia pneumoniae." Infect Immun. **66**(8): 3848-3855.

Popov, V. L., A. A. Shatkin, et al. (1991). "Ultrastructure of Chlamydia pneumoniae in cell culture." FEMS Microbiol Lett. **68**(2): 129-134.

Pospischil, A. (2009). "From disease to etiology: historical aspects of Chlamydia-related diseases in animals and humans." Drugs Today (Barc). **45**(Suppl B): 141-146.

Pucciarelli, M. G. and F. Garcia-del Portillo (2003). "Protein-peptidoglycan interactions modulate the assembly of the needle complex in the Salmonella invasion-associated type III secretion system." Mol Microbiol. **48**(2): 573-585.

Puolakkainen, M., A. Lee, et al. (2008). "Retinoic acid inhibits the infectivity and growth of Chlamydia pneumoniae in epithelial and endothelial cells through different receptors." Microb Pathog. **44**(5): 410-416. Epub 2007 Nov 2023.

Riordan, K. E., J. A. Sorg, et al. (2008). "Impassable YscP substrates and their impact on the Yersinia enterocolitica type III secretion pathway." J Bacteriol. **190**(18): 6204-6216. Epub 2008 Jul 6218.

Ripa, K. T. and P. A. Mardh (1977). "Cultivation of Chlamydia trachomatis in cycloheximide-treated mccoy cells." J Clin Microbiol. **6**(4): 328-331.

Ross, J. A. and G. V. Plano (2011). "A C-terminal region of Yersinia pestis YscD binds the outer membrane secretin YscC." J Bacteriol. **193**(9): 2276-2289. Epub 2011 Feb 2225.

Rurangirwa, F. R., P. M. Dilbeck, et al. (1999). "Analysis of the 16S rRNA gene of micro-organism WSU 86-1044 from an aborted bovine foetus reveals that it is a member of the order Chlamydiales: proposal of Waddliaceae fam. nov., Waddlia chondrophila gen. nov., sp. nov." Int J Syst Bacteriol. **49**(Pt 2): 577-581.

Sadowski, I., J. C. Stone, et al. (1986). "A noncatalytic domain conserved among cytoplasmic protein-tyrosine kinases modifies the kinase function and transforming activity of Fujinami sarcoma virus P130gag-fps." Mol Cell Biol. **6**(12): 4396-4408.

Sanowar, S., P. Singh, et al. (2010). "Interactions of the transmembrane polymeric rings of the Salmonella enterica serovar Typhimurium type III secretion system." MBio. **1(3).**(pii): e00158-00110.

Sauer, R. T., D. N. Bolon, et al. (2004). "Sculpting the proteome with AAA(+) proteases and disassembly machines." Cell. **119**(1): 9-18.

Schachter, J., R. S. Stephens, et al. (2001). "Radical changes to chlamydial taxonomy are not necessary just yet." Int J Syst Evol Microbiol. **51**(Pt 1): 249; author reply 251-243.

Schreiner, M. and H. H. Niemann (2012). "Crystal structure of the Yersinia enterocolitica type III secretion chaperone SycD in complex with a peptide of the minor translocator YopD." BMC Struct Biol. **12**(1): 13.

Schultz, J., R. R. Copley, et al. (2000). "SMART: a web-based tool for the study of genetically mobile domains." Nucleic Acids Res. **28**(1): 231-234.

Scidmore, M. A., E. R. Fischer, et al. (2003). "Restricted fusion of Chlamydia trachomatis vesicles with endocytic compartments during the initial stages of infection." Infect Immun. **71**(2): 973-984.

Scidmore, M. A., D. D. Rockey, et al. (1996). "Vesicular interactions of the Chlamydia trachomatis inclusion are determined by chlamydial early protein synthesis rather than route of entry." Infect Immun. **64**(12): 5366-5372.

Shaw, E. I., C. A. Dooley, et al. (2000). "Three temporal classes of gene expression during the Chlamydia trachomatis developmental cycle." Mol Microbiol. **37**(4): 913-925.

Shea, J. E., M. Hensel, et al. (1996). "Identification of a virulence locus encoding a second type III secretion system in Salmonella typhimurium." Proc Natl Acad Sci U S A. **93**(6): 2593-2597.

Shima, K., G. Kuhlenbaumer, et al. (2010). "Chlamydia pneumoniae infection and Alzheimer's disease: a connection to remember?" Med Microbiol Immunol. **199**(4): 283-289. Epub 2010 May 2016.

Silva-Herzog, E., F. Ferracci, et al. (2008). "Membrane localization and topology of the Yersinia pestis YscJ lipoprotein." Microbiology. **154**(Pt 2): 593-607.

Silva-Herzog, E., S. S. Joseph, et al. (2011). "Scc1 (CP0432) and Scc4 (CP0033) function as a type III secretion chaperone for CopN of Chlamydia pneumoniae." J Bacteriol. **193**(14): 3490-3496. Epub 2011 May 3413.

Simonetti, A. C., J. H. Melo, et al. (2009). "Immunological's host profile for HPV and Chlamydia trachomatis, a cervical cancer cofactor." Microbes Infect **11**(4): 435-442.

Sorg, J. A., B. Blaylock, et al. (2006). "Secretion signal recognition by YscN, the Yersinia type III secretion ATPase." Proc Natl Acad Sci U S A. **103**(44): 16490-16495. Epub 12006 Oct 16418.

Spreter, T., C. K. Yip, et al. (2009). "A conserved structural motif mediates formation of the periplasmic rings in the type III secretion system." Nat Struct Mol Biol. **16**(5): 468-476. Epub 2009 Apr 2026.

Stamm, L. M. and M. B. Goldberg (2011). "Microbiology. Establishing the secretion hierarchy." Science. **331**(6021): 1147-1148.

Stephens, R. S., G. Myers, et al. (2009). "Divergence without difference: phylogenetics and taxonomy of Chlamydia resolved." FEMS Immunol Med Microbiol. **55**(2): 115-119.

Stock, A. M., V. L. Robinson, et al. (2000). "Two-component signal transduction." Annu Rev Biochem. **69**: 183-215.

Stone, C. B., D. C. Bulir, et al. (2011). "Chlamydia Pneumoniae CdsL Regulates CdsN ATPase Activity, and Disruption with a Peptide Mimetic Prevents Bacterial Invasion." Front Microbiol. **2**: 21. Epub 2011 Feb 2014.

Stone, C. B., D. C. Bulir, et al. (2010). "Interactions between flagellar and type III secretion proteins in Chlamydia pneumoniae." BMC Microbiol. **10**: 18.

Stone, C. B., D. L. Johnson, et al. (2008). "Characterization of the putative type III secretion ATPase CdsN (Cpn0707) of Chlamydophila pneumoniae." J Bacteriol. **190**(20): 6580-6588. Epub 2008 Aug 6515.

Stone, C. B., S. Sugiman-Marangos, et al. (2012). "Structural characterization of a novel Chlamydia pneumoniae type III secretion-associated protein, Cpn0803." PLoS One. **7**(1): e30220. Epub 32012 Jan 30217.

Stuart, E. S., W. C. Webley, et al. (2003). "Lipid rafts, caveolae, caveolin-1, and entry by Chlamydiae into host cells." Exp Cell Res. **287**(1): 67-78.

Su, H., G. McClarty, et al. (2004). "Activation of Raf/MEK/ERK/cPLA2 signaling pathway is essential for chlamydial acquisition of host glycerophospholipids." J Biol Chem. **279**(10): 9409-9416. Epub 2003 Dec 9415.

Su, H., L. Raymond, et al. (1996). "A recombinant Chlamydia trachomatis major outer membrane protein binds to heparan sulfate receptors on epithelial cells." Proc Natl Acad Sci U S A. **93**(20): 11143-11148.

Subtil, A., C. Parsot, et al. (2001). "Secretion of predicted Inc proteins of Chlamydia pneumoniae by a heterologous type III machinery." Mol Microbiol. **39**(3): 792-800.

Sudler, C., L. E. Hoelzle, et al. (2004). "Molecular characterisation of chlamydial isolates from birds." Vet Microbiol **98**(3-4): 235-241.

Sullivan, J. L. and E. D. Weinberg (1999). "Iron and the role of Chlamydia pneumoniae in heart disease." Emerg Infect Dis. **5**(5): 724-726.

Swietnicki, W., D. Carmany, et al. (2011). "Identification of small-molecule inhibitors of Yersinia pestis Type III secretion system YscN ATPase." PLoS One. **6**(5): e19716. Epub 12011 May 19718.

Tam, J. E., C. H. Davis, et al. (1994). "Expression of recombinant DNA introduced into Chlamydia trachomatis by electroporation." Can J Microbiol. **40**(7): 583-591.

Teankum, K., A. Pospischil, et al. (2007). "Prevalence of chlamydiae in semen and genital tracts of bulls, rams and bucks." Theriogenology. **67**(2): 303-310. Epub 2006 Aug 2028.

Thanabalu, T., E. Koronakis, et al. (1998). "Substrate-induced assembly of a contiguous channel for protein export from E.coli: reversible bridging of an inner-membrane translocase to an outer membrane exit pore." Embo J. **17**(22): 6487-6496.

Thomas, N. A., W. Deng, et al. (2005). "CesT is a multi-effector chaperone and recruitment factor required for the efficient type III secretion of both LEE- and non-LEE-encoded effectors of enteropathogenic Escherichia coli." Mol Microbiol. **57**(6): 1762-1779.

Toor, R. K., C. B. Stone, et al. (2012). "Chlamydia pneumoniae CdsQ functions as a multi-cargo transport protein, delivering chaperone-effector complexes to the type III secretion ATPase, CdsN." Translational Biomedicine **3**(1:2): 1-11.

Tseng, T. T., B. M. Tyler, et al. (2009). "Protein secretion systems in bacterial-host associations, and their description in the Gene Ontology." BMC Microbiol. **9**(Suppl 1): S2.

Tyagi, N., K. Anamika, et al. (2010). "A framework for classification of prokaryotic protein kinases." PLoS One. **5**(5): e10608.

Vardhan, H., A. R. Bhengraj, et al. (2009). "Chlamydia trachomatis alters iron-regulatory protein-1 binding capacity and modulates cellular iron homeostasis in HeLa-229 cells." J Biomed Biotechnol. **2009**: 342032. Epub 342009 Aug 342016.

Verma, A. and A. T. Maurelli (2003). "Identification of two eukaryote-like serine/threonine kinases encoded by Chlamydia trachomatis serovar L2 and characterization of interacting partners of Pkn1." Infect Immun. **71**(10): 5772-5784.

Verma, A. and A. T. Maurelli (2003). "Identification of Two Eukaryote-Like Serine/Threonine Kinases Encoded by Chlamydia trachomatis Serovar L2 and Characterization of Interacting Partners of Pkn1." Infect Immun **71**(10): 5772-5784.

Wang, J. Y. and D. E. Koshland, Jr. (1978). "Evidence for protein kinase activities in the prokaryote Salmonella typhimurium." J Biol Chem. **253**(21): 7605-7608.

Wang, Y., S. Kahane, et al. (2011). "Development of a transformation system for Chlamydia trachomatis: restoration of glycogen biosynthesis by acquisition of a plasmid shuttle vector." PLoS Pathog. **7**(9): e1002258. Epub 1002011 Sep 1002222.

Watson, C. and N. J. Alp (2008). "Role of Chlamydia pneumoniae in atherosclerosis." Clin Sci (Lond) **114**(8): 509-531.

Wattiau, P., B. Bernier, et al. (1994). "Individual chaperones required for Yop secretion by Yersinia." Proc Natl Acad Sci U S A. **91**(22): 10493-10497.

Wehrl, W., T. F. Meyer, et al. (2004). "Action and reaction: Chlamydophila pneumoniae proteome alteration in a persistent infection induced by iron deficiency." Proteomics. **4**(10): 2969-2981.

Wilson, D. P., J. A. Whittum-Hudson, et al. (2009). "Kinematics of intracellular chlamydiae provide evidence for contact-dependent development." J Bacteriol. **191**(18): 5734-5742. Epub 2009 Jun 5719.

Wolf, K., E. Fischer, et al. (2000). "Ultrastructural analysis of developmental events in Chlamydia pneumoniae-infected cells." Infect Immun. **68**(4): 2379-2385.

Wolf, K. and T. Hackstadt (2001). "Sphingomyelin trafficking in Chlamydia pneumoniae-infected cells." Cell Microbiol. **3**(3): 145-152.

Wylie, J. L., G. M. Hatch, et al. (1997). "Host cell phospholipids are trafficked to and then modified by Chlamydia trachomatis." J Bacteriol. **179**(23): 7233-7242.

Wyrick, P. B. (2000). "Intracellular survival by Chlamydia." Cell Microbiol. **2**(4): 275-282.

Xu, X., L. M. Tsvetkov, et al. (2002). "Chk2 activation and phosphorylation-dependent oligomerization." Mol Cell Biol. **22**(12): 4419-4432.

Yip, C. K., B. B. Finlay, et al. (2005). "Structural characterization of a type III secretion system filament protein in complex with its chaperone." Nat Struct Mol Biol. **12**(1): 75-81. Epub 2004 Dec 2026.

Appendices

Appendix A – The annotation of T3S-associated proteins in *C. pneumoniae, Salmonella, Yersinia, Shigella,* and Flagellar apparatuses (IM=inner membrane; OM=outer membrane; NF=needle filament; CP=cytoplasm; HCM=host cell membrane)

Gene ID	Common Protein Name						Location
C. pneumoniae	*Chlamydia*	*Salmonella (SPI-1)*	*Salmonella (SPI-2)*	*Yersinia (Ysc)*	*Shigella (Mxi)*	Flagella	
Cpn0702	CdsC	InvG	SsaC	YscC	MxiD	--	OM
Cpn0712	CdsD	PrgH	SsaD	YscD	MxiG	FliG	IM
Cpn0710	CdsF	PrgI	SsaG	YscF	MxiH	--	NF
Cpn0828	CdsJ	PrgK	SsaJ	YscJ	MxiJ	FliF	IM
Cpn0826	CdsL	--	SsaK	YscL	MxiN	FliH	CP
Cpn0707	CdsN	InvC	SsaN	YscN	Spa47	FliI	CP
CPn0705	CdsP	InvJ	SsaP	YscP	Spa32	--	Secreted?
Cpn0704	CdsQ	SpaO	SsaQ	YscQ	Spa33	FliN	CP
Cpn0825	CdsR	SpaP	SsaR	YscR	Spa24	FliP	IM
Cpn0824	CdsS	SpaQ	SsaS	YscS	Spa9	FliQ	IM
Cpn0823	CdsT	SpaR	SsaT	YscT	Spa29	FliR	IM
Cpn0322	CdsU	SpaS	SsaU	YscU	Spa40	FlhB	IM
Cpn0323	CdsV	InvA	SsaV	YscV	MxiA	FlhA	IM
Cpn0324	CopN	InvE	--	YopN	MxiC	FlhE	CP
Cpn0808	CopD	SipC	SseD	YopD	IpC	--	HCM
Cpn1019	CopD2	--	--	--	--	--	HCM
Cpn0809	CopB	SipB	SseC	YopB	IpaB	--	HCM
Cpn1020	CopB2	--	--	--	--	--	HCM

Appendix B – List of primers used in Gateway cloning system (Invitrogen)

Primer Name	Primer Length (in base pairs)	Primer Sequence (5'-3')
CdsD (Forward)	95	GGGGACAAGTTTGTACAAAAAAGCAGGCTTAGA TTACGATATCCCAACGACCGAAAACCTGTATTTT CAGGGCATGGCAGTACGATTAATTGTTG
CdsD (Reverse)	57	GGGGACCACTTTGTACAAGAAAGCTGGGTCTTAT TTATTGTAGTCTATTTTATATTT
kPknD (Forward)	97	GGGGACAAGTTTGTACAAAAAAGCAGGCTTAGA TTACGATATCCCAACGACCGAAAACCTGTATTTT CAGGGCATGGAGCGCTATGATATTGTTAGA

kPknD (Reverse)	54	GGGGACCACTTTGTACAAGAAAGCTGGGTCTTA CCCTTTCAGATGACTCTCGAT
CdsF (Forward)	95	GGGGACAAGTTTGTACAAAAAAGCAGGCTTAGA TTACGATATCCCAACGACCGAAAACCTGTATTTT CAGGGCATGGCTACAAATAAAAGTTGCA
CdsF (Reverse)	52	GGGGACCACTTTGTACAAGAAAGCTGGGTCTTA ACTTCCTTTAACTGCTCTA
CdsV (Forward)	94	GGGGACAAGTTTGTACAAAAAAGCAGGCTTAGA TTACGATATCCCAACGACCGAAAACCTGTATTTT CAGGGCATGAATAAGCTACTCAATTTC
CdsV (Reverse)	51	GGGGACCACTTTGTACAAGAAAGCTGGGTCTTA GAAAATCTGAATTCTTCC
CdsP (Forward)	94	GGGGACAAGTTTGTACAAAAAAGCAGGCTTAGA TTACGATATCCCAACGACCGAAAACCTGTATTTT CAGGGCATGGAATTAAAGAAAACAGCA
CdsP (Reverse)	51	GGGGACCACTTTGTACAAGAAAGCTGGGTCTTAT AAACGTGCTTCTTCGAT
CdsC (Forward)	94	GGGGACAAGTTTGTACAAAAAAGCAGGCTTAGA TTACGATATCCCAACGACCGAAAACCTGTATTTT CAGGGCGTGAAAACTGTGATATTGAAC
CdsC (Reverse)	51	GGGGACCACTTTGTACAAGAAAGCTGGGTCCTA CTGAGCTTCTATTTCTAT
CdsJ (Forward)	94	GGGGACAAGTTTGTACAAAAAAGCAGGCTTAGA TTACGATATCCCAACGACCGAAAACCTGTATTTT CAGGGCATGGTTCGTCGATCTATTTCT
CdsJ (Reverse)	51	GGGGACCACTTTGTACAAGAAAGCTGGGTCCTA AGCACCCTCAATTTCATT
CdsQ (Forward)	91	GGGGACAAGTTTGTACAAAAAAGCAGGCTTAGA TTACGATATCCCAACGACCGAAAACCTGTATTTT CAGGGCATGGCAGTAGCAGCCGAT
CdsQ (Reverse)	51	GGGGACCACTTTGTACAAGAAAGCTGGGTCTTAT ACCTCTAAAACGCGAAT
CdsU (Forward)	94	GGGGACAAGTTTGTACAAAAAAGCAGGCTTAGA TTACGATATCCCAACGACCGAAAACCTGTATTTT CAGGGCATGGGTGAAAAAACAGAAAAG
CdsU (Reverse)	51	GGGGACCACTTTGTACAAGAAAGCTGGGTCTTAT AAATGATCAGGTTGGTT
CdsS (Forward)	94	GGGGACAAGTTTGTACAAAAAAGCAGGCTTAGA TTACGATATCCCAACGACCGAAAACCTGTATTTT CAGGGCGTGTTAGCATTTTTCGCAACT

CdsS (Reverse)	54	GGGGACCACTTTGTACAAGAAAGCTGGGTCTTATTTCCATTTATAGAAGTTTTG
CdsT (Forward)	94	GGGGACAAGTTTGTACAAAAAAGCAGGCTTAGATTACGATATCCCAACGACCGAAAACCTGTATTTTCAGGGCTTGCAGGTCAGATTTTCCAAA
CdsT (Reverse)	51	GGGGACCACTTTGTACAAGAAAGCTGGGTCTTAGAGTACTTGAGGGTTGGA
CdsL (Forward)	96	GGGGACAAGTTTGTACAAAAAAGCAGGCTTAGATTACGATATCCCAACGACCGAAAACCTGTATTTTCAGGGCATGAAGTTTTTTAGCTTAATTTT
CdsL (Reverse)	51	GGGGACCACTTTGTACAAGAAAGCTGGGTCTTATTCTTTCTTATCCTGATC